

## 1 Response to Referee #1

2 Thanks for the review and interest in our measurements. We are pleased with the reviewer's  
3 overall evaluation of our manuscript, which acknowledges the novelty and quality of our  
4 measurements. However, the reviewer also expressed skepticism about the subsection that  
5 describes the smoke case study, based primarily on the fact that similar results have not been  
6 observed before. We must disagree with this. There are no other published depolarization  
7 measurements of smoke at 355 nm that we are aware of, so there is not enough information  
8 available to the science community about the spectral depolarization of smoke, or whether there  
9 is significant variability depending on factors like age, composition, combustion efficiency, and  
10 humidity. Indeed the reviewer's confirmation that these are unusual measurements makes us all  
11 the more eager to publish them and get them out into public discussion. We feel we have  
12 provided ample explanation of the measurement technique and uncertainties to support our  
13 measurements and stated conclusions. We do partially agree with the reviewer's feelings that  
14 the current state of particle modeling is insufficient to thoroughly explain the observed spectral  
15 dependencies (either in the more familiar dust cases or in the more unusual smoke case). But  
16 again, we do not agree that this means that discussion of these results should be curtailed rather  
17 than subjected to open scientific scrutiny. We discuss the current state of modeling because it is  
18 the best that is currently available for explaining spectral depolarization measurements. We hope  
19 that more researchers with modeling expertise may also become interested in these observations  
20 and move this work forward so we as a community will gain a better understanding of the  
21 observations. Similarly, we hope that other researchers will publish their 355 nm depolarization  
22 measurement of smoke, and multi-wavelength depolarization measurements generally, whether  
23 or not they agree with ours, to help move the field forward.

24 Below, the reviewer's comments are in blue and our responses are in black.

### 25 General

26 This is an exciting contribution to the lidar literature. For the first time, airborne polarization lidar  
27 measurements are performed simultaneously at three wavelengths. Several case studies are  
28 presented and corroborate that high quality observations with a unique lidar setup could be  
29 realized. However several points must be improved. The smoke case study triggers many  
30 questions that must be checked and answered.

### 31 Detailed comments:

32 Page 24754, second paragraph:

33 The introduction should be improved. In such an important paper, the field of aerosol  
34 depolarization studies must be better reviewed. References to the work of Japanese groups  
35 (Sugimoto, Nishizawa and further papers) must be given. The milestone-like work of the  
36 SAMUM and SALTRACE groups should be cited (Freudenthaler, Gross, and Tesche papers in  
37 Tellus 2009 and 2011). These efforts including the use of the measured particle linear  
38 depolarization ratio to separate dust from non-dust aerosol components (Tesche JGR 2009,  
39 Ansmann JGR 2011, ACP 2012, Mamouri-Ansmann, AMT 2014) pushed the depolarization lidar  
40 work really forward and offered many new opportunities for important quantitative aerosol  
41

1 studies. CALIPSO and EarthCARE benefit from all this basic work (e.g., via Amiridis, ACP 2013).  
2 A nice and well balanced introduction increases the importance of the next large step presented  
3 in this paper (three wavelength depolarization lidar). Do not hesitate to cite your own recent  
4 papers (Burton in ACP and AMT, 2012, 2013, 2014) together with the Gross papers (2011, 2013,  
5 2015: :). All these aerosol-typing papers are important contributions to the field and should show  
6 up in a compact brief introduction.  
7

8 I understand that a paper from a NASA group wants to put all the spaceborne lidar activities into  
9 the center of interest. But polarization lidar is clearly a stand-alone science field and offers exciting  
10 possibilities. So, at least in the second paragraph, one should provide a brief introduction into the  
11 field of polarization lidar for aerosol studies (not for cloud studies, that is not necessary here).

12 It should also be mentioned, that there is another group that does these simultaneous three-  
13 wavelength depolarization measurements (27 ILRC paper, Haarig et al.). The Leipzig group gave  
14 a presentation at the ILRC conference at New York and showed many desert dust cases from their  
15 Barbados SALTRACE campaigns which seem to match very well with your results if I remember  
16 all the numbers right. Maybe it is possible to compare these results, but I am not sure whether an  
17 extended ILRC paper is available or not. Usually they publish 4-page papers in the conference  
18 proceedings.  
19

20 OK, we have revised and reorganized the introduction as the reviewer suggests and included  
21 these references. New text:

22 *Polarization lidar is an a large and active field, with recent contributions from ground-based*  
23 *networks such as EARLINET (Pappalardo et al., 2014; Mamouri and Ansmann, 2014; Nisantzi*  
24 *et al., 2014) and the National Institute of Environmental Studies East Asian network of lidars*  
25 *(Sugimoto et al., 2005; Nishizawa et al., 2011); directed field campaigns, such as SAMUM*  
26 *(Freudenthaler et al., 2009; Tesche et al., 2011) and SALTRACE (Groß et al., 2015; Haarig et al.,*  
27 *2015); and others.*

28 *There is also considerable interest in global lidar observations from satellites {...continues with*  
29 *similar text as before...} NASA's airborne HSRL-2 is the first HSRL system making depolarization*  
30 *measurements at three wavelengths. A ground-based Raman system operated by the Leibniz*  
31 *Institute of Tropospheric Research has also been recently upgraded to make three-wavelength*  
32 *depolarization measurements (Haarig et al., 2014).*  
33

34 *Aerosol classification is one specific application of aerosol polarization measurements (Burton et*  
35 *al., 2012; Groß et al., 2013; Burton et al., 2013; Groß et al., 2014). Aerosol particle depolarization*  
36 *ratio from lidar is of key importance for the detection and assessment of dust and volcanic ash since*  
37 *it is a clear indicator of non-spherical particles. The particle depolarization ratio is also used to infer*  
38 *the amount of dust or ash in a mixture (Sugimoto and Lee, 2006; Tesche et al., 2009a; Tesche et al.,*  
39 *2011; Ansmann et al., 2011; Ansmann et al., 2012; David et al., 2013; Burton et al., 2014;*  
40 *Mamouri and Ansmann, 2014). It is also sensitive to the size of the non-spherical particles*  
41 *(Ansmann et al., 2009; Sakai et al., 2010; Gasteiger et al., 2011; Gasteiger and*  
42 *Freudenthaler, 2014).*  
43

1 {Continues with original text about dust and smoke measurements specifically.}

2  
3 Page 24755, second paragraph:

4 Regarding smoke and dust separation with polarization lidar, I like this Tesche paper in Tellus  
5 2011 very much. They distinguished African biomass burning smoke from desert dust and came  
6 finally even up with single scattering albedo values for the smoke part. That paper should also  
7 be included in the references here.

8 It has been added. See above.

9 Page 24756, Sect. 2, Instrumentation:

10 Can we have detailed information on the aircraft flight heights a.s.l. for all the case studies  
11 discussed later on? I have strong doubts that this strange smoke case with very large 355 nm  
12 depolarization ratio is based on good signals. I speculate that overlap or overloading problems  
13 may have caused these strange results. I will come to this point later again.

14 We added flight altitude to the description here in the instrumentation section (“The typical flight  
15 altitude of the B200 during lidar operations is 9 km”), and for the smoke flight specifically, the  
16 caption to figure 14 now notes that the flight altitude is 8970 m.

17 See below for responses regarding the overlap.

18 Page 24759, Eq.(2), please provide a reference for the equation

19 Thanks for pointing out this omission. It is Cairo, F., Di Donfrancesco, G., Adriani, A., Pulvirenti,  
20 L., and Fierli, F.: Comparison of Various Linear Depolarization Parameters Measured by Lidar,  
21 Appl. Opt., 38, 4425-4432, 1999.

22 Page 24761, Sect.3.1,

23 Line 22, particle depolarization ratios of 30.4% indicate desert dust backscatter fraction of only  
24 80-90%? I would say the fraction is then close to 100%.

25 Sugimoto and Lee (2006) give the mixing ratio as

$$X = \frac{(1 + \delta_{d532})\delta_{532}}{\delta_{d532}(1 + \delta_{532})}$$

26  
27 Plugging in 0.304 for  $\delta_{532}$  and the same value they use, 0.35, for  $\delta_{d532}$ , yields 90%. There was no  
28 good reason for us to include a wider range for the dust fraction estimate than for the quoted  
29 particle depolarization ratio so in the revision it has been changed to “approximately 90% dust”.

30 It would be really nice if we can have a full set of profiles of all the retrieved optical properties,  
31 maybe based on 10 sec or 30 sec signal averages or what ever is appropriate in case of aircraft  
32 HSRL observations. Then we could best compare your results with other publications in this field.  
33 I would recommend: left plot: profiles of particle backscatter at all three wavelengths, center left:  
34 profiles of particle extinction coefficient at both wavelength, center right: profiles of lidar ratio at  
35 both wavelength, right panel: particle linear depol ratio at all three wavelength. Profiles showing  
36 the depol ratio and the lidar ratio together provide the essential basis of all the aerosol typing  
37 studies (which includes your own paper Burton et al, AMT,2012, but also Gross et al., 2013 and  
38 2015, even in Illingworth et al., EarthCARE paper in BAMS, 2015, such a plot with lidar ratio  
39 versus depol ratio is given).

1 As mentioned in the manuscript, range dependence of the aerosol and molecular signals in the  
2 overlap region prevents us from calculating extinction (and therefore lidar ratio) within the  
3 smoke plume (but not particle depolarization ratio, which we discuss below). We prefer not to  
4 rely on simulations of the overlap region or perform analytical formulations to correct the overlap  
5 of the system, since these would introduce additional uncertainties. However, this is not  
6 primarily a typing study but a study of the spectral dependence of depolarization, so we think it  
7 should be acceptable to focus only on the depolarization. It's not that we don't agree with the  
8 researcher that it would be nice to have the lidar ratio for the smoke case, but in this case,  
9 unfortunately, the aircraft altitude was not high enough to allow that. In any case, the broad  
10 characterizations of "dust" and "smoke" that aerosol typing methodologies (like Burton et al.  
11 2012, Gross et al. 2013, etc.) allow would not add much information to these particular cases. The  
12 two dust cases are not really in doubt; there is no other aerosol type in the typing methodologies  
13 with such high 532 nm and 1064 nm particle depolarization ratios (except volcanic ash which is  
14 unlikely in the circumstances). For the smoke case, the identification of smoke is well supported  
15 by back-trajectories, knowledge from satellite data that smoke was blanketing the entire region,  
16 and most importantly, an out-of-the-window visual ID of the smoke plume. Certainly a  
17 measurement of lidar ratio would be extremely interesting from the point of view of expanding  
18 our understanding of aerosol typing methodologies for an unusual case which may indicate  
19 differences between different ages or compositions of smoke, and also for linking 355 nm and 532  
20 nm, which is wanted for future satellite measurements. Unfortunately, that's just not possible in  
21 this case, since we cannot calculate high confidence profiles of extinction and lidar ratio within  
22 the plume. However, we can provide high confidence profiles of particle depolarization ratio at  
23 three wavelengths, since quantities that are the ratio of two channels are not affected by range-  
24 dependence in the overlap region, so that is what we discuss in this manuscript. The reviewer  
25 says both particle depolarization and particle lidar ratio are necessary for aerosol typing studies,  
26 but this is not an aerosol typing study. As the reviewer points out in comments about the  
27 introduction, particle depolarization is an important and relevant field of study even by itself.

28 [Page 24763, Sect. 3.2](#)

29 [Line 17, The AOT of the layer on 8 Feb is just 0.02 at 532 nm, and you can still have good particle  
30 depol ratios? The 1064nm backscatter and the 532-1064nm Angstrom exponent should at least be  
31 rather uncertain. Sakai et al \(Appl. Opt 2010\) found values close to 39% depol for 'pure' coarse-  
32 mode dust. So your results seem to be in agreement with these measurements.](#)

33 The AOT is low because the layer is so shallow, but the scattering is very strong. Total aerosol  
34 scattering ratio at 532 nm is 3.1, higher than the other two cases. This is primarily what drives  
35 the uncertainty. We've added total scattering ratio values in the revised text.

36 [Page 24765, line 22, please mention here also Sakai et al. \(2010\)](#)

37 We added it in the introduction, where we note that particle depolarization depends on the size  
38 of the particles. At this particular spot on page 24765, the text is specifically about spectral  
39 dependence, and since Sakai et al. (2010) measured only at one wavelength, the introduction  
40 seemed more appropriate.

41

42 [Page 24766, last two paragraphs of Sect.3.2:](#)

1 Simulation studies are at all not just trustworthy and should therefore be interpreted with caution  
2 The unknown shape characteristics does not allow proper conclusions from simulations of the  
3 wavelength dependence of particle linear depol ratio.

4 We agree that the results should be used with caution. We don't mean to suggest that the  
5 theoretical results should be used quantitatively, but we think that these calculations can be  
6 reasonably interpreted to suggest that (1) particle depolarization ratio spectral dependence is  
7 broadly sensitive to size and (2) specifically, it is reasonable to suppose that a shift in the  
8 wavelength of the peak of particle depolarization ratio may be an indicator of increasing particle  
9 size. We simplified the discussion of the theoretical papers and tried to make it clear what the  
10 limitations are, and that we are drawing only very general conclusions from them. Here is the  
11 revision for these paragraphs:

12 *Theoretical calculations to date have shown that it is difficult to quantitatively predict the spectral*  
13 *dependence of the particle depolarization ratio for dust (Gasteiger et al., 2011; Wiegner et al., 2009;*  
14 *Gasteiger and Freudenthaler, 2014), due in part to the need for parameterizing the shape of the*  
15 *dust aerosols as spheroids or other simplified shapes.*

16 *In a theoretical treatment of a particular measurement case, Gasteiger et al. (2011) modeled particle*  
17 *depolarization ratio at multiple wavelengths using size distributions and refractive indices*  
18 *appropriate for SAMUM measurements, parameterizing the shapes of dust particles using*  
19 *spheroids. For their reference distribution, the modeled particle depolarization ratio reflects a*  
20 *spectral dependence with a peak in the middle of the wavelength range. Calculated values at 355,*  
21 *532, 710 and 1064 nm were 0.275, 0.306, 0.311, 0.298, consistent with the measurements we report*  
22 *for the Saharan dust-dominated cases from the NASA HSRL-1 and HSRL-2. However, for the*  
23 *dust-dominated cases in the immediate vicinity of North American sources, the measured*  
24 *maximum shifts to longer wavelengths, and there is no longer agreement with the modeled values*  
25 *at 1064 nm.*

26 *Gasteiger et al. (2011) do not show results for size distributions with different size particles, but*  
27 *Gasteiger and Freudenthaer (2014) perform theoretical calculations using spheroids for various*  
28 *size parameters (single particles). These calculations show that the first peak in the spectral*  
29 *depolarization ratio shifts to larger wavelengths as particle size increases. This result, based on*  
30 *highly simplified modeling of dust aerosol, should be used only cautiously, but in general supports*  
31 *the notion that the spectral particle depolarization ratio is sensitive to particle size.*

32  
33

34 Page 24767, Sect 4.:

35 You observed a smoke plume at 8 km, and the aircraft was a bit higher. Then you should have an  
36 impact of the overlap problem on your measurements. Can you exclude such an impact caused  
37 by slightly different beam paths from the telescope to the photomultipliers of the cross and co-  
38 polarized channels. Maybe you made tests at ground and found an almost height –independent  
39 depolarization ratio throughout a well mixed PBL and this down to very small ranges to your  
40 lidar?

1 The incomplete geometric overlap is not expected to affect depolarization measurements. We are  
2 aware of the range dependent effects of a lidar system and agree that this can be an issue if it is  
3 not properly designed or implemented. That is not the case for the system presented here.

4 As noted in the manuscript, the smoke plume is indeed in the overlap region, which extends  
5 approximately 2km below the lidar based our estimates from the extinction calculations when in  
6 clear air. The loss of light in the overlap region occurs when the atmospheric target is in the near  
7 field and the image is focused beyond the field stop such that the cone of unfocused light overfills  
8 the field stop. (Since the system is co-axial, the beam is centered at the field stop even in the near  
9 field.) However, there is no range-dependent overlap effect on the ratio measurements such as  
10 the volume depolarization ratio (ratio of perpendicular and parallel channels) and the total  
11 aerosol scattering ratio (ratio of aerosol and molecular channels), since both channels are equally  
12 affected by loss of light from overfilling the range stop. Furthermore, range-dependent effects in  
13 the detectors are avoided by imaging the entrance pupil of the telescope (not the field stop) onto  
14 the detector, so that the illuminated area on the detector is not range dependent. All the channels  
15 have similar optical designs, including pupil imaging, careful optical design to eliminate clipping,  
16 and detailed characterization of the detectors and electronics. In addition, the instrument includes  
17 an active boresight system to align the incoming beam, and thus all the receiver channels, to the  
18 receiver telescope. These considerations mean that ratios of two channels such as the volume  
19 depolarization ratio or the total aerosol scattering ratio are not range dependent. This can be  
20 checked in cases where the signals are measured in nearly clear air. For example, Figure 5 shows  
21 volume depolarization ratios up to approximately 500 m below the lidar and illustrate that there  
22 is no range dependence near the top of this profile. (The total aerosol scattering ratio which is  
23 not shown also is free of range dependence near the top of the profile). We certainly do not see a  
24 significant increase in the 355 nm volume depolarization ratio near the aircraft. In the smoke case  
25 shown, aircraft was flying at 8970 m and the top of the smoke layer was 1 km below the aircraft.  
26 A range-dependent effect would have to be extreme to see the enhancements in the  
27 depolarization shown in Figure 14. Considering this evidence and the design of the system, we  
28 are confident the depolarization ratio measurements are not impacted by range dependent  
29 effects. To avoid confusion for readers, we added this sentence to the manuscript "Volume  
30 depolarization ratio measurements and total aerosol scattering ratio measurements are ratios of  
31 two channels that are equally affected and therefore have no range-dependent overlap function."  
32

33 I do not believe this value of 25% depol at 355nm when, at the same time, the other wavelengths  
34 show depol ratios below of less than 10 or even less than 3%. There must be something wrong  
35 with the 355 nm signals. Are you sure that the signals were well aligned, no overlap problems.  
36 Such a strong wavelength dependence between 355 and 532 nm has never been observed). And  
37 there are several 355/532nm lidars available now and produced a lot of 355/532 nm depol ratio  
38 observations. Simulation studies do not help because of the always unknown shape  
39 characteristics.

40 We don't share the reviewer's doubts about the good signals for the 355 nm depolarization ratio.  
41 See above for comments about the system, lack of overlap effect on the depolarization ratio, and  
42 auto-boresighting to ensure good alignment.

1 As for the statement that such a strong wavelength dependence between 355 and 532 nm has  
2 never been observed, in fact, we were unable to find any published depolarization measurements  
3 from smoke cases at 355 nm. Rather we found only published measurements of depolarization  
4 from dust at both 355 nm and 532 nm, and published measurements of depolarization from  
5 smoke at 532 nm (some cases with “negligible” depolarization and some with linear particle  
6 depolarization values up to 8% or so in cases with no evidence of entrained dust or higher for  
7 cases that may include some entrained dust or fine mode dust). That is, there are no available  
8 measurements that show this strong wavelength dependence *or any other wavelength dependence*  
9 for smoke. If we missed some papers on this topic, we’d be happy to have them pointed out to  
10 us. In any case, they appear to be rare. We can only speculate on the reasons for the lack of  
11 literature about this. Possibly, like the reviewer believes, it is because smoke simply doesn’t in  
12 any circumstance create a spectral dependence with larger depolarization at 355 nm, but that is  
13 not the only possible explanation or, in our opinion, the most likely one. Based on our own  
14 experience, depolarization is a difficult measurement to make and uncertainties at 355 nm are  
15 larger than at 532 nm, so it may be not surprising that published measurements at 355 nm are  
16 relatively rare. The very fact that reliable three-wavelength observations of depolarization are  
17 uncommon is the motivation for this manuscript. We hope that other groups making two and  
18 three-wavelength measurements of depolarization will publish more measurements of the  
19 spectral dependence of smoke depolarization, because from this first glimpse, it seems that this  
20 is a field of study where there is a lot to learn.

21 The reviewer’s assertion that “There must be something wrong with the 355 nm signals” appears  
22 to be based on expectations extrapolated from a sparse data set, and not on the measurements  
23 and careful assessment of the uncertainties we have presented. This is unfortunate, but we do  
24 believe our measurements and feel that we have presented sufficient information about the  
25 instrument and systematic uncertainties, to allow them to be published.

26 [The layer is about 300m in depth and the AOT was estimated to be 0.05 in the green. So it should  
27 be possible to compute extinction coefficients and lidar ratios for 355 and 532nm. Based on this  
28 optical data set one may be in a better position to discuss this strange observation...](#)

29 As stated in the manuscript, the optical depth was estimated with an assumed lidar ratio. There  
30 is not enough independent information to retrieve a lidar ratio because the overlap prevents a  
31 retrieval of lidar ratio or extinction. However, while we have already agreed that lidar ratio  
32 would provide additional very interesting information, it’s not clear why the lidar ratio would  
33 make the large depolarization in the 355 nm channel more believable to the reviewer. Regardless  
34 of whether the lidar ratio is high or low, the unusual spectral dependence of the particle  
35 depolarization ratio is still unlike anything previously published, which seems to be the  
36 reviewer’s main objection.

37  
38 [Page 24769, line 11-28, please include in this discussion \(soil dust injection during fire  
39 events\) the paper of Nisantzi et al., \(ACP, 2014\).](#)

40 [Nisantzi, A., Mamouri, R. E., Ansmann, A., and Hadjimitsis, D.: Injection of mineral dust into the  
41 free troposphere during fire events observed with polarization lidar at Limassol, Cyprus, Atmos.  
42 Chem. Phys., 14, 12155-12165, doi:10.5194/acp-14-12155-2014, 2014.](#)

1 This is interesting because it offers another different speculation about the cause of depolarization  
2 (at 532 nm) in smoke, which is “fine mode dust”. It’s appropriate to add that alternate explanation  
3 in the manuscript where we discuss different theories about smoke depolarization, and we do so  
4 in the revision. However, the explanation by Nisantzi (2014) is based only on the assertion that  
5 “anthropogenic haze, biomass-burning smoke, and marine particles do not produce strong  
6 depolarization of backscattered light” for which they reference five lidar papers, four of which  
7 do not show any measurements of unmixed biomass burning smoke (three of them concern  
8 SAMUM measurements where a significant amount of desert dust, including coarse mode, was  
9 considered to be mixed with the smoke). Gross et al. (2012) includes aged biomass burning  
10 aerosol with linear particle depolarization ratios of  $7\pm 2\%$  which is not insignificant. It seems to  
11 be just a rule-of-thumb that is not supported by enough evidence to warrant it being taken as  
12 evidence itself. We don’t debate that dust can be entrained in smoke and affect the  
13 depolarization; we quote Fiebig et al. (2002) who presents a fairly compelling case which includes  
14 coincident chemical analysis. However, we also believe that it can also occur that biomass  
15 burning aerosol can exhibit depolarization of backscattered light without necessarily having a  
16 dust component, like the observations of Murayama (2004) who observed depolarization at 532  
17 nm but a chemical analysis of the plume showed no mineral content (incidentally, Nisantzi et al.  
18 (2014) also reference this case but for some reason discount the chemical analysis and claim that  
19 this case also includes fine mode dust.) The lab measurements of dust by Sakai et al. are well  
20 done and show that fine mode dust can cause depolarization, but not that it actually causes the  
21 observed depolarization in any particular atmospheric observation. The Kahnert et al. (2012)  
22 modeling study discussed in this manuscript demonstrates that there is at least one more possible  
23 explanation: smoke particles themselves can cause depolarization.

24 [Page 24770, simulations: All the simulations with a spheroidal dust shape model are not](#)  
25 [trustworthy. The results must be handled with care. Especially the spectral dependence of the](#)  
26 [depol ratio is rather erroneous.](#)

27 We cut out most of this paragraph and left only this:

28 *Referring back to the theoretical calculations of spectral depolarization for spheroids discussed in*  
29 *Section 3.c., the larger particle depolarization ratio at 355 nm compared to longer wavelengths may*  
30 *indicate a smaller size for the non-spherical particles than the dust cases, although of course these*  
31 *results may be only qualitatively applicable to more general particle shapes.*

32 [Page 24771, I am not a friend of speculations as given on this page. Figure 15 is simply useless. I](#)  
33 [would just remove all this, but leave it open to the authors what to do with this strange case study](#)  
34 [and all the simulation-based discussions.](#)

35 The reviewer appears to generally disapprove of current modelling efforts to interpreting lidar  
36 observations, which is perhaps a somewhat extreme point of view. We believe that  
37 intercomparisons of observations and theoretical studies are useful and necessary. On the one  
38 hand, measurements are indispensable for guiding the development of models. So at the very  
39 least, Figure 15 contains useful information for model developers. On the other hand, models are  
40 needed in all Bayesian retrieval algorithms to invert observations. We do agree with the reviewer  
41 that all modelling studies face great challenges related to the large variability of particle  
42 morphologies. We also share his reservations about the use of over-simplified particle models for

1 interpreting depolarization measurements. The model we use for intercomparison in the smoke  
2 case is based on a morphologically sophisticated particle model. Its main weakness is that we  
3 cannot assume that the morphological parameters used in the model apply to our case study - a  
4 point that we clearly pointed out in the text. Given this uncertainty, Figure 15 is a comparison of  
5 the current state-of-the-art in measurement technology and modelling capabilities. It illustrates  
6 the level of consistency and discrepancies that we can presently expect from comparing  
7 observations and model calculations of depolarization. As we understand the reviewer, it is not  
8 a requirement that we remove the figure. We therefore decided, for the reasons stated above, that  
9 we would like to keep it.

10 Sect. 5, Summary, second half of this Sect. 5: You make a dangerous conclusion concerning the  
11 355 nm depolarization ratio (EarthCARE) . When looking into the literature (for example  
12 Illingworth, 2015, depol vs lidar ratio figure) then there is no doubt that 355 nm depol  
13 observations can indeed be used for aerosol typing. Dangerous means here: Your statement is  
14 based on the fact that you only observed depol values from 20-25% at 355 nm with your HSRL,  
15 disregarding what type of aerosol was present. So these measurements are at least to some extent  
16 questionable (at least for me) so that such severe conclusions are not justified, ... is my opinion.  
17 Sure if this is found by many groups in future, yes then we have to change our mind, but at the  
18 moment, one should better leave out such statement regarding EarthCARE.

19  
20 The reviewer has read a more definitely negative tone in our remark than what was intended.  
21 We don't suggest that our observations negate any of the observations in the Illingworth (2015)  
22 figure. But any such figure (including the ones for 532 nm and 1064 nm measurements from  
23 HSRL-1 in Burton et al. 2012, our own paper) include only specific datasets and, so far, none of  
24 these datasets are global and can't be taken to be all-inclusive. We don't suggest that all smoke  
25 observations will have a wavelength dependence of the particle depolarization ratio similar to  
26 this case that we observe, just that the existence of at least one such case brings up the possibility  
27 that there may be aerosol types or subtypes that aren't captured in these figures, or that some of  
28 the distributions may be broader than what is shown in these figures. Note that there are two  
29 smoke types shown in Illingworth (2015) Figure 8. "Smoke" is shown to have linear particle  
30 depolarization ratio approximately from 0-5% and "Aged boreal biomass burning" is shown to  
31 have linear particle depolarization ratio of approximately 7-13% for the cases shown. We know  
32 nothing about the depolarizing biomass burning cases except that they were observed in Leipzig,  
33 from the caption, since there is no publication listed for them; in particular, we do not know the  
34 wavelength dependence, since the 532 nm and 1064 nm particle depolarization isn't shown.  
35 Could it be that aged biomass burning aerosol of a different age, composition, or combustion type  
36 observed on another continent or possibly in different meteorological conditions (temperature,  
37 relative humidity) may have different intensive parameters? We believe that our measurements  
38 show that it can happen, but we do not know what circumstances drive it or how frequent this  
39 occurrence is. The language in the manuscript was actually fairly soft, saying, "if this is not an  
40 isolated case ... the EarthCARE satellite *may* observe significant particle depolarization in *some*  
41 *types* of smoke as well as in dust." This is such a provisional statement that it seems that the only  
42 basis for disagreement with it is that the reviewer disregards the possibility that our observations  
43 are valid, or perhaps does not believe that this layer was actually smoke. As we said above, we

1 believe our measurements are valid and we have carefully described potential sources of  
2 systematic error and characterized the uncertainties to show evidence for the validity of our  
3 measurements. Also, we have no reason to think this observation was anything other than smoke.  
4 Given that, we think it is worth calling attention to the potential implications of this observation.  
5 Note that our first discussed implication was not even remotely a criticism. Rather we are  
6 enthusiastic about the prospect of obtaining global measurements of smoke depolarization in  
7 many different circumstances from EarthCARE, which will hopefully help to sort out what  
8 circumstances control the incidence of high depolarization ratio values at 355 nm. However, we  
9 still do wish to point out the other potential implication, that values of particle depolarization  
10 ratio near 20-25% at 355 nm may be more ambiguous than similar values at 532 nm are, in terms  
11 of the aerosol classification. We are willing to revise the final paragraph to repeat the caveats  
12 again to try to avoid offense, however. Here is the new wording:

13 *“On the other hand, the third case study presented here showed that smoke particle depolarization*  
14 *ratio can be significantly larger at 355 nm than at 532 nm, and in fact the particle depolarization*  
15 *ratio at 355 nm for this smoke case was quite comparable to the dust-dominated cases. If this is not*  
16 *an isolated case, and this signature proves typical for some subsets of smoke aerosol in particular*  
17 *conditions, the EarthCARE satellite may observe significant particle depolarization in some types*  
18 *of smoke as well as in dust-dominated aerosol. If this is the case, global observations of smoke*  
19 *depolarization will present an exciting opportunity for improving our understanding of the optical*  
20 *properties of smoke and how they change with age and processing; however, it will also present a*  
21 *challenge. That is, a significant particle depolarization ratio signature at the single wavelength of*  
22 *532 nm has been sufficient for distinguishing dust-dominated aerosol from smoke aerosol, but at*  
23 *355 nm this signature by itself is more ambiguous, if the smoke case presented here is not an isolated*  
24 *case. EarthCARE will also measure lidar ratio at 355 nm; this is related to absorption but has*  
25 *significant variability for smoke (Groß et al., 2014). EarthCARE will not have backscatter or*  
26 *extinction measurements at a second wavelength to give an indicator of particle size. Therefore, for*  
27 *any cases where particle depolarization ratio is ambiguous, smoke and dust may not be easily*  
28 *separable.”*

29 Furthermore, to try to meet the reviewer halfway, we changed the abstract so that EarthCARE is  
30 not mentioned specifically, saying only *“We note that in these specific case studies, the linear particle*  
31 *depolarization ratio for smoke and dust-dominated aerosol are more similar at 355 nm than at 532 nm,*  
32 *having possible implications for using particle depolarization ratio at a single wavelength for aerosol*  
33 *typing.”*

34 [This brings me to the question: Did you ever observe particle depolarization ratios \(in aerosol  
35 layers\) at 355 nm clearly below 10%?](#)

36 Yes, of course. For example, see the same case study, but at lower altitudes. Figure 14 shows  
37 linear particle depolarization ratio of approximately 1% for most of the boundary layer and the  
38 residual layer. Figure 4 shows another example. On 13 July 2014, the upper layer (altitude above  
39 approximately 3.5 km) has 355 nm linear particle depolarization ratio of 4-7%.

40 [Final remark: Appenix, Page 24776. line 14 Do you observe any wavelength dependence in the  
41 ellipticity angle? If yes, please provide the numbers for the different wavelengths.](#)

1 Yes, this was partially left out of the manuscript and was confusing. The revision says, *“we have*  
2 *historically measured minimum depolarization ratios in clear air that exceed the theoretical value, namely*  
3 *values of approximately 0.006 in the 355 nm channel, approximately 0.008 in the 1064 nm channel, and*  
4 *0.0085-0.0135 in the 532 nm channel.”*

5

6 Table 1: Lidar ratios at 355 and 532 nm in addition would be fine.

7 Figure 3: There is space to the right... for two more color plots (355nm and 532nm lidar ratios). At  
8 least for this excellent dust observation, we need to bring together all the information, we have  
9 and on which all the aerosol-typing papers are based on. As mentioned I would like to have an  
10 additional four-panel figure: height profiles of backscatter (three wavelengths), extinction (two  
11 wavelengths), lidar ratio (two wavelengths), depolarization ratio (three wavelengths).

12 See above. We cannot derive lidar ratios for the smoke case and, given that, we prefer not to  
13 include them for the dust cases either. Lidar ratio for dust is a popular field and it would require  
14 a significant amount of work, probably a whole separate paper, to do that topic justice. We feel  
15 it would add significantly to the amount of analysis we would have to present in this paper, both  
16 to describe the measurement technique to a degree of detail consistent with the depolarization  
17 instrument characterization, and also to discuss comparisons with prior published measurements  
18 of dust lidar ratio. We chose to focus on the spectral depolarization of dust for this paper and we  
19 feel that other measurements are outside the scope of the current manuscript.

20 Figure 10: smoke is practically invisible, can you use arrows or something else to point to the  
21 smoke fields...?

22 There is a lot of smoke in the image and a circle around the smoke field would encompass a third  
23 or so of the image so perhaps not be so useful. It is a little difficult to distinguish the gray smoke  
24 from the white clouds at first, though. We added these few sentences to the caption to try to help  
25 the reader visually lock onto the smoke: “The bright white is clouds and snow cover and the gray  
26 is smoke. Several distinct smoke plumes indicate sources in the U.S. Pacific Northwest and in  
27 Western Canada within the cloud-free area on the western part of the continent. Significant smoke  
28 layers from these fires blanket the mid-continent cloud-free areas in the northern portion of the  
29 image. The HSRL-2 measurements are close to the southern edge of the extensive smoke field.

30 Figure 13: I am still wondering what the reason for the strange observation is ? Overload in the  
31 co-polarized 355nm channel, could be an explanation?

32 We checked for saturation effects in this case and found no evidence that either channel is  
33 saturated.

34 All in all, the paper is very good and it was fun to study it! I know the group and know that the  
35 lidar is excellent, and the data analysis is carefully done by an experienced scientist (professional).  
36 So my comments are just to trigger to re-think and to re-check some of the results and to keep the  
37 discussion on the very safe side ....

38

## 1 Response to Referee #2

2 Response to Anonymous Referee #2 on the manuscript "Observations of the spectral dependence  
3 of particle depolarization ratio of aerosols using NASA Langley airborne High Spectral  
4 Resolution Lidar".

5 Thank you for your supportive and helpful comments. Responses to the specific comments can  
6 be found below. Reviewer comments are in blue and author responses are in black.

7 The discussion paper of Burton et al. presents very interesting measurements of the  
8 linear depolarization ratio at three wavelengths for cases with long-range transported  
9 Saharan aerosols, with locally-generated desert aerosols, and with transported smoke  
10 aerosols. The measured data is discussed in context of existing literature. The paper  
11 is well-structured and overall well-written. It is a valuable contribution and should be  
12 published in ACP after some minor corrections.

13 1) For someone starting to read this paper, it remains unclear for a long time which  
14 depolarization ratio (linear or circular?) is meant. Please explicitly write "linear depolarization  
15 ratio" in the title, the abstract, the main text (at least once per section), and  
16 the figure captions.

17 We will revise the manuscript to say "linear particle depolarization ratio" in the title, abstract,  
18 and body text.

19 2) The abstract (p24753 l18) says "... is inferred to be ...": In my view, "coated soot aggregates"  
20 are one possible explanation for the smoke measurements, but there are certainly  
21 other types of soot-like particles that would explain these measurements. Thus,  
22 I suggest to write "... can be explained ..." or something similar.

23 We have no objection to making the suggested change in the abstract. As a side note, we would  
24 be interested to learn more specifics about the other explanations the reviewer has in mind,  
25 perhaps in another comment in this discussion forum. This manuscript is part of a learning  
26 process for us and we are very open to learning more about possible explanations for  
27 depolarization in smoke measurements.

28 3) Eq. 2: The definition of  $\beta_{\text{parallel}}$  and  $\beta_{\text{perpendicular}}$  is unclear. The text  
29 calls them "signal", but  $\beta$  usually is the backscatter coefficient.

30 Agreed. As Gimmetstad (2008) points out, adding parallel and perpendicular subscripts for the  
31 backscatter coefficient is imprecise since that notation mixes an atmospheric parameter  
32 (backscatter) with instrument-specific factors. In the manuscript, we were really just looking for  
33 a way for readers to see in a glance which of two frequently-used ratios we use. However,  
34 Equation 1 does this in a more correct way. We will simply delete the middle portion of the  
35 double-equality in Equation 2.

36 4) Fig. 4 at about 150km distance on track and 4km altitude: The linear depolarization  
37 ratio increases from  $<0.1$  at 355nm to  $\sim 0.2$  at 532nm and  $\sim 0.25$  at 1064nm. As this  
38 wavelength dependence is quite uncommon, I wonder if these numbers are real aerosol  
39 properties or just a measurement artefact. Can you comment on this?

40 It's somewhat difficult to see on the curtain plots, but the local maximum of the depolarization at  
41 that location corresponds to a local minimum in the aerosol backscatter coefficient (conversely,  
42 the peak in backscattering is at an altitude just below the quoted linear depolarization ratios and  
43 this backscatter peak corresponds to a local minimum in depolarization values). The total

1 scattering ratio (R in the manuscript) at 532 nm is about 1.4 at that spot. The estimated systematic  
2 error (at 532 nm) is therefore approximately 17% relative error. Taking these into account, I  
3 would say that there is non-zero depolarization at 532 nm and 1064 nm and that the values at  
4 these wavelengths exceed the 355 nm value (indicating perhaps some coarse-mode dust aerosol)  
5 but that the relatively low backscatter in that thin layer precludes drawing a conclusion about  
6 whether the spectral dependence definitely increases between 532 nm and 1064 nm or not.

7 5) "pure dust", "pure Saharan dust" in several places of the paper: Though these terms  
8 have been used in the literature, they are, strictly speaking, wrong. Dust particles  
9 are solid particles, but desert aerosols usually contain also a non-negligible number  
10 of small spherical particles that are no dust particles. This was shown in measurements  
11 during field campaigns, for example SAMUM. The "desert mixture" of the aerosol  
12 database OPAC also contains small spherical particles. They are very important for the  
13 depolarization ratio at 355nm and thus the spectral dependence of the depolarization  
14 ratio. The spectral dependence of the depolarization ratio presented in Sect. 3 shows  
15 that such non-dust particles were present in both measured "dust" cases. Thus, I suggest  
16 to write "pure desert aerosol", "pure Saharan aerosol", "dust-containing aerosol",  
17 or something similar, but not "pure dust".

18 We will make that change in the manuscript.

19 6) More generally, I like to encourage the authors to replace "dust", where appropriate,  
20 by "desert aerosol", "Saharan aerosol", "dust-containing aerosol", "dust-dominated  
21 aerosol", etc., throughout the paper, to take into account that the measured aerosols  
22 contain also non-dust particles as discussed in comment 5. I admit that this is not  
23 always considered in the literature, nonetheless the suggested naming would be more  
24 precise.

25 We will support the effort to introduce more precise descriptions of dust-dominated aerosol by  
26 making this change in the manuscript as well.

27 7) p24767 l16ff.: Does the incomplete geometrical overlap not increase the uncertainties  
28 of the depolarization measurements?

29 The depolarization measurement is made as a ratio of two channels, which are affected the same  
30 way by the incomplete geometrical overlap, so therefore there is no increase in uncertainty, except  
31 through a decrease in signal strength. That is, since the amount of light reaching the detectors for  
32 both channels is reduced, there can be an increase in the amount of noise relative to the signal;  
33 however, for the smoke plume featured here, the amount of scattering was quite high and loss of  
34 signal is not a concern.

35 8) p24770 l24 and Fig. 15: Please mention how the size of the soot aggregates is  
36 defined? Volume-equivalent, maximum dimension, or?

37 Volume-equivalent particle radius. We will put this description in the caption to Fig 15 and the  
38 main text.

39 I find the technical details of the system and the error analysis well-described. However,  
40 since I am not so familiar with all the effects that can happen in the optics and the  
41 electronics of such an advanced lidar system, I hope that other reviewers are more  
42 familiar with this topic.

43  
44 Technical corrections:

45 A) p24756 l8: "6-km" -> "6 km" Corrected in the revision

- 1 B) p24762 l18: "The particle depolarization spectral dependence..." -> "The spectral
- 2 dependence of the particle depolarization ..." Changed in the revision
- 3 C) Fig. 3 caption: "Aerosol backscatter and extinction curtains ..." -> "Curtains of
- 4 aerosol backscatter and extinction coefficients ..." Changed in the revision
- 5 D) Fig. 6 and 12 caption: "backscatter" -> "backscatter coefficient" Corrected in the revision
- 6

1 **Response to Referee #3**

2 Response to Anonymous Referee #3 on the manuscript “Observations of the spectral  
3 dependence of particle depolarization ratio of aerosols using NASA Langley airborne High  
4 Spectral Resolution Lidar”.

5 We're pleased that the reviewer seems to very interested in our instrument and put so much  
6 effort into carefully reading our manuscript. However, some of the suggestions seem to be  
7 driving towards corrections or improvements that are quite small compared to the estimated  
8 error bars, and would not affect our conclusions. We feel that this is a very carefully  
9 designed and well calibrated instrument which it would be difficult to improve significantly at  
10 this time. However, any instrument will have potential sources of systematic error, and it  
11 may be quite difficult to assess them, the more so for a well-calibrated instrument where the  
12 remaining sources are subtle. We reiterate that this paper is primarily about the  
13 measurement case studies and the primary purpose of the discussion of systematic error  
14 sources and estimation of systematic uncertainty is to demonstrate that the measurements  
15 are accurate enough to support the conclusions we draw about them in the manuscript. It  
16 may be possible to refine some of estimates of component systematic uncertainties further  
17 with some future work, but this is out of the scope of the paper. All that being said, we  
18 certainly appreciate that many of these comments have helped us improve the exactness of  
19 our written descriptions.

20 Responses to specific comments can be found below. Reviewer comments are in blue and  
21 author responses are in black (manuscript text in italics)

22 *The paper is well written, well suited for ACP. The measurement cases are well described and  
23 put into relation with other measurements and model results. Although the title of the paper  
24 emphasizes the three reported measurement cases of the linear depolarization ratio of  
25 aerosols, the part describing the instrument, its errors and the error calculation seems to be the  
26 more important of this paper, because it will serve as the reference for future papers about the  
27 depolarisation measurements with this instrument. I propose to publish the paper under  
28 consideration of following remarks concerning the description of the system set-up and the  
29 error calculations.*

30 **Chap. 2 Instrument description and measurement methodology**

31 *Because measurements of the linear depolarization ratio with the HSRL-1 and HSRL-2  
32 are directly compared, the set-up differences between both instruments, in case they exist,  
33 should be explicitly mentioned, which could be relevant for the measurement of the  
34 linear depolarization ratio.*

35 We will add text similar to this in the revised manuscript: *“For measurements at 532 nm and  
36 1064 nm, HSRL-2 is identical to HSRL-1. HSRL measurements of extinction and backscatter at  
37 355 nm are made using an interferometer rather than an iodine filter. For 355 nm  
38 measurements of depolarization discussed here, the setup is very similar to the other  
39 channels; the small differences are explained in section 2a.”* Those differences between the  
40 355 nm and 532 nm depolarization measurements are already discussed in the first version of  
41 the manuscript.

42

1 **Page 24757 Line 2**

2 *The polarization axis of the outgoing light is matched to that of the receiver with an approach*  
3 *similar to that outlined by Alvarez et al. (2006) using seven fixed polarization angles between*  
4  *$\pm 45^\circ$ , using the half-wave calibration wave plates indicated in Fig. 1.*

5 How accurate can the offset angle between the outgoing polarization and the receiver be  
6 determined? This should be determinable from the uncertainty of the fit of the Alvarez-  
7 calibration with the seven polarization angles. It is conjecturable that the offset angle  
8 changes during a flight and between different flights due to thermal and pressure  
9 influences e.g. on the birefringence of the exit window, wherefore I would not average  
10 between different calibrations, especially not for a conservative error estimate (further  
11 discussion about the systematic error below).

12 The fit of the Alvarez calibration with seven polarization angles is typically excellent, with  
13 chi-squared values  $>99\%$ . An example can be seen below. It is a non-linear fit and we have  
14 not explicitly calculated the errors in angle or the other parameters from this fit. We  
15 acknowledge that there is a potential for the offset angle to change during a flight or  
16 between flights, which is why we have specifically examined the change in offset angle during  
17 flight when two or more calibrations could be made during a flight. We do not average  
18 between calibrations, and only look at this change in order to assess the uncertainty. We  
19 conclude that the angle is good to within 0.4 degrees over the course of a flight, as stated in  
20 the text.

21 **Page 24757 Line 5**

22 *Following the alignment, the gain ratio between the cross-polarized and co-polarized channels is*  
23 *routinely determined in flight by rotating the transmitted polarization  $45^\circ$  relative to the receiver,*  
24 *...*

25 How accurate can the  $45^\circ$  angle be adjusted with respect to the receiver?

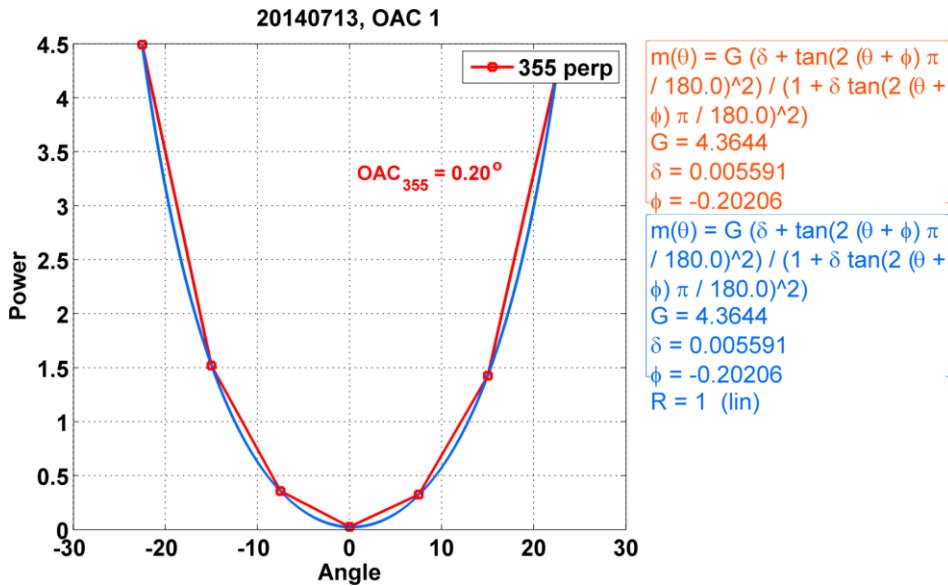
26  
27 I guess that the precision is high by means of position encoders or similar. But what about  
28 the absolute accuracy? As shown by Freudenthaler et al. (2009), the high precision of the  
29 angular positioning can be used to achieve a high accuracy for the polarization calibration  
30 by means of the  $\pm 45^\circ$  calibration regardless of the polarization offset angle. This could  
31 easily be done with the two of the seven calibration positions which are exactly  $90^\circ$  apart.  
32

33 As an example, Fig.1 below shows the calibration factor (with  $I_c / I_p = I_{\text{cross}} / I_{\text{parallel}}$ )  
34 with assumed electronic gain ratio = 1, calculated with Eqs. (1), (A1), and (A2) of this  
35 paper for  $\delta_{\text{tot}} = 0.1$ , a polarization ellipticity angle  $\theta = 5^\circ$ , and a polarization offset angle  
36 offset =  $-2^\circ$ . The red marks show the seven measurements at nominal positions  $\psi$  as used  
37 by the authors of this paper, and the large error of the calibration factor at  $+45^\circ$  or  $-45^\circ$   
38 positions. The green line shows the calibration factors calculated with the square root of  
39 the geometric mean of measurement pairs of the blue line which are  $90^\circ$  apart (e.g.  $-60^\circ$   
40 and  $+30^\circ$ ).

1 ...

2 It would be very helpful for the readers if such a calibration measurement (with statistical  
3 and systematic error bars) could be shown in the paper.

4  
5 Yes, the 7 angle fit does indeed give another estimate of the gain ratio which is another one  
6 of the parameters obtained in the non-linear fit. Here is an example of the 7-angle  
7 calibration from one of the flights highlighted in the paper. The red dots indicate the  
8 measured ratios and the blue curve indicates the fitted curve. The chi-squared goodness-of-  
9 fit statistic for this non-linear fit is typically >99%, computed by doing a regression on the  
10 relationship between the measured ratios and the fitted ratios.



11

12

13 The equation for the curve is Equation 10 from Alvarez et al.

14

$$m_j = G \left\{ \frac{(\delta + \tan^2[2(\theta + \varphi_j)])}{1 + \delta \tan^2[2(\theta + \varphi_j)]} \right\}$$

15 Where  $m_j$  are the measured ratios for each of the 7 angles,  $\varphi_j$ , and the parameters to be fit  
16 are  $\theta$ , the offset angle; G, the gain ratio; and  $\delta$ , the minimum depolarization value. This  
17 fitted gain ratio could reasonably be used as the inferred gain ratio without the need to do a  
18 subsequent gain ratio calibration, as the reviewer suggests. These two estimates are  
19 consistent (in this case agreeing to within less than 1%), supporting the use of the 45°  
20 calibration results.

1 Both calibration procedures (the 7 angle calibration and the single-angle 45° calibration)  
2 require the atmosphere to be stable, and the 45° calibration can of course be done more  
3 quickly. So, generally we are able to perform more 45° calibrations during the course of a  
4 flight. Since the system parameters may change during flight (due to environmental factors  
5 such as temperature changes), we use the polarization gain ratio calculated during the 45°  
6 calibration. The reviewer has a good point that we may have sufficient time to do the  
7 calibration at both  $\pm 45^\circ$  even if there is not time for a full 7 angle calibration, but historically  
8 we haven't done this.

9 The reviewer will notice that the values of the ratios at  $\pm 45^\circ$  are not equal. However, please  
10 note that after the 7 angle calibration, the waveplate is rotated to the zero-point that is  
11 inferred from the center of the 7 angle fit. The 45° adjustment for the subsequent  
12 polarization gain ratio calibration is done with respect to this new, improved angle, and so  
13 should have a smaller error. If there was an error such that the adjustment of the wave plate  
14 angle is inaccurate or that it changes during flight, it would be evident when the next  
15 polarization angle calibration (i.e. the 7-angle calibration) is performed later in the flight.  
16 That's why we use the change during flight to estimate the uncertainties.

17 **Page 24757 Line 28**

18 *The polarization extinction ratio measured in the system is 300 : 1 ....*

19 The extinction ratio is the ratio of the transmission of the unwanted component to the  
20 wanted component. It is defined like that, e.g., by Tompkins and Irene (2005), by Bennett  
21 (2009) in OSA's Handbook of Optics, and Goldstein (2003) writes in Chap. 26.2.1: "The  
22 extinction ratio should be a small number and the transmittance ratio a large number; if  
23 this is not the case, the term at hand is being misused." Unfortunately, searching the  
24 literature, I find "misuse" by the larger part.

25 We have changed it to "transmittance ratio" in the revised manuscript.

26 **Page 24757 Line 28**

27 *The co-polarized signal and cross-polarized signal are used to determine total depolarization.*

28 Although for an insider it is clear from the instrument description what is meant with  
29 total depolarization, the correct naming for the measured quantities are linear  
30 depolarization ratio and volume (or total) linear depolarization ratio, etc.. This is  
31 important, because some lidar systems measure the circular depolarization ratio, and it  
32 should be at least mentioned once at the begin of the paper before proceeding with the  
33 short-cuts.

34 Agreed. We have inserted "linear" in the revised version of the manuscript in the title,  
35 abstract, and at several places in the text.

36 **Page 24758 Line 12**

37 *The separation of the aerosol and molecular signals is the basis of the HSRL technique for*  
38 *extinction and backscatter retrieval. Since it is also relevant to the systematic error in particle*  
39 *depolarization ratio, it will be discussed again in Sect. 2.2, below.*

1 The discussion of the errors of the backscatter ratio and its influence on the error of the  
2 linear depolarization ratio are described not sufficiently. Page 24758 Line 15 refers to Sect.  
3 2.2, which refers to the appendix, but there just a value for the error is given and little  
4 explained. In Hair et al. (2008) Chap. 7 a detailed error analysis was promised in a  
5 following paper: *An analysis of the systematic errors for all data products from the airborne*  
6 *HSRL is beyond the scope of this paper. A manuscript focused on a complete error analysis and*  
7 *validation of extinction measurements is currently in preparation.*

8 I couldn't find this paper.

9 It's true there's just a number in Section 2.2; both references should direct the reader to the  
10 Appendix, where the number is explained. That has been changed in the revision. In the  
11 Appendix, there are already several paragraphs of discussion about the potential sources of  
12 error in the total aerosol scattering ratio (i.e. backscatter ratio) including how the calibration  
13 factor (aerosol-to-molecular gain ratio) is assessed, how we estimated the uncertainty in the  
14 aerosol-to-molecular gain ratio, and how this propagates to uncertainty in the particle  
15 depolarization ratio. This information is sufficient for quantifying the uncertainty in the 355  
16 nm depolarization ratio. We're not sure what else is wanted.

17 Likewise, we're not sure what's considered to be missing from Hair et al. 2008. That paper  
18 has very detailed information about the HSRL-1 instrument, calibration procedures, and  
19 random and systematic errors. It has served well as a useful and sufficient instrument  
20 description paper. What it didn't contain was much validation, but HSRL-1 measurements  
21 were subsequently validated in a paper by Rogers et al. [2009] in this journal. The current  
22 manuscript is not meant to be a further follow-on to Hair et al. [2008] and is not primarily  
23 meant as an instrument description paper. We consider the descriptions of the instrument in  
24 this manuscript to be sufficient to support and explain the measurements we are highlighting.

#### 25 **Page 24759 Line 21**

26 Different names are used for the same thing, e.g. volume depolarization, total  
27 depolarization, volume depolarization ratio, which is confusing. Please decide for only  
28 one short-cut (see comment above Page 24757 Line 28) throughout the paper.

29 Similar: there are several calibrations: polarization angle calibration, backscatter gain  
30 ratio calibration, depolarization gain ratio calibration, etc.. Please use unique names and  
31 only one for the same in the whole paper, and always use the full unique name.

32 Similar: fractional error = relative error?

33 We revised the manuscript to have only one term per concept and remove most synonyms and  
34 shortcuts. We are using "relative uncertainty", "volume depolarization ratio", "particle  
35 depolarization ratio", "polarization angle calibration", "polarization gain ratio calibration",  
36 "aerosol-to-molecular gain ratio", and "total aerosol scattering ratio".

#### 37 **Page 24760 Line 2**

38 ... we estimate a reasonable upper bound on the systematic error in the volume depolarization ratio  
39 measurement to be 4.7 % (fractional error) in the 355 nm channel, the larger of 5 % fractional  
40 error or 0.007 absolute error in the 532 nm channel, and the larger of 2.6 % fractional error or  
41 0.007 absolute error in the 1064 nm channel.

1 **Why is there no absolute error (offset) at 355 nm?**

2 The absolute portion is for the uncertainty due to cross-talk that results in an offset of the  
3 observed clear air depolarization, reduced for a partial correction we applied (explained in  
4 the text and see also below). The observed offset for 355 nm is much smaller than for the  
5 other channels, so we initially didn't include it, but the reviewer is right: it is more consistent  
6 if we include it. We also realized the text was unclear about how the different channels are  
7 affected. Adding the component to 355 makes only a small change in the uncertainty, and  
8 only where the particle depolarization ratio is small. Only the lower layer (below the smoke  
9 layer) in Figure 14 is affected with now slightly larger error bars; none of the other figures or  
10 tables are affected. We will replace figure 14 in the revision. We also clarify the text like  
11 this: "*Since 2006, we have historically measured minimum depolarization ratios in clear air  
12 that exceed the theoretical value, namely values of approximately 0.006 in the 355 nm  
13 channel, approximately 0.008 in the 1064 nm channel, and 0.0085-0.0135 in the 532 nm  
14 channel, .... An ellipticity angle of  $5.8^\circ$  ( $\chi=0.980$ ) would explain the error in the  
15 depolarization ratio at 532 nm where the error is largest.... Taking the partial correction into  
16 account, we include a component of 0.007 (absolute) due to cross-talk in the estimated  
17 volume depolarization ratio error for the 532 nm and 1064 nm channels and 0.001 (absolute)  
18 for the 355 nm channel.*"

19

20 **Page 24760 Line 13**

21 *... the molecular depolarization arises only from the central Cabannes line and is very well  
22 characterized, with a value of 0.0036...*

23 **The molecular (air) linear depolarization ratio is wavelength dependent and actually  
24 0.003946 at 355 nm, 0.003656 at 532 nm, and 0.003524 at 1064 nm. (Own calculations for  
25 air with 385 ppmv CO<sub>2</sub> and 0% RH).**

26 Thanks for the additional information. This is a very small difference that does not affect the  
27 results in the manuscript. We feel that we cannot quote these values in the manuscript  
28 because we don't know of an appropriate way to reference unpublished communication from  
29 an anonymous source. However, we changed the text to more precisely reflect the  
30 provenance and limitations of the calculation we use: "the molecular depolarization ratio is  
31 temperature independent and is calculated to be 0.0036 using N<sub>2</sub> and O<sub>2</sub> molecules (ignoring a  
32 negligible wavelength dependence due to non-linear molecules like CO<sub>2</sub>) (Behrendt and  
33 Nakamura, 2002)".

34 **Page 24760 Line 14**

35 *More critically important is a potential systematic error in the total scattering gain(?) ratio. We  
36 estimate the effective upper bound of this error to be 4.1 % in the 532 nm channel from an analysis  
37 of the stability of the gain (?) ratio;...*

38 **Stability (precision) is not accuracy. Furthermore, how is the error of the of the total  
39 scattering ratio determined?**

40 The excerpt was correct as originally written, although we have clarified the revision by using  
41 the full names "total aerosol scattering ratio" and "aerosol-to-molecular gain ratio". What we  
42 are saying is that the uncertainty in the aerosol-to-molecular gain ratio gives the uncertainty  
43 in the total aerosol scattering ratio (the quantities are linearly related, so the relative

1 uncertainties are the same). The aerosol-to-molecular gain ratio is calculated either by  
2 direct calibration (for 532 nm) or by transfer of the calibration from 532 nm to the other  
3 channels (discussed in the text). The calibration is performed one to three times during a  
4 flight, but not continuously. The difference between precision and accuracy for the 532 nm  
5 case would occur only if there was some mechanism that would cause the gain ratio to  
6 consistently be measured incorrectly during calibration. We know of no such mechanism;  
7 however, it is possible for the gains to change in flight, so the change in the measured gain  
8 ratio during a flight really is our best estimate of the uncertainty in the 532 nm aerosol-to-  
9 molecular gain ratio. The calibration transfer to the 355 nm and 1064 nm channels might  
10 conceivably result in a consistent bias, so we estimated the size of such a (potential) bias and  
11 used that to increase the calculated uncertainty for those channels, as discussed in the  
12 original manuscript.

13 **Page 24760 Line 21**

14 *The estimates given above are intended to be a conservative upper bound on the systematic errors.*  
15 *The systematic errors on the three quantities,  $\delta_{mol}$ ,  $\delta_{tot}$ , and  $R$ , are combined in quadrature*  
16 *using standard propagation of errors for independent variables, as described in the Appendix.*  
17 I do not agree, that this "standard" propagation of errors is the right one for the systematic  
18 errors mentioned here (see discussion Systematic errors below).  
19 Response below.

20 **Page 24762 Line 8**

21 *For that case, the particle depolarization ratios at 532 and 1064 nm are  $0.33 \pm 0.02$  (standard*  
22 *deviation) ...*

23 What does "standard deviation" mean here? Probably the propagated error due to  
24 (random) signal noise is meant (see discussion Systematic errors below).

25 This wasn't meant to be a systematic uncertainty. It's the standard deviation of a sample  
26 measurements immediately around the quoted measurement. It is described fully in the  
27 caption to Table 1 "samples were taken at specific times and altitudes comprising 400-4500  
28 distinct measurement points ... the values are reported as median plus-or-minus standard  
29 deviation for the sample." Also in the text on page 24761 line 19 (of the discussion  
30 manuscript), it says "standard deviation for the sample". After that first usage, we shortened  
31 it for readability.

32 **Figure 14**

33 *The x-scales could be adjusted for each wavelength to make the data better visible.*  
34 We feel that the full range is needed to capture the large values in the smoke plume at 355  
35 nm.

36 **Page 24776 Line 20**

37 *The calibration procedure has been carefully designed and used successfully on both the HSRL-1*  
38 *and HSRL-2 systems since 2006, and the stability of the offset angle is high. Changes indicated*  
39 *during calibrations are at most  $0.4^\circ$  of polarization ( $0.2^\circ$  rotation of the half-wave plate) for all*  
40 *channels (assessed, as before, using the mean plus two standard deviations for all flights having*  
41 *multiple calibrations during the latest field mission).*

1 This tells us only something about the stability (or precision) of the 45° angle adjustment,  
2 but nothing about the accuracy, which is the basic important value.  
3 See above for why we consider the stability of the calibration to be a good measure of its  
4 uncertainty.

5 What does "Changes indicated" mean?

6 If the Alvarez calibration indicates that the center of the polarization curve shown in the  
7 Reviewer's Figure 1 is not at 0 degrees, the waveplate angle is adjusted so that it is at zero  
8 degrees. This has been clarified in the text.

9 **Page 24777 Line 12**

10 Change:

11 *This effect on the measured gain will be reflected in the ~~stability~~-error of the gain ratio, ...*

12 Changed as suggested.

13 **Page 24777 Line 18**

14 *The stability of this gain ratio was assessed in a similar manner to the offset angle and polarization*  
15 *gain ratios given above.*

16 Again: precision (stability) is not accuracy. Please explain.

17 The same explanation applies. The aerosol-to-molecular gain ratio calibration measurements  
18 occur at least once during flight and twice when possible (occasionally 3 or more times), but  
19 not continuously. There is some possibility of the gain ratio changing during a flight due to  
20 environmental factors (e.g. thermal changes). Therefore the amount of change during a  
21 flight is the best estimate of the size of the uncertainty. The uncertainty was estimated to  
22 be the amount of change in flights where two or more calibrations took place. For this study,  
23 we calculated statistics of this change over multiple flights to give a confidence limit for the  
24 uncertainty.

25 **Systematic errors**

26 A well-founded error calculation for lidar products is a really laborious task. The effort  
27 done in this paper is ambitious. Nevertheless, I would like to make a general remark and  
28 some comments in the following:

29 Error bars are essential in several respects, e.g. for the retrieval of micro-physical aerosol  
30 parameters with model calculations, for the comparison of results from different  
31 instruments, or for aerosol classification. The two scenarios A and B in Fig. 2 show their  
32 importance: in scenario A the two values 1 and 2 cannot be measurements of the same  
33 object, because the error bars don't overlap.

34 At least if we take the error bars seriously. In scenario B we cannot exclude that value 1  
35 and 2 are measurements of the same object. They are not distinguishable considering the  
36 accuracy of the measurements.

37 ...

38 Furthermore, if we know from other measurements that object 1 and 2 are actually the  
39 same, as it is sometimes the case from simultaneous measurements in multi-sensor field  
40 campaigns, we must conclude from scenario A that there are unaccounted instrumental

1 errors, and from scenario B that the true value of the object is in the small overlap region  
2 of the two measurements.

3 This shows first, that error bars are very valuable and powerful information, and second,  
4 that we must be careful because other scientist will take our error bars and interpret them  
5 in their context if we don't specify them sufficiently.

6 We agree on the general discussion and philosophy of error bars. I don't think we said  
7 anything in the manuscript that goes counter to these general statements.

8 Models need the experimental error bars as constraints. They often produce results with  
9 statistical probabilities from many trials. Often Gaussian like distributions arise due to  
10 the central limit theorem, even if the original parameters are evenly distributed. But for  
11 that more than about ten different input values for each parameter are required.

12 But an instrument like a lidar system has only one set of system parameters at the time  
13 of a certain measurement, which usually shouldn't change during the measurement.  
14 Therefore the application of the statistical error propagation for independent parameters  
15 (sum of squares), which assumes a Gaussian distribution of the "erroneous" parameters,  
16 is not appropriate for the error propagation of fixed systematic errors. Should a system  
17 parameter nevertheless change during a measurement, its behaviour should be  
18 determined and an appropriate error propagation developed. This would be the  
19 preferred method, but it is often too complex to accomplish. Also in this case an error  
20 calculation using the extreme bounds is the conservative way.

21 Here is where we disagree. First, it is not true that statistical error propagation for  
22 independent parameters assumes a Gaussian distribution. Statistical error propagation and  
23 summation in quadrature are only dependent on the definition of variance, and variance is a  
24 concept that is applicable to any distribution. The variance is defined as  $E[X^2]-E[X]^2$  where  
25  $E[]$  denotes the expectation value, and so this is not dependent on Gaussian distributions.  
26 The proof that variances add depends only on this definition (see the proof given here, for  
27 example:  
28 [http://apcentral.collegeboard.com/apc/members/courses/teachers\\_corner/50250.html](http://apcentral.collegeboard.com/apc/members/courses/teachers_corner/50250.html),  
29 accessed 11/3/2015).

30 Second, while we agree that it would be inappropriate to use statistical error propagation for  
31 repeated (fixed) systematic errors, that is not what we are doing. That is, to determine the  
32 error from repeated trials with a system having fixed systematic errors, you would not assess  
33 the error for each trial and then add them in quadrature or indeed add them at all. However,  
34 what we are doing in this section is different: assessing the overall effect of multiple  
35 independent sources of uncertainty (which happen to be systematic sources). Since they are  
36 independent and the value of the actual error for each source is unknown, it is appropriate to  
37 add them in quadrature. It would only be appropriate to add them absolutely if they were  
38 exact known values. That is, if we knew that the error due to the polarization gain ratio was  
39 exactly x and the error due to the aerosol-to-molecular gain ratio was exactly y, etc., then it  
40 would be appropriate to say the total error is x plus y. Although in that case, if so much was  
41 known exactly, we would probably choose to correct the errors rather than report them as

1 error bars. In fact, we do not know the values: they are unknown values from an unknown  
2 distribution.

3 So, it's calculating the variance that's problematic, not adding them in quadrature. For  
4 random, normally distributed errors, the variance is well defined, and assessing multiple  
5 trials is usually the best and most straightforward way to calculate it. Granted, systematic  
6 errors are not best described as "random". For a constant systematic error from a single  
7 source, if the distribution is a delta function, it would not make much sense to talk about  
8 variance, as the reviewer points out. But in our case, even though it may not be right to  
9 describe the errors as "random", the errors are unknown so they each belong to some  
10 probability distribution which is not a delta function. Unfortunately the probability  
11 distribution is also unknown. So, we don't know a formula for how to calculate the variance.  
12 Instead we do the best we can to make an estimate of a confidence interval for these errors,  
13 such that we expect that the error from a given source is most likely less than the limit we  
14 specify (and which we therefore called a bound or limit in the discussion paper). We do not  
15 say that the error is exactly equal to that confidence limit. In fact, we do not know these  
16 values but they are unlikely to all be equal to the upper limit. So adding the errors absolutely  
17 would result in unnecessarily large error bars, which, as the reviewer points out below, are  
18 not particularly helpful to data users. On further reflection, we see that calling these  
19 confidence limits an "upper bound" may have added to confusion if the reviewer took that to  
20 mean all our uncertainty estimates denote absolute maximum. We really intend this to be  
21 analogous to 95% confidence interval (although we don't wish to take "95%" too literally,  
22 since the distributions are not Gaussian), a threshold that the systematic error is "most  
23 likely" to be below with high confidence. In the revision, we use "uncertainty", making a  
24 more correct distinction between the systematic error (the amount by which a measurement  
25 is incorrect due to system parameters) and "systematic uncertainty" (our best estimate of the  
26 value below which the error should fall) and we think this greatly clarifies the discussion. It's  
27 true that if we knew more about the probability density of the true errors within our  
28 uncertainty, it would be possible (though probably still challenging) to make the estimates of  
29 the variance and confidence interval more exact and the results might differ from what we  
30 reported. However, we still would need to add the errors from different sources, and since  
31 they are unknown values and independent, we believe that adding them in quadrature is the  
32 most reasonable approach.

33 [Furthermore, if the lidar error bars are too large, a too large variety of model results fall  
34 within the error bars, and if the lidar error bars are too small, the model solutions which  
35 would come close to the reality might be excluded. If lidar error bars are getting smaller  
36 and reliable, the lidar measurements can be really helpful to improve the model  
37 developments.](#)

38 We have no disagreement with this statement. We have made fair estimates of the  
39 systematic uncertainty of our measurement system and demonstrated that the error bars are  
40 small enough to support the conclusions we draw about the measurement cases.

41  
42 [Detailed comments:](#)

1 1. The details of the error calculation should not fall back behind the one presented by  
2 Freudenthaler et al. (2009).

3 We are not sure what the reviewer means by this. While we do compare our measurements  
4 to those of Freudenthaler et al. (2009) for a dust case, to show that our results are consistent  
5 with earlier published results, there is nowhere in the manuscript that suggests that the  
6 Freudenthaler et al. (2009) error calculation should be used to understand our own  
7 measurements.

8 The equations for the  $F_x$ -values should be presented as well as the ones for the calculation  
9 of the error of the backscatter ratio due to the HSRL technique.

10 Equation A6 of the Appendix gives the  $F_x$  factors as partial derivatives calculated from Eq. (2).  
11 In the revision we will add a sentence clarifying this: "*The partial derivatives are calculated*  
12 *easily from Eq. (2) which relates the particle depolarization ratio to the factors  $R$ ,  $\delta_{tot}$ , and*  
13  *$\delta_m$ .*" We don't write out the partial derivatives, since they are straightforward for any reader  
14 to calculate.

15 As already mentioned, the "manuscript focused on a complete error analysis and  
16 validation of extinction measurements" promised by Hair et al. (2008) is missing.

17 This is a criticism of an earlier published paper, not the manuscript under review. However,  
18 we will point out again that Hair et al (2008) does indeed include a "complete error analysis"  
19 of the extinction– and depolarization– measurements of HSRL-1. The validation was  
20 demonstrated in a later paper, Rogers et al. (2009). The current manuscript does not present  
21 any extinction measurements, so the error analysis of HSRL-2 extinction measurements is  
22 outside the scope of this paper. To the extent that the extinction and backscatter retrieval is  
23 relevant to the depolarization ratio uncertainties, we have discussed it already in the  
24 manuscript.

25 2. The absolute error (offset) of the volume linear depolarization ratio can only be  
26 positive. The only way to decrease the depolarization is a polarization filter, which is the  
27 case if the receiver optics has diattenuation. But this effect is in principle fully corrected  
28 with the polarization calibration. (I propose to use "polarization calibration" instead of  
29 "depolarization calibration".)

30 Therefore, this error would have a one-sided distribution if many different instrument  
31 adjustments were done, which is clearly not a Gaussian distribution.

32 Our calculation does not depend on its being Gaussian. Please see above. We acknowledge  
33 that an offset error is one-sided; however, like the reviewer, we think it is reasonable to try  
34 to correct for it (as described in the text). This correction may overshoot in particular cases,  
35 so the error after correction is not necessarily one-sided. Furthermore, the other potential  
36 systematic error sources are not one-sided (errors in the gain ratios, for example), so adding  
37 them all absolutely would result in an unnecessary overestimate. We feel that what we have  
38 done is the most reasonable way to combine all the various sources of uncertainty, given that  
39 it is impossible to assess systematic error by repeated trials. (We agree about using  
40 "polarization calibration" and have revised the manuscript accordingly.)

41 3. Eq. (1) of this paper corrects only for different electronic gain and optical transmission  
42 after the polarizing beam splitter, but not for the cross talk of the polarizing beam splitter

1 as shown by Freudenthaler et al. (2009) Eqs. (15) and (16). Although the extinction ratios  
2 of the polarizing beam splitter assemblies used in the HSRL-2 receiver are quite good, the  
3 error from neglecting their cross talk is maximal for low depolarization and amounts for  
4 the molecular linear depolarization ratios to +0.0023 at 355 nm and +0.0010 at 532 and  
5 1064 nm using the transmission ratios in page 24757 line 29. The linear depolarization  
6 ratio values presented in the paper could be easily corrected for that effect.  
7 However, this calculation also shows, that the effect is not sufficient to explain the  
8 assumed molecular linear depolarization ratios of 0.0085 to 0.0135 measured since 2006  
9 (Page 24775 Line 14).

10 The molecular linear depolarization ratio is the only calibration standard we have for  
11 depolarization measurements. Deviations from that can be due to an offset, due to a  
12 calibration factor, and due to a combination of both. Assuming that the error of the  
13 calibration factor can be reduced to a few percent, the offset can be determined and all  
14 measurements can be corrected for that error with the appropriate equations. The  
15 remaining error is then the unexplained spread of the assumed-molecular linear  
16 depolarization ratios of 0.0085 to 0.0135.

17 As the reviewer points out, the correction for cross-talk in the polarization beam splitter is  
18 not sufficient to correct the total systematic error due to presumed cross-talk. So we have  
19 used the molecular linear depolarization ratio as the means of estimating this source of  
20 systematic uncertainty, as the reviewer suggests. Since, as the reviewer points out, the  
21 offset error will be in one direction and fairly consistent, we feel that we can correct for it,  
22 as already described in the Appendix. However, even this correction is not perfect, and so  
23 we include an offset portion in our reported uncertainty as well.

24 4. Elliptically polarized output light can be separated in the Stokes vector in a pure  
25 linearly polarized and a pure circularly polarized part. The circularly polarized part is  
26 detected by the linear polarization analyser, i.e. the polarizing beam splitter in the lidar  
27 receiver, as depolarization and gives a more or less constant offset contribution to the  
28 linear depolarization ratio (decreasing slightly with increasing atmospheric  
29 depolarization). It doesn't influence the polarization calibration factor.

30 If by "polarization calibration factor" the reviewer means "polarization gain ratio" we agree  
31 that ellipticity does not affect that quantity. It does affect the measured depolarization  
32 ratio; the amount is given by Equation A3.

33 In contrast, if there is a rotation of the plane of polarization of the emitted light with  
34 respect to the receiver, it is probably also there for the polarization calibration, which  
35 results in a relative error of the gain and therefore in a relative error of the linear  
36 depolarization ratio (see above comment to Page 24757 Line 5). Therefore, the two  
37 systematic errors, i.e. elliptical polarization and angle of the plane of polarization, cannot  
38 be treated identically as cross-talk (Page 24776 Line 8).

39 We agree that there is also a relative uncertainty due to the effect of cross-talk on the gain  
40 ratio, which we discussed separately in the paper in the following paragraph. The cross-talk  
41 also has an offset effect, described by Equation A3. The offset portion does not depend on

1 whether the problem is a rotation of the plane of polarization or an ellipticity. Although this  
2 was already discussed in the manuscript, we have attempted to clarify this by changing the  
3 wording. We now say, “Eqs (6) and (7) make no distinction between the ellipticity and  
4 polarization offset angles  $\theta$  and  $\psi$ . Therefore, we can model cross talk due to either source  
5 using the same correction, although noting that an offset angle would additionally affect the  
6 polarization gain ratio.”

7 **Page 24776 Line 17**

8 *Taking this into account, we include a factor of 0.007 (absolute) due to cross-talk in the estimated*  
9 *volume depolarization error.*

10 The value 0.007 is not a factor, but an absolute offset. The cross-talk error should be a  
11 relative error. See discussions above.

12 We agree it is not a factor; we changed the word to “component”. As discussed above, the  
13 cross-talk has both a (fairly constant) offset and a relative portion, both of which are  
14 discussed in the text. This sentence refers to the offset portion.

15 **Table 2**

16 Instead of somehow arbitrary value combinations the real values for Table 1 should be  
17 used, and maybe some extreme values to show certain aspects. Furthermore, the  
18 equations used to calculate the factors and errors should be shown, which would be  
19 valuable for the readers to improve their own error calculation.

20 We included Table 2 to help build a sense of how the functions behave. If we used  
21 measurements for Table 2, all quantities would vary simultaneously, and it would be more  
22 difficult to discern the effects of varying each column. The actual measurements are used in  
23 the calculation of the error bars quoted in Table 1 (the table that shows the measurements)  
24 and in the figures, so we are not losing any information by additionally illustrating arbitrary  
25 combinations in Table 2. The equations are already given: A5 and A6 of the appendix. The  
26 partial derivatives aren't written out, but they are easily derived from Equation (2), which we  
27 have now clarified, as stated above.

28 *The uncertainty for R is only +5%, but for 1064 nm +20% are mentioned in the paper.*

29 Yes, table 2 is arbitrary values as already noted. However, Table 1 and the figures use the  
30 larger error bars for 1064 nm as discussed in the text, so there is no inconsistency that needs  
31 to be corrected.

32 **Summary**

33 *The offset errors and the errors of the calibration factors should be separated as much as*  
34 *possible.*

35 They are already separated in the discussions in the paper. We have added some clarification  
36 to the text as described above.

37 *The polarization calibration error can be decreased and separated from the*  
38 *measurements error of the polarization angle by using the +45° calibration.*

39 See above. The waveplate is physically rotated to the inferred zero point (i.e. the angle that  
40 minimizes the depolarization), and so the offset angle is removed before science  
41 measurements are made; therefore we do not agree that the polarization calibration error

1 can be decreased. If we had obtained  $\pm 45^\circ$  calibration measurements after rotating the  
2 waveplate, it might be useful to confirm that there is no lingering error in the offset angle  
3 after the adjustment but we have not seen any indication of a consistent bias in setting the  
4 angle, which would be evident when looking at consecutive polarization calibrations. In any  
5 case, after adjusting the waveplate as indicated by the 7 angle calibration, we only did  
6 calibrations at  $+45^\circ$ , so we cannot make the suggested change to the measurements in this  
7 paper.

8 [The error of the polarization angle should be determined for each calibration separately  
9 and propagated to the corresponding measurements.](#)

10 See response above. The waveplate is physically rotated to the inferred zero point as part of  
11 the calibration procedure, so there is no error in the polarization angle for subsequent  
12 measurements, as far as we can tell. We do not do another assessment of the angle  
13 immediately after adjusting the waveplate, so we have no information to use for correcting  
14 for an error in the angle. However, a small error is possible to the extent that the waveplate  
15 position may change between measurements, which is why we use the in-flight change of the  
16 measured calibration to estimate the systematic uncertainty for measurements obtained  
17 between calibrations.

18 [The cross talk error from the polarizing beam splitters should be corrected.](#)

19 As noted in the text, the cross-talk error from the polarizing beam splitter is made negligible  
20 compared to other error sources by the addition of “clean-up” PBS cubes. This is already  
21 acknowledged in the reviewer’s comments “the extinction ratios of the polarizing beam  
22 splitter assemblies used in the HSRL-2 receiver are quite good” and “the effect is not  
23 sufficient to explain the assumed molecular linear depolarization ratios”. The reported  
24 systematic uncertainties cover all sources of cross-talk. For the purpose of this paper, which  
25 is to highlight the spectral dependence of the aerosol linear depolarization ratio for the  
26 selected case studies, the systematic uncertainty estimates are sufficient small to show that  
27 the highlighted differences are real differences.

28 [The determination of the backscatter ratio error should be described more detailed and  
29 its influence on the error of the linear depolarization ratio should be made more clear.](#)

30 We have included a fair amount of detail about the total aerosol scattering ratio uncertainty  
31 and its influence on the linear depolarization ratio. We point out that the systematic  
32 uncertainty for the total aerosol scattering ratio is the systematic uncertainty in the gain, and  
33 that for 532 nm, the aerosol-to-molecular gain ratio calibration is the only source. For the  
34 other channels, there is additional uncertainty related to transferring the gain ratio  
35 calibration from 532 nm, and we describe how we estimated that additional uncertainty. The  
36 influence of the uncertainty in the total aerosol scattering ratio on the uncertainty in the  
37 linear depolarization ratio is given by equation A5. The uncertainty in the total aerosol  
38 scattering ratio is  $\Delta R$  and the uncertainty in the linear particle depolarization ratio is  $\Delta\delta_a$  on  
39 the left-hand side. The propagation factor  $F_R$  is a partial derivative given by equation A6  
40 operating on Equation 2.

41 [With a small error of the calibration factor, the more or less constant offset error can be  
42 accurately determined, and the values of the linear depolarization ratio can be corrected  
43 for that.](#)

1 We already discussed correcting the more or less constant offset error in the original  
2 manuscript. We included a correction, and because the correction is not perfect, we also  
3 included a component in the uncertainty.

4 **References:**

5 Alvarez, J. M., Vaughan, M. A., Hostetler, C. A., Hunt, W. H., and Winker, D. M.: Calibration Technique for Polarization-  
6 Sensitive Lidars, *J Atmos Ocean Tech*, 23, 683-699, 10.1175/jtech1872.1, 2006.

7 Rogers, R. R., et al. (2009), NASA LaRC airborne high spectral resolution lidar aerosol measurements during MILAGRO:  
8 observations and validation, *Atmos Chem Phys*, 9(14), 4811-4826, doi: 10.5194/acp-9-4811-2009.

9

10

1 Revised Manuscript with Mark-up

2 **Observations of the spectral dependence of linear particle depolarization**  
3 **ratio of aerosols using NASA Langley airborne High Spectral Resolution**  
4 **Lidar**

5 S. P. Burton<sup>1</sup>, J. W. Hair<sup>1</sup>, M. Kahnert<sup>2,3</sup>, R. A. Ferrare<sup>1</sup>, C. A. Hostetler<sup>1</sup>, A. L. Cook<sup>1</sup>, D. B. Harper<sup>1</sup>, T. A. Berkoff<sup>1</sup>,  
6 S. T. Seaman<sup>1,4</sup>, J. E. Collins<sup>1,5</sup>, M. A. Fenn<sup>1,5</sup>, R. R. Rogers<sup>1,6</sup>

7 <sup>1</sup>NASA Langley Research Center, MS 475, Hampton, VA, 23681, USA

8 <sup>2</sup>Research Department, Swedish Meteorological and Hydrological Institute, Folkborgsvägen 17, 60176 Norrköping,  
9 Sweden

10 <sup>3</sup>Department of Earth and Space Science, Chalmers University of Technology, 41296 Gothenburg, Sweden

11 <sup>4</sup>National Institute of Aerospace, 100 Exploration Way, Hampton, VA, 23666, USA

12 <sup>5</sup>Science Systems and Applications, Inc., One Enterprise Pkwy, Hampton, VA, 23666, USA

13 <sup>6</sup>now at Lord Fairfax Community College, Middletown, VA 22645, USA

14 Email: Sharon.P.Burton@NASA.gov

15 **Abstract**

16 Linear pParticle depolarization ratio is presented for three case studies from the NASA Langley  
17 airborne High Spectral Resolution Lidar-2 (HSRL-2). Particle depolarization ratio from lidar is an  
18 indicator of non-spherical particles and is sensitive to the fraction of non-spherical particles and  
19 their size. The HSRL-2 instrument measures depolarization at three wavelengths: 355 nm, 532  
20 nm, and 1064 nm. The three measurement cases presented here include two cases of dust-  
21 dominated aerosol and one case of smoke aerosol. These cases have partial analogs in earlier  
22 HSRL-1 depolarization measurements at 532 nm and 1064 nm and in literature, but the  
23 availability of three wavelengths gives additional insight into different scenarios for non-  
24 spherical particles in the atmosphere. A case of transported Saharan dust has a spectral  
25 dependence with a peak of 0.30 at 532 nm with smaller particle depolarization ratios of 0.27 and  
26 0.25 at 1064 and 355 nm, respectively. A case of aerosol containing locally generated wind-  
27 blown North American dust has a maximum of 0.38 at 1064 nm, decreasing to 0.37 and 0.24 at  
28 532 nm and 355 nm, respectively. The cause of the maximum at 1064 nm is inferred to be very  
29 large particles that have not settled out of the dust layer. The smoke layer has the opposite spectral  
30 dependence, with the peak of 0.24 at 355 nm, decreasing to 0.09 and 0.02 at 532 nm and 1064 nm.  
31 The depolarization in the smoke case may be explained by ~~is inferred to be due to~~ the presence of  
32 coated soot aggregates. We note that in these specific case studies, the linear particle  
33 depolarization ratio for smoke and dust-dominated aerosol are more similar at 355 nm than at  
34 532 nm, having possible implications for using particle depolarization ratio at a single wavelength  
35 for aerosol typing. ~~We also point out implications for the upcoming EarthCARE satellite, which~~  
36 ~~will measure particle depolarization ratio only at 355 nm. At 355 nm, the particle depolarization~~  
37 ~~ratios for all three of our case studies are very similar, indicating that smoke and dust may be~~  
38 ~~more difficult to separate with EarthCARE measurements than heretofore supposed.~~

## 1 1. Introduction

2 The impact of aerosols on climate depends on their horizontal and vertical distribution and  
3 microphysical properties. Lidar is an important tool for remote sensing of aerosol, because it  
4 provides vertically resolved information on aerosol abundance and aerosol type. One extremely  
5 useful lidar aerosol measurement is the linear particle depolarization ratio, an indicator of non-  
6 spherical particles. Polarization lidar is an a large and active field, with recent contributions from  
7 ground-based networks such as the European Aerosol Research Lidar Network (EARLINET;  
8 (Pappalardo et al., 2014; Mamouri and Ansmann, 2014; Nisantzi et al., 2014) and the National  
9 Institute of Environmental Studies (NIES) East Asian network of lidars (Sugimoto et al., 2005;  
10 Nishizawa et al., 2011); directed field campaigns, such as the Saharan Mineral Dust Experiment  
11 (SAMUM); (Freudenthaler et al., 2009; Tesche et al., 2011) and the Saharan Aerosol Long-range  
12 Transport and Aerosol-Cloud Experiment (SALTRACE); (Groß et al., 2015; Haarig et al., 2015);  
13 and others.

14 There is also considerable interest in global lidar observations from satellites. Global lidar  
15 observations of aerosol have been provided by the Cloud-Aerosol Lidar and Infrared Pathfinder  
16 Satellite Observations (CALIPSO) satellite since 2006 (Winker et al., 2007). Another satellite lidar,  
17 the experimental Cloud-Aerosol Transport System (CATS) instrument on the International Space  
18 Station (ISS) (McGill et al., 2012) was recently launched in January 2015, and the Earth Clouds  
19 Aerosols and Radiation Explorer (EarthCARE) satellite (Illingworth et al., 2015) is due to launch  
20 in 2018. CALIPSO linear particle depolarization ratio data have been used, for example, to assess  
21 the global distribution and transport of dust (e.g. Johnson et al., 2012; Liu et al., 2013; Yang et al.,  
22 2013). This measurement will also be part of the suite of measurements made by the ATLID  
23 (Atmospheric Lidar) on EarthCARE; however, CALIPSO measures depolarization at 532 nm and  
24 ATLID will measure it at 355 nm (Groß et al., 2014; Illingworth et al., 2015).

25 NASA Langley airborne High Spectral Resolution Lidars, HSRL-1 and HSRL-2, have participated  
26 in many process-oriented field campaigns, have provided validation and calibration data for  
27 CALIPSO since 2006 (Rogers et al., 2011; Rogers et al., 2014), and will also be useful for validating  
28 the EarthCARE lidar measurements. Since the airborne HSRL-2 measures particle depolarization  
29 ratio at both the CALIPSO and EarthCARE wavelengths and also at 1064 nm, observations from  
30 this instrument are useful for assessing how the measurements from the two satellite instruments  
31 will correspond. NASA's airborne HSRL-2 is the first HSRL system making depolarization  
32 measurements at three wavelengths. A ground-based Raman system operated by the Leibniz  
33 Institute of Tropospheric Research has also been recently upgraded to make three-wavelength  
34 depolarization measurements (Haarig et al., 2014).

35 Global lidar observations of aerosol have been provided by the Cloud-Aerosol Lidar and Infrared  
36 Pathfinder Satellite Observations (CALIPSO) satellite since 2006 (Winker et al., 2007). Another  
37 satellite lidar, the experimental Cloud-Aerosol Transport System (CATS) instrument on the  
38 International Space Station (ISS) (McGill et al., 2012) was recently launched in January 2015, and  
39 the Earth Clouds Aerosols and Radiation Explorer (EarthCARE) satellite (Illingworth et al., 2015)  
40 is due to launch in 2018. NASA Langley airborne High Spectral Resolution Lidars, HSRL-1 and  
41 HSRL-2, have participated in many process-oriented field campaigns, have provided validation

1 and calibration data for CALIPSO since 2006 (Rogers et al., 2011; Rogers et al., 2014), and will also  
2 be useful for validating the EarthCARE lidar measurements.

3 One extremely useful lidar aerosol measurement is the particle depolarization ratio, an indicator  
4 of non-spherical particles. CALIPSO particle depolarization ratio data have been used, for  
5 example, to assess the global distribution and transport of dust (e.g. Johnson et al., 2012; Liu et  
6 al., 2013; Yang et al., 2013). This measurement will also be part of the suite of measurements made  
7 by the ATLID (Atmospheric Lidar) on EarthCARE; however, CALIPSO measures depolarization  
8 at 532 nm and ATLID will measure it at 355 nm (Groß et al., 2014; Illingworth et al., 2015). Since  
9 the airborne HSRL-2 measures particle depolarization ratio at both of these wavelengths and also  
10 at 1064 nm, observations from this instrument are useful for assessing how the measurements  
11 from the two satellite instruments will correspond.

12 Aerosol classification is one specific application of aerosol polarization measurements (Burton et  
13 al., 2012; Groß et al., 2013; Burton et al., 2013; Groß et al., 2014) ~~(Burton et al., 2013)~~. Aerosol  
14 particle depolarization ratio from lidar is has long been of key importance used for the detection  
15 and assessment of dust and volcanic ash since it is a clear indicator of non-spherical particles. The  
16 particle depolarization ratio is known to be sensitive to the amount of dust or ash in a mixture is  
17 also used to infer the amount of dust or ash in a mixture (Sugimoto and Lee, 2006; Tesche et al.,  
18 2009a; Tesche et al., 2011; Ansmann et al., 2011; Ansmann et al., 2012; David et al., 2013; Burton  
19 et al., 2014; Mamouri and Ansmann, 2014). ~~and~~ It is also sensitive to the size of the non-spherical  
20 particles (Ansmann et al., 2009; Sakai et al., 2010; Gasteiger et al., 2011; Gasteiger and  
21 Freudenthaler, 2014; Gasteiger et al., 2014).

22 While a significant amount of study has been made of depolarization by dust and ash, smoke has  
23 also been observed to produce significant depolarization of lidar light in some cases (e.g. Fiebig  
24 et al., 2002; Sassen and Khvorostyanov, 2008; Sugimoto et al., 2010; Dahlkötter et al., 2014), but  
25 not in others (e.g. Müller et al., 2005). Even for cases with significant depolarization, the  
26 depolarization signature for smoke is generally smaller than for dust, at the wavelengths of 532  
27 nm and 1064 nm where most lidar depolarization measurements of smoke have been made.

28 We will describe two dust-dominated cases and a smoke-dominated case where depolarizing  
29 aerosol was observed simultaneously at three wavelengths by the NASA Langley airborne HSRL-  
30 2 instrument. We show consistency between the three HSRL-2 cases and three previously  
31 published cases from the predecessor HSRL-1 instrument in which similar measurements were  
32 made at 532 nm and 1064 nm, and we also discuss similarities and differences with published  
33 lidar measurements globally. We find that the three cases each have a different spectral  
34 dependence of the particle depolarization ratio. Accordingly, we discuss possible explanations  
35 for these differences with reference to published studies. We also point out implications for future  
36 space-based observations of aerosol depolarization. We begin in Section 2 with a description of  
37 the NASA Langley airborne HSRL instruments and the methodology for ~~de~~depolarization  
38 measurements, including an assessment of systematic uncertainty error assessment. In Section 3  
39 we describe and discuss the dust cases and in Section 4 we describe and discuss the smoke case.  
40 We summarize the discussion and conclude in Section 5. In the Appendix we give more details  
41 about the estimation of systematic uncertainty errors.

## 1 2. Instrument Description and Measurement Methodology

2 The NASA Langley second-generation airborne High Spectral Resolution Lidar-2 (HSRL-2) uses  
3 the HSRL technique (Shiple et al., 1983) to independently measure aerosol extinction and  
4 backscatter at 355 and 532 nm and the standard backscatter technique (Fernald, 1984) to measure  
5 aerosol backscatter at 1064 nm. It also measures linear depolarization ratio at all three  
6 wavelengths. It is a follow-on to the successful airborne HSRL-1 instrument (Hair et al., 2008),  
7 which has made measurements at 532 nm and 1064 nm since 2006 (Rogers et al., 2009). For  
8 measurements at 532 nm and 1064 nm, HSRL-2 is essentially identical to HSRL-1. HSRL  
9 measurements of extinction and backscatter at 355 nm are made using an interferometer rather  
10 than an iodine filter. For 355 nm measurements of depolarization discussed here, the setup is  
11 very similar to the other channels; the small differences are explained in section 2a. Data are  
12 sampled at 0.5-s temporal and 30-m vertical resolutions. Aerosol backscatter and depolarization  
13 products are averaged 10-s horizontally (~1-km at nominal aircraft speed) and aerosol extinction  
14 products are averaged 60-s (~6-km) horizontally and 150-m vertically. Besides aerosol  
15 backscatter, extinction, and depolarization ratio, products also include horizontally- and  
16 vertically-resolved curtains of backscatter Ångström exponent and extinction Ångström  
17 exponent. Operational retrievals also provide mixing ratio of nonspherical-to-spherical  
18 backscatter (Sugimoto and Lee, 2006), aerosol type and partitioning of aerosol optical depth  
19 (AOD) by type (Burton et al., 2012), aerosol mixed-layer height (Scarino et al., 2014), and aerosol  
20 microphysics for spherical particles (Müller et al., 2014). HSRL-2 has been successfully deployed  
21 from the NASA LaRC King Air B200 aircraft on four field missions since 2012 and has obtained  
22 over 350 science flight hours. The typical flight altitude of the B200 during lidar operations is 9  
23 km. The data for the case studies presented here are available on the DISCOVER-AQ (Deriving  
24 Information on Surface Conditions from Column and Vertically Resolved Observations Relevant  
25 to Air Quality) data archive at [http://www-air.larc.nasa.gov/missions/discover-aq/discover-](http://www-air.larc.nasa.gov/missions/discover-aq/discover-aq.html)  
26 [aq.html](http://www-air.larc.nasa.gov/missions/discover-aq/discover-aq.html) or using the data doi: [10.5067/Aircraft/DISCOVER-AQ/Aerosol-TraceGas](https://doi.org/10.5067/Aircraft/DISCOVER-AQ/Aerosol-TraceGas).

### 27 a. Depolarization Optics

28 In this paper, we will focus on the measurements of linear particle depolarization ratio. Figure 1  
29 shows a simplified diagram of the optics of the transmission system that are relevant to the  
30 measurement of depolarization. The primary optical components for the polarization of the  
31 transmitted beams are Glan Laser Polarizers, which have a very high polarization  
32 ~~transmittance~~extinction ratio of 2e5:1 (i.e. the light is highly linear polarized with an extremely  
33 small fraction of cross-polarized light). The calibration of depolarization for HSRL-2 is done in a  
34 manner similar to HSRL-1 (Hair et al., 2008) for all three wavelengths. The polarization axis of  
35 the outgoing light is matched to that of the receiver with an approach similar to that outlined by  
36 Alvarez et al. (2006) using seven fixed polarization angles between  $\pm 45^\circ$ , using the half-wave  
37 calibration wave plates indicated in Figure 1. Following the alignment, the polarization gain ratio  
38 between the cross-polarized and co-polarized channels is routinely determined in flight by  
39 rotating the transmitted polarization  $45^\circ$  relative to the receiver, so that both channels measure  
40 equal components of the co-polarized and cross-polarized backscatter returns, in a cloud-free  
41 portion of the profile. See Hair et al. (2008) for a detailed description of the calibrations. See the  
42 caption accompanying Figure 1 for more details of the HSRL-2 transmission optics.

1 The receiver optics relevant to depolarization measurements are shown in Figure 2. The  
2 collimated light arrives from the telescope and is split into the three wavelengths using dichroic  
3 beam splitters. Each beam is then passed through an interference filter (1064 nm) or a  
4 combination of interference filter and etalon (355 and 532 nm) to remove background scattering.  
5 The effective full-width half-max (FWHM) bandwidths for the three channels are 0.4 nm (3.5 cm<sup>-1</sup>)  
6 at 1064 nm, 0.03 nm (1.1 cm<sup>-1</sup>) at 532 nm, and 0.045 nm (3.6 cm<sup>-1</sup>) at 355 nm. Note that these  
7 bandwidths are narrow enough to completely exclude the rotational Raman sidebands from the  
8 receiver optics, which are found starting at ±11.9 cm<sup>-1</sup> for N<sub>2</sub> and ±14.4 cm<sup>-1</sup> for O<sub>2</sub> (Behrendt and  
9 Nakamura, 2002). The 1064 nm channel includes a half-wave plate which can be used to correct  
10 any small polarization misalignment in the receiver system, since the 532 nm and 1064 nm beams  
11 are transmitted together. This half-wave plate is set during installation and is not rotated during  
12 normal operations. Next, each beam passes through Polarization Beam Splitters (PBS) to be  
13 separated into components that are co-polarized and cross-polarized with respect to the  
14 transmitted beam. Since the ~~transmittance~~ ~~extinction~~ ratio of the light exiting a PBS is greater in  
15 the transmitted direction than in the reflected direction, a second “clean-up” PBS is included for  
16 each detector wavelength to further improve the extinction ratio for the co-polarized light. The  
17 polarization ~~transmittance~~ ~~extinction~~ ratio measured in the system is 300:1 for the cross-polarized  
18 light at 355 nm, 431:1 for the co-polarized light at 355 nm (with two PBS) and greater than 1000:1  
19 for both polarization states at 532 nm and 1064 nm. After exiting the polarization optics, the light  
20 in the 1064 nm channel goes directly to the Avalanche Photodetectors (APD). The co-polarized  
21 signal and cross-polarized signal are used to determine ~~the total volume~~ depolarization ~~ratio~~. As  
22 described by Hair et al. (2008) for HSRL-1, the co-polarized 532 nm channel is also split into a  
23 portion that is passed through an iodine cell leaving only molecular return and a channel with  
24 both molecular and aerosol return. At 355 nm, a portion of the co-polarized light is captured for  
25 the determination of the ~~volume~~ ~~total~~ depolarization ~~ratio~~, while the rest of the co-polarized light  
26 is transmitted through an interferometer to produce one channel that is dominated by the aerosol  
27 return with little signal from molecular scattering and a complementary channel that is  
28 dominated by the molecular signal with much less aerosol backscatter signal. The separation of  
29 the aerosol and molecular signals is the basis of the HSRL technique for extinction and backscatter  
30 retrieval. Since it ~~is also~~ ~~affects the relevant to the~~ systematic ~~uncertainty~~ ~~error~~ in particle  
31 depolarization ratio, it ~~is included in the systematic uncertainty budget discussed will be~~  
32 ~~discussed again~~ in Section 2b, below, ~~and more details can be found in the Appendix~~.  
33 The volume (or total) ~~linear~~ depolarization ratio is the ratio of the signal in the cross-polarized  
34 channel to that in the co-polarized channel, normalized by the measured ~~polarization~~ gain ratio.

$$\delta_{tot} = G_{dep} \frac{P^{\perp}}{P^{\parallel}} \quad (1)$$

35 In Eq (1), P<sup>∥</sup> and P<sup>⊥</sup> are proportional to the light measured by the photodetectors or  
36 photomultipliers in the co-polarized channel and the cross-polarized channel, respectively; G<sub>dep</sub>  
37 is the electro-optical gain ratio between the two (for each wavelength) and δ<sup>tot</sup> is the volume  
38 depolarization ratio, which is the ratio of the cross-polarized to co-polarized channel returns  
39 using the ~~appropriate~~ ~~polarization~~ gain ratio.

1 The particle depolarization ratio is calculated from the volume depolarization ratio using the  
2 following (Cairo et al., 1999):

$$\delta_a = \frac{\beta_{\perp}^{\pm}}{\beta_{\parallel}^{\pm}} \frac{R\delta_{tot}(\delta_m + 1) - \delta_m(\delta_{tot} + 1)}{R(\delta_m + 1) - (\delta_{tot} + 1)} \quad (2)$$

3 where  $\delta_a$  indicates the particulate depolarization ratio which will be used in all of the following  
4 discussion;  $\delta_m$  indicates the estimated molecular depolarization ratio;  $\beta_{\perp}^{\pm}$  and  $\beta_{\parallel}^{\pm}$  indicate the  
5 aerosol backscatter signal from the cross-polarized and co-polarized channels, respectively; and  
6 R indicates the total aerosol scattering ratio, which is the ratio of the aerosol plus molecular  
7 backscatter to the molecular backscatter, including both polarization components.

$$R = \frac{\beta_a + \beta_m}{\beta_m} \quad (3)$$

8

## 9 b. Systematic Errors

10 Systematic error can be a concern for depolarization measurements. Potential sources of  
11 systematic error in volume depolarization ratio arise in the depolarization optics and calibration.  
12 The retrieval of particle aerosol depolarization ratio can potentially introduce additional  
13 systematic error related to the total aerosol scattering ratio or uncertainty in the molecular  
14 depolarization ratio value. We will provide an overview of the potential systematic errors here,  
15 including bounds on the systematic uncertainty errors for volume depolarization ratio and on the  
16 propagated systematic uncertainty errors for the particle aerosol depolarization ratio. More  
17 details about these potential errors and the means of estimating the systematic uncertainty error  
18 bounds are given in the Appendix.

19 The linear volume depolarization ratio, given by Eq (1), is the more basic measurement.  
20 Systematic errors in the volume depolarization ratio can arise from various sources, including  
21 calibration errors either in the polarization angle calibration or the polarization gain ratio  
22 calibration. A major concern for the measurement of depolarization is the potential for cross-talk,  
23 which can arise from a number of sources, including imperfect polarization angle alignment,  
24 signal impurities due to imperfections in the polarization beam splitter (particularly the reflected  
25 channel), or other optics, including the aircraft window. Considering these sources, we estimate  
26 a reasonable upper bound on the systematic uncertainty error in the volume depolarization ratio  
27 measurement to be the larger of 4.7% (relative fractional error) or 0.001 (absolute) in the 355 nm  
28 channel, the larger of 5% (relative) fractional error or 0.007 (absolute) error in the 532 nm channel,  
29 and the larger of 2.6% fractional (relative) error or 0.007 (absolute) error in the 1064 nm channel.  
30 Further discussion of these estimates is given in the Appendix.

31 As can be seen in Eq. (2), the aerosol-particle depolarization ratio,  $\delta_a$ , depends on the volume  
32 depolarization ratio, the molecular depolarization ratio, and the total aerosol scattering ratio.  
33 Therefore, an error in the assumed value of  $\delta_{mol}$  or any systematic error in the total aerosol  
34 scattering ratio, R, can also cause systematic error in the particle aerosol depolarization ratio.  
35 Since the rotational Raman scattering sidebands are completely excluded from the receiver by the  
36 narrow-bandwidth background filters, the molecular depolarization arises only from the central

1 Cabannes line and is very well characterized, ~~with a value of 0.0036~~ (She, 2001; Behrendt and  
2 Nakamura, 2002). More critically important is any potential systematic error in the total aerosol  
3 scattering ratio, R. We estimate the ~~effective upper bound of this error~~ systematic uncertainty to  
4 be 4.1% in the 532 nm channel from an analysis of the stability of the aerosol-to-molecular gain  
5 ratio; 5% in the 355 nm channel including potential errors associated with gain ratio calibration  
6 transfer from the 532 nm channel; and 20% in the 1064 nm channel taking into account the  
7 retrieval of backscatter using an estimated lidar ratio. Again, further discussion can be found in  
8 the Appendix.

9 The estimates given above are intended to be a conservative estimates of the systematic  
10 uncertainty upper bound on the systematic errors confidence limit, such that we expect a high  
11 probability that the systematic error is less than this value. The systematic ~~uncertainty errors~~  
12 on the three quantities,  $\delta_{\text{mol}}$ ,  $\delta_{\text{tot}}$ , and R, are combined in quadrature using standard propagation of  
13 errors for independent variables, as described in the Appendix. The propagated systematic  
14 ~~uncertainty errors~~ for the case studies are included in the figures and tables in Sections 3 and 4.

### 15 3. Dust

16 In this section we discuss two case studies in which HSRL-2 made three-wavelength  
17 measurements of the depolarization of dust.

#### 18 a. Case study: 13 July 2014, Dust in the residual layer in North American Midwest

19 On 13 July 2014, HSRL-2 aboard the B200 made measurements at three wavelengths on a transit  
20 flight from Virginia to Colorado for the DISCOVER-AQ field mission ([http://discover-  
21 aq.larc.nasa.gov/](http://discover-aq.larc.nasa.gov/)). The aerosol backscatter at three wavelengths and aerosol extinction at two  
22 wavelengths are shown in Figure 3 for a 180 km portion of the flight track in Missouri and Kansas,  
23 in the Midwestern United States. Several aerosol layers are evident. For this case study, we will  
24 focus on a dust-dominated layer that extends from just above the boundary layer to about 3200  
25 m ASL. Back-trajectories derived from the NOAA Hybrid Single Particle Lagrangian Integrated  
26 Trajectory Model (HYSPLIT) tool ([ready.arl.noaa.gov](http://ready.arl.noaa.gov)) indicate that this ~~dust~~  
27 layer probably has a Saharan origin and has undergone a very long transport period of about 14 days. Non-spherical  
28 particles, such as dust, have a distinct signature in lidar particle depolarization measurements.  
29 The linear particle depolarization ratio measurement curtains for all three wavelengths are shown  
30 in Figure 4. Peak values of particle depolarization ratio in the 1600-2300 m altitude range are  
31 approximately  $0.246 \pm 0.018$  (standard deviation for the sample)  $\pm$  (0.055 systematic),  
32  $0.304 \pm 0.005 \pm (0.022)$ , and  $0.270 \pm 0.005 \pm (0.009)$  at 355 nm, 532 nm, and 1064 nm, respectively. These  
33 high values of the particle depolarization ratio indicate that the layer is dominated by mostly dust  
34 (~~80 approximately~~ 90% dust using the methodology of Sugimoto and Lee (2006)). Note that the  
35 particle depolarization ratio at 532 nm for this layer is larger than at either 355 nm or 1064 nm.  
36 The 532 nm layer optical depth is approximately 0.1 and the total aerosol scattering ratio at 532  
37 nm is 2.3. The backscatter Ångström exponent (532/1064 nm) is  $0.45 \pm 0.03$  (standard deviation) for  
38 this layer. Table 1 includes these values for this sample and for the other cases discussed here.  
39 Values for the particle depolarization ratios and backscatter Ångström exponents are within the  
40 interquartile range we previously reported for ~~pure~~ dust-dominated aerosol measurements from  
41 HSRL-1 (Burton et al., 2013).

1 Figure 5 shows both the ~~aerosol depolarization~~particle depolarization ratio and volume  
2 depolarization ratio measurements for all altitudes at time = 17.2 UT (17:12 UT). The ~~aerosol~~  
3 ~~depolarization~~particle depolarization ratio random and systematic uncertainties (~~estimated~~  
4 ~~upper bounds~~) are also shown.

5 The predecessor of the HSRL-2, the NASA Langley HSRL-1 instrument, observed several cases  
6 of transported Saharan dust in the Caribbean in August 2010, for example the case on 18 August  
7 2010 that is shown by Burton et al. (2012). For that case, the particle depolarization ratios at 532  
8 nm and 1064 nm are  $0.33 \pm 0.02$  (standard deviation) and  $0.28 \pm 0.01$ , slightly higher than the 13 July  
9 2014 case but agreeing within the spread of the measurement sample. The backscatter Ångström  
10 exponent (532/1064 nm) is  $0.68 \pm 0.13$  (Table 1). As on 13 July 2014, the particle depolarization ratios  
11 and the backscatter Ångström exponent are within the interquartile range of values for ~~pure dust-~~  
12 dominated aerosol reported for HSRL-1. The backscatter Ångström exponents (532/1064 nm) are  
13 larger than the value reported for pure Saharan ~~aerosol-dust~~ in Morocco (Tesche et al., 2009b),  
14 which is  $0.28 \pm 0.16$ . The larger values may be consistent with large particle loss during transport,  
15 discussed in more detail below.

16 The spectral dependence of the ~~particle depolarization ratios~~spectral dependence can also be  
17 compared to measurements of ~~Saharan~~pure dust particle depolarization ratio reported by  
18 Freudenthaler et al. (2009) for the ~~Saharan Mineral Dust Experiment (SAMUM I)~~  
19 campaign. For the four dates presented in their Figure 7, the minimum and maximum values for 355 nm  
20 from the Portable Lidar System POLIS were 0.21-0.31 (compare 0.25 for NASA HSRL-2 case); at 532 nm  
21 they were 0.29-0.33 from the German Aerospace Center (DLR) HSRL (compare 0.30 and 0.33 from  
22 NASA HSRL-2 and HSRL-1) and at 1064 nm they were 0.22-0.29 from the DLR HSRL (compare  
23 0.27 and 0.28 from NASA HSRL-2 and HSRL-1). Again, the reported values at 532 nm exceed  
24 those at the other wavelengths. Indeed all three of these case studies, Saharan dust close to the  
25 source (Freudenthaler et al., 2009), transported ~~pure~~ Saharan dust observed in the Caribbean by  
26 HSRL-1 and transported Saharan dust observed by HSRL-2 in the Midwestern U.S., have similar  
27 wavelength dependence of the particle depolarization ratio.

#### 28 **b. Case study: 8 February 2013, Dust in North American Southwest**

29 A less typical observation of ~~pure dust-dominated aerosol~~ was made by the HSRL-2 instrument  
30 on 8 February 2013. On a transit flight to Virginia at the conclusion of the DISCOVER-AQ  
31 California field campaign, HSRL-2 aboard the B200 made three-wavelength measurements of a  
32 locally produced dust layer very close to the source in the U.S. Southwest. Figure 6 shows the  
33 lidar curtain of the aerosol backscatter coefficient at 532 nm for a segment of approximately 280  
34 km in Arizona and New Mexico. The highest backscatter values are near the surface and are  
35 associated with the dust layer. More tenuous layers are also visible between 3 and 5 km, which  
36 are probably smoke. The discussion will focus primarily on the dust layer for this example. Figure  
37 7 shows particle depolarization ratio at three wavelengths for the same flight segment.

38 The maximum backscatter values occur within 400 m of the ground at about 17:08 UT (17:14 UT),  
39 near the Potrillo volcanic fields in New Mexico in the Chihuahuan Desert. The layer is shallower  
40 than the previous case, and the layer AOD is only about 0.02 at 532 nm, but it is very strongly  
41 scattering, with 532 nm total aerosol scattering ratio of 3.1. The peak particle depolarization ratio

1 is  $0.24 \pm 0.05 \pm (0.05)$ ,  $0.37 \pm 0.01 \pm (0.02)$ , and  $0.383 \pm 0.006 \pm (0.011)$  at 355, 532, and 1064 nm respectively  
2 (the first uncertainty value represents standard deviation and parenthesis indicate systematic  
3 ~~uncertainty error bounds~~). Given that these very large depolarization ~~ratio~~ values occur very close  
4 to the ground, we infer that this observation is close to the source region. This observed dust layer  
5 is locally generated, wind driven ~~dust aerosol~~ from a bare soil surface in desert scrubland. The  
6 large particle depolarization ratios provide confidence that this air mass is ~~dominated by dust~~  
7 ~~aerosol nearly pure dust and rather than not~~ a mixture ~~from distinct sources~~. The backscatter  
8 Ångström exponent (532/1064 nm) is  $-0.09 \pm 0.04$ .

9 Figure 8 shows line plots of the profiles of volume depolarization ratio and ~~aerosol~~  
10 ~~depolarization particle depolarization~~ ratio, plus error bars. The systematic ~~uncertainty errors~~  
11 are generally larger at 355 nm. This error magnification at 355 nm occurs in both ~~dust-dominated~~  
12 cases because of the spectral dependence of the scattering and consequent small total ~~aerosol~~  
13 scattering ratio at 355 nm ( $\text{FSR} = 1.2$  at 355 nm). However, the systematic ~~uncertainties error~~  
14 ~~bounds~~ are small enough to clearly reveal that the wavelength dependence of the particle  
15 depolarization ratio is quite different from the Saharan dust cases discussed previously, both  
16 those measured by the NASA Langley HSRL-1 and HSRL-2 instruments and by other researchers.  
17 In our previous observations of transported Saharan ~~aerosol dust~~, the particle depolarization ratio  
18 at 532 nm exceeds the value at 1064 nm, but this case differs in that the 1064 nm particle  
19 depolarization ratio slightly exceeds the 532 nm value. The difference is primarily in the 1064 nm  
20 value, since the 355 nm and 532 nm particle depolarization ratios are similar to the Saharan  
21 ~~aerosol dust~~ cases. However, there was a previous observation by HSRL-1 of windblown North  
22 American dust on the slope of the Pico de Orizaba near Veracruz, Mexico on 12 March 2006  
23 (Burton et al., 2014; de Foy et al., 2011) which provides an analogous case for comparison. In this  
24 case the particle depolarization ratios are  $0.33 \pm 0.02$  (standard deviation) and  $0.40 \pm 0.01$  at 532 nm  
25 and 1064 nm, respectively, similar to the Chihuahuan desert ~~dust aerosol~~ on 8 Feb 2013, and the  
26 backscatter Ångström exponent (532/1064 nm) is  $-0.9 \pm 0.4$ . Note that these backscatter Ångström  
27 exponents are significantly smaller than the transported Saharan dust ~~dominated aerosol~~ cases  
28 discussed in Section 3a.

### 29 c. Discussion of spectral dependence of particle depolarization ratio of dust ~~dominated aerosol~~

30 Figure 9 shows the ~~linear~~ particle depolarization ratio at all three wavelengths for the four HSRL-  
31 1 and HSRL-2 cases discussed so far. The HSRL-2 observations of transported Saharan  
32 ~~aerosol dust~~ have spectral dependence consistent with the elevated Saharan dust ~~dominated~~  
33 ~~aerosol~~ reported by Freudenthaler et al. (2009) for the DLR airborne HSRL and ground-based  
34 lidar. However, the NASA HSRL-1 and HSRL-2 observations of North American dust at low  
35 altitude close to the source appear to fall into a different category. Although all of the observations  
36 discussed here from the NASA HSRL-2 and those of Saharan ~~desert aerosol dust~~ in Africa  
37 (Freudenthaler et al., 2009) have particle depolarization ratios at 355 nm that are less than those  
38 at 532 nm, there is a large difference at the longest wavelength, with larger 1064 nm particle  
39 depolarization ratios for the local dust ~~dominated~~ cases.

40 Furthermore, the backscatter Ångström exponents in the Chihuahuan desert observation on 8 Feb  
41 2013 and on Pico de Orizaba on 12 March 2006 are much smaller compared to 0.45-0.68 for the  
42 cases of transported Saharan dust. These smaller values are an indication of larger particle sizes

1 (Sasano and Browell, 1989) (although it must be noted that the backscatter Ångström exponent is  
2 also sensitive to other factors besides particle size, such as relative humidity (Su et al., 2008)).  
3 Maring et al. (2003) shows measured size distributions for dust layers over the Canary Islands  
4 and Puerto Rico at different stages of transport, and concluded by modeling of these distributions  
5 that a combination of Stokes gravitational settling and an offset upward velocity would explain  
6 these observations. According to that model, the volume mean diameter decreases only 20% after  
7 10 days of atmospheric transport, but 80% of that change occurs within the first 2 days. In other  
8 words, the size distributions for transported dust-dominated aerosol are similar whether  
9 transported long distances or short distances, but even layers transported short distances  
10 probably have already lost the largest particles to settling. This model applies to Saharan dust  
11 transport, but it raises the possibility that dust-dominated aerosol size distributions immediately  
12 over the source such as the North American dust cases presented here will have some proportion  
13 of particles significantly larger than those found in the transported layers.

14 The spectral dependence of particle depolarization ratio is known to be related to the size of the  
15 non-spherical particles (Mishchenko and Sassen, 1998). We infer that the difference in  
16 depolarization spectral dependence, and in particular the 1064 nm values, are due to larger  
17 particles in the observations of windblown dust close to the surface. Ground-based lidar  
18 observations by Ansmann et al. (2009) of convective plumes of dust and sand being lifted from  
19 the surface in Morocco included extremely large particle depolarization ratios of 0.50-1.0 at 710  
20 nm. This supports the connection between large particle depolarization ratios at the longer  
21 wavelengths and large particles sizes. However, the long-wavelength values in the current case  
22 study are not nearly as extreme, suggesting perhaps that the particle sizes are not as large.

23 Theoretical ~~calculations~~~~treatments~~ to date have shown that it is difficult to quantitatively predict  
24 the spectral dependence of the particle depolarization ratio for dust (Gasteiger et al., 2011;  
25 Wiegner et al., 2009; Gasteiger and Freudenthaler, 2014), due in part to the need for  
26 parameterizing the shape of the dust aerosols as spheroids or other simplified shapes.

27 ~~In these previous studies, single particle depolarization calculations tend to be monotonically~~  
28 ~~increasing with wavelength for large particle sizes (Gasteiger et al., 2011) with a more~~  
29 ~~complicated spectral dependence for smaller particles (Gasteiger and Freudenthaler, 2014), which~~  
30 ~~generally supports that the increasing spectral dependence in the North American cases~~  
31 ~~presented here is due to the presence of larger particles. The theoretical calculation of multi-~~  
32 ~~wavelength particle depolarization for more complex distributions of particles has occurred only~~  
33 ~~for limited cases.~~

34 ~~For example, In a theoretical treatment of a particular measurement case,~~ Gasteiger et al. (2011)  
35 modeled particle depolarization ratio at multiple wavelengths ~~for parameterizations of dust and~~  
36 using size distributions and refractive indices appropriate for SAMUM measurements,  
37 parameterizing the shapes of dust particles using spheroids. For their reference distribution, the  
38 modeled particle depolarization ratio reflects a spectral dependence with a peak in the middle of  
39 the wavelength range. Calculated values at 355, 532, 710 and 1064 nm were 0.275, 0.306, 0.311,  
40 0.298, consistent with the measurements we report for the Saharan dust-dominated cases from  
41 the NASA HSRL-1 and HSRL-2. However, for the dust-dominated cases in the immediate vicinity

1 of North American sources, the measured maximum shifts to longer wavelengths, and there is  
2 no longer agreement with the modeled values at 1064 nm.

3  
4 Gasteiger et al. (2011) do not show results for size distributions with different size particles, but  
5 Gasteiger and Freudenthaer (2014) perform theoretical calculations using spheroids for various  
6 size parameters (single particles). These calculations show that the first peak in the spectral  
7 depolarization ratio shifts to larger wavelengths as particle size increases. This result, based on  
8 highly simplified modeling of dust aerosol, should be used only cautiously, but in general  
9 supports the notion that the spectral particle depolarization ratio is sensitive to particle size.

#### 10 4. Smoke

##### 11 a. Case study: 17 July 2014 North American Wildfire Smoke

12 Our third three-wavelength case study is an observation of a smoke plume with large particle  
13 depolarization ratios measured during the Colorado deployment of the DISCOVER-AQ field  
14 mission on 17 July 2014 at about 8 km altitude. At this time, wildfire smoke from fires in the  
15 Pacific Northwest of the United States blanketed much of the region, visible in a composited  
16 Moderate Resolution Imaging Spectroradiometer (MODIS) true color image in Figure 10. (The  
17 smoke situation on that day is also discussed in University of Maryland Baltimore County's U.S.  
18 Air Quality Smog Blog, see [http://alg.umbc.edu/usaq/archives/2014\\_07.html](http://alg.umbc.edu/usaq/archives/2014_07.html),  
19 accessed 26 Feb 2015). Figure 11 shows a view of the smoke plume from the B200.

20 Figure 12 and Figure 13 show HSRL-2 measurements of 532 nm backscatter and three wavelength  
21 linear particle depolarization ratio as time-height curtains and Figure 14 illustrates a profile at  
22 19.3 UT (19:18 UT) as a line plot with random and systematic ~~uncertainty~~ error bars. The  
23 pictured flight segment began near the Boulder Atmospheric Observatory tall tower north of  
24 downtown Denver and proceeded south for about 70 km to Chatfield Park, then turned north  
25 again on a parallel track for 135 km to Fort Collins. The layer optical thickness is about 0.05 at 532  
26 nm and the total aerosol scattering ratio is 2.9. This layer was at high altitude near the aircraft, in  
27 the overlap region, where there is a range dependence of the detected backscattered light (Hair  
28 et al., 2008). While backscattered light from a distant target is fully imaged in the detector, light  
29 from a near-field target is focused beyond the field stop, resulting in overfilling of the field stop  
30 at small range from the lidar. This loss of signal is range dependent and prevents the retrieval of  
31 aerosol extinction. —due to incomplete geometrical overlap between the transmitted beam and  
32 the receiver system. For this reason, ~~the aerosol extinction was not retrieved for this layer and~~ the  
33 layer optical depth given above is an estimate using the backscatter measurements and an  
34 assumed lidar ratio of 70 sr, which is typical for smoke. Volume depolarization ratio  
35 measurements and total aerosol scattering ratio measurements are ratios of two channels that are  
36 equally affected and therefore have no range-dependent overlap function. For this layer, the  
37 particle depolarization ratio is greatest at 355 nm, about  $0.24 \pm 0.01 \pm (0.02)$  at the southern end of  
38 the flight track, and about 0.17-0.22 in the more northern portions. The particle depolarization  
39 ratio at 532 nm is as large as  $0.09 \pm 0.02 \pm (0.01)$  at the southern end of the flight track and down to  
40 about 0.06 at the northern end. Particle depolarization ratio at 1064 nm is about  
41  $0.018 \pm 0.002 \pm (0.008)$  throughout the region (parenthesis indicate systematic ~~uncertainty~~ errors).

1 Note that the wavelength dependence of the particle depolarization [ratio](#) is opposite to what was  
2 observed for dust on 8 February 2013, in that the smoke plume has significantly larger particle  
3 depolarization ratio at the shorter wavelengths. Since this smoke layer has a very high total  
4 [aerosol scattering ratio](#), the systematic ~~uncertainties~~[error bounds](#) are relatively small, and it is  
5 clear even at the upper ~~bound of potential systematic error~~[limit of the systematic uncertainty](#) that  
6 the 355 nm ~~aerosol depolarization~~[particle depolarization ratio](#) value significantly exceeds the 532  
7 nm value and the 532 nm value significantly exceeds the 1064 nm value.

8 The pattern of larger particle depolarization ratio at 532 nm compared to 1064 nm has regularly  
9 been observed for smoke with the HSRL-1 instrument; indeed the HSRL-1 aerosol classification  
10 methodology (Burton et al., 2012) takes advantage of this spectral dependence. One such example  
11 is the aged southwest Canadian smoke plume observed on the eastern seaboard of the U.S. on 2  
12 August 2007 that was shown by Burton et al. (2012). For that prior case, the particle depolarization  
13 ratios were  $0.07 \pm 0.01$  and  $0.019 \pm 0.005$  at 532 and 1064 nm, respectively. The observation by HSRL-  
14 2 is the first time to our knowledge that particle depolarization ratio has been reported for pure  
15 smoke at three wavelengths. Note that while the 532 nm particle depolarization ratio for the  
16 smoke case is only about 25-30% of the value for pure dust, the large particle depolarization ratio  
17 at 355 nm for the smoke layer is quite comparable to the 355 nm value for dust.

#### 18 **b. Discussion of particle depolarization ratio of smoke**

19 Observed [linear](#) particle depolarization ratios for smoke are quite variable. Frequently the 532 nm  
20 particle depolarization ratio is observed to be only a few percent at most and often discounted as  
21 negligibly close to zero (e.g. Mattis et al., 2003; Müller et al., 2005). For example, small values of  
22 about 2-3% at 532 nm were observed by HSRL-1 in smoke plumes in Mexico City during the  
23 Megacity Initiative: Local and Global Research Observations (MILAGRO) field mission described  
24 by de Foy et al. (2011). In the published images of HSRL-1 measurements, the smoke plumes are  
25 obvious as local minima in the particle depolarization ratio compared to the relatively high  
26 ambient values which are due to regional dusty background conditions. However, higher values  
27 of particle depolarization ratio at 532 nm of 0.05-0.11 have sometimes been observed in aged  
28 smoke layers, as for example 0.07 observed by HSRL-1 on 2 August 2007 noted above (Burton et  
29 al., 2012), 0.06-0.11 for transported Canadian smoke reported in Lindenberg, Germany during the  
30 Lindenberg Aerosol Characterization Experiment (LACE) 1998 by Fiebig et al. (2002), [0.06 to 0.08](#)  
31 [for 3-4 day old smoke from North America observed over Germany in 2011 by Dahlkötter et al.](#)  
32 [\(2014\)](#), 0.06 for transported Siberian smoke observed in Tokyo in 2003 by Murayama et al. (2004)  
33 and 0.05 for Alaskan forest fire smoke observed by Sassen and Khvorostyanov (2008) in 2004.  
34 Sugimoto et al. (2010) discuss a case in which much higher 532 nm particle depolarization ratios  
35 were observed for smoke from a Mongolian forest fire transported to Japan in 2007. The particle  
36 depolarization ratios measured for this smoke were 0.12, 0.14 and 0.15 for layers at two different  
37 altitudes observed at Nagasaki and Tsukuba. [Nisantzi et al. \(2014\) observe values of 0.09 to 0.18](#)  
38 [at 532 nm for aerosol from Turkish fires observed in Cyprus after one to four days of transport.](#)

39 The causes of depolarization by smoke are not well understood. Two possible explanations are  
40 frequently cited in literature: lifting and entrainment of surface soil into the smoke plume and  
41 asymmetry of smoke particles themselves.

1 For example, the smoke observed by Sugimoto et al. (2010) was associated with  
2 pyrocumulonimbus and therefore it is inferred that strong convection lifted soil particles from  
3 the surface into the smoke plume, explaining the unusually large particle depolarization ratios.  
4 Lifting of soil particles is also cited as a possible explanation of the more moderate but still non-  
5 negligible particle depolarization ratios reported by Fiebig et al. (2002), since chemical  
6 composition analysis of this plume reveals the presence of aluminosilicates and iron  
7 oxides/hydroxides. [Nisantzi et al. \(2014\) assume that the depolarization is due to fine mode dust  
8 and infer the mass fraction of dust mixed in the smoke plumes using lab measurements of fine  
9 and coarse dust by Sakai et al. \(2010\).](#) However, this explanation is not sufficient in every case.  
10 Murayama et al. (2004) discount soil lifting for their observations of depolarizing smoke since no  
11 signature of mineral dust is found in a chemical analysis of this plume. Instead, they cite non-  
12 sphericity of smoke particle aggregates as the probable cause. Martins et al. (1998) discuss the  
13 non-sphericity of smoke particles observed by scanning electron microscope images and an  
14 electro-optical aerosol asymmetry analyzer for a variety of smoke types during the Smoke,  
15 Clouds, and Radiation – Brazil (SCAR-B) project in 1995. They concluded that most of the non-  
16 spherical particles in the observed smoke were chain aggregates of small black carbon particles,  
17 and that the non-sphericity tends to increase with the black carbon ratio. Young smoke (<1 hour)  
18 is composed of open clusters of high non-sphericity while aged smoke is composed of tighter  
19 clusters with lesser non-sphericity. They also point out that flaming fires (high combustion  
20 efficiency) tend to produce more non-spherical particles than smoldering fires.

21 Referring back to the theoretical calculations of spectral depolarization [for spheroids](#) discussed  
22 in Section 3.c., [the larger particle depolarization ratio at 355 nm compared to longer wavelengths  
23 may indicate a smaller size for the non-spherical particles than the dust cases, although of course  
24 these results may be only qualitatively applicable to more general particle shapes.](#) ~~Gasteiger and  
25 Freudenthaler (2014) show that spectral dependence monotonically decreasing with wavelength  
26 would be possible for non-spherical particles approximately the size of the smallest measured  
27 wavelength and one third the size of the longest wavelength, that is, about 355 nm. Therefore, it  
28 seems likely that the large particle depolarization ratio at 355 nm in the HSRL-2 case of 17 July  
29 2014 indicates that the cause of the depolarization in this case is non-sphericity of the relatively  
30 smaller soot particles themselves, rather than entrained dust particles or ice crystals which would  
31 be expected to be larger. Note, these calculations were performed by modeling the non-spherical  
32 particles as spheroids, so may be only qualitatively applicable to carbon aggregates.~~

33 Theoretical calculations of [linear](#) particle depolarization [ratio](#) by aggregates of soot are given by  
34 (e.g. Sorensen, 2001; Bescond et al., 2013; Kahnert et al., 2012). Calculations for bare carbon  
35 aggregates (Sorensen, 2001; Bescond et al., 2013) tend to produce small values of the particle  
36 depolarization ratio, much smaller than what was measured in the HSRL-2 case study. However,  
37 Kahnert et al. (2012) model the scattering properties of [a more realistic particle morphology](#), light  
38 absorbing carbon (LAC)-aggregates embedded in a sulfate shell, and obtain larger values. They  
39 use the discrete dipole method to calculate the depolarization ratio of the aggregate particle in  
40 the backscatter direction at 304.0, 533.2 and 1010.1 nm. They show that the particle depolarization  
41 [ratio](#) generally increases with aggregate particle radius ([defined as volume-equivalent radius](#))  
42 and with the volume fraction of LAC in the aggregate. The values also increase with decreasing

1 wavelength for aggregate ~~volume-equivalent radii~~~~particle sizes~~ of 400 nm and smaller; but for  
2 500 nm particles, the particle depolarization ~~ratio~~ peaks at the middle wavelength, 533.2 nm. The  
3 maximum calculated particle depolarization ~~ratios~~~~values~~ for 7% LAC fraction by volume is 0.08-  
4 0.11 for 500 nm particles at 533.2 nm. This is comparable to the 532 nm measurement on 17 July  
5 2014; however, the calculated value at 304.0 nm for the same size and LAC volume fraction is  
6 0.05-0.07, much smaller than the measured value (at 355 nm) of 0.24. The largest values calculated  
7 for the 304.0 nm wavelength are about 0.12-0.21, occurring for the case of 400 nm particle ~~volume-~~  
8 ~~equivalent~~ radius~~s~~ and 20% LAC volume fraction. The full set of theoretical calculations of particle  
9 depolarization ratio for 20% LAC volume fraction are replotted in Figure 15 for all three  
10 wavelengths to highlight the wavelength dependence. Figure 15 also indicates the HSRL-2  
11 observed particle depolarization ratio in the 17 July smoke plume (at 355, 532, and 1064 nm). The  
12 calculated particle depolarization ratios are roughly comparable in magnitude to the HSRL-2  
13 measurements for ~~volume-equivalent radii~~~~particle sizes~~ in the 400-500 nm range, but the  
14 wavelength dependence matches better for smaller particle sizes. LAC volume fraction of 20% is  
15 quite high and may be unrealistic for this smoke layer and the modeled single scattering albedos  
16 for 20% LAC volume fraction, shown by Kahnert et al. (2012), are quite low (below 0.7 at 533.2  
17 nm), indicating exceptionally absorbing particles, so this model is probably not an exact match  
18 for the observation in this case. Yet, it is encouraging that an estimate of particle depolarization  
19 ratio of the right magnitude can be made by modeling coated soot aggregates. The model results  
20 were for a constant fractal dimension of 2.6, structural prefactor of 1.2, and a monomer radius of  
21 25 nm, values chosen to be consistent with the findings for soot aerosol in Mexico City (Adachi  
22 and Buseck, 2008). In the HSRL-2 case study, there could be a different fractal dimension, different  
23 size monomer component, different coating or a different fraction of soot per aggregate. In  
24 addition, the spectral dependence of the refractive index is not well known, and this will have a  
25 significant effect on the spectral dependence of the particle depolarization ratio. While the  
26 current state of knowledge is not sufficient to perform a retrieval of particle size using the  
27 depolarization measurements alone, it is certainly worth noting that the particle depolarization  
28 ratio at three wavelengths is sensitive to and contains some information about the particle size of  
29 smoke particles, information that may play a role in future microphysical retrievals.

## 30 5. Summary and Discussion

31 We have presented three case studies of depolarizing aerosol observed at three wavelengths (355  
32 nm, 532 nm and 1064 nm) by the NASA airborne HSRL-2 instrument. These three aerosol layers,  
33 two dust-~~dominated~~ layers and a smoke layer, each have a different spectral dependence of ~~linear~~  
34 particle depolarization ~~ratio~~, but in each case, the 532 nm and 1064 nm values agree well with  
35 prior analogs in the long record of observations by the predecessor instrument, HSRL-1, and with  
36 comparable measurements in literature. The first case, transported Saharan ~~desert aerosol~~~~sst~~, has  
37 a peak in the spectral dependence of the particle depolarization ~~ratio~~ at 532 nm. This is in  
38 accordance with prior measurements of Saharan ~~dust~~ ~~desert aerosol~~ aloft both close to the source  
39 and transported to the Caribbean Sea. The second case, also a dust-~~dominated~~ measurement, but  
40 near the surface and very close to the source, has a spectral dependence increasing monotonically  
41 with wavelength, differing from the previous case primarily at the longest wavelength, 1064 nm.  
42 We infer the cause of this difference to be a greater fraction of very large particles due to proximity

1 to the source region; we believe that the largest particles have settled out of the observed Saharan  
2 layers but not the locally produced North American dust plumes in this case and a prior HSRL-1  
3 case. Our third case study is of an elevated, transported smoke layer and has spectral  
4 depolarization ratio decreasing monotonically with wavelength. Again we infer that the  
5 difference in spectral dependence is due to the size of the non-spherical particles, and specifically,  
6 that the depolarization is probably due to smoke aerosols and may be explained by ~~ation in this~~  
7 ~~case is probably attributable to soot aggregates in the smoke.~~

8 Microphysical retrievals (Müller et al., 2014) were not available for these HSRL-2 measurement  
9 cases, because the current state of these retrievals is limited to spherical particles. However, as  
10 suggested by Gasteiger and Freudenthaler (2014) for dust and ash, these observations suggest the  
11 possibility that the particle depolarization ratio measurements may aid in retrievals of particle  
12 size of non-spherical dust and smoke particles in the future.

13 More immediately, since the upcoming EarthCARE satellite mission will include a lidar  
14 instrument that measures particle depolarization ratio and lidar ratio at 355 nm only, it is valuable  
15 to have measurements of the spectral dependence of depolarization ratio for depolarizing aerosol  
16 types. These data will help to build the basis for comparing observations from EarthCARE to  
17 existing measurements at 532 nm from the CALIPSO satellite. Studying such correspondence is  
18 particularly motivated by the desire to identify different aerosol types observed by the  
19 EarthCARE satellite. Particle depolarization ratio is hoped to be particularly useful for  
20 distinguishing dust and ash from smoke and other aerosol types (Groß et al., 2014; Illingworth et  
21 al., 2015), as it already is for CALIPSO (Omar et al., 2009).

22 However, as illustrated by the case studies presented here, there is not a single consistent spectral  
23 dependence of particle depolarization ratio. On the positive side (from the perspective of  
24 corresponding CALIPSO and EarthCARE measurements), for ~~pure aerosols dominated by~~ dust  
25 the 355 nm and 532 nm particle depolarization ratios appear to be fairly consistent even for  
26 different particle sizes and may be relatively easily converted. Variation in the 532 nm and 355  
27 nm particle depolarization ratio for dusty aerosols has been primarily linked to the fraction of  
28 dust particles in a sample (Sugimoto et al., 2003) so ~~there is no reason to think that~~ inferences of  
29 dust mixing ratio (e.g. Sugimoto and Lee, 2006; Tesche et al., 2009a; Nishizawa et al., 2011; Burton  
30 et al., 2014) may ~~not be done proceed~~ with 355 nm measurements. However, in the case of dust-  
31 dominated aerosol, the 355 nm signal consistently is significantly both smaller and more difficult  
32 to measure accurately than the 532 nm signal, and so the signature of dust may be harder to detect  
33 from space at 355 nm than at 532 nm for dilute dust mixtures.

34 On the other hand, the third case study presented here showed that smoke particle depolarization  
35 ratio can be significantly larger at 355 nm than at 532 nm, and in fact the particle depolarization  
36 ratio at 355 nm for this smoke case was quite comparable to the dust-dominated cases. If this is  
37 not an isolated case, and this signature proves typical for some subset types of smoke aerosol in  
38 particular conditions, the EarthCARE satellite may observe significant particle depolarization in  
39 some types of smoke as well as in dust-dominated aerosol. If this is the case, global observations  
40 of smoke depolarization will present an exciting opportunity for improving our understanding

1 of the optical properties of smoke and how they change with age and processing; however, it will  
2 also present a challenge. That is, a significant particle depolarization ratio signature at the single  
3 wavelength of 532 nm has been sufficient for distinguishing dust-dominated aerosol from smoke  
4 aerosol, but at 355 nm this signature by itself is more ambiguous, if the smoke case presented here  
5 is not an isolated case. if particle depolarization ratio measurements are made at 355 nm only, a  
6 significant particle depolarization ratio signature alone will not be sufficient for the  
7 discrimination of dust and smoke from satellite lidar measurements. EarthCARE will also  
8 measure lidar ratio at 355 nm; this is related to absorption but has significant variability for smoke  
9 (Groß et al., 2014). EarthCARE will not have backscatter or extinction measurements at a second  
10 wavelength to give an indicator of particle size. Therefore, for any cases where particle  
11 depolarization ratio is ambiguous, it seems that smoke and dust may not be easily separable.

## 12 **Appendix: Systematic ~~Uncertainties~~Errors**

13 In Section 2.b. we provided systematic uncertainties~~bounds on the systematic errors~~ in the linear  
14 volume depolarization ratio of the larger of 4.7% (fractional relative error) or 0.001 (absolute) in  
15 the 355 nm channel, the larger of 5% fractional (relative) error or 0.007 (absolute) error in the 532  
16 nm channel, and the larger of 2.6% fractional (relative) error or 0.007 (absolute) error in the 1064  
17 nm channel. For R (total aerosol scattering ratio) we estimate the upper bound on the systematic  
18 uncertainty error to be 4.1% for the 532 nm channel, 5% for the 355 channel, and 20% for the 1064  
19 nm channels. The systematic uncertainties are estimated conservatively as confidence limits, such  
20 that we expect a high probability that the true systematic error is within this uncertainty. Here in  
21 the Appendix, we discuss the error sources and estimates of the uncertainties~~upper bounds~~ in  
22 more detail.

23 For the linear volume depolarization ratio, potential sources of systematic errors include an error  
24 in the polarization gain ratio calibration or cross-talk between the co-polarized and cross-  
25 polarized signals. The polarization gain ratio calibration generally occurs once or twice per flight  
26 as described above in Section 2.a. Since gain ratios can potentially change during a flight, due to  
27 temperature changes for example, our best estimate of uncertainty in the gain ratio during a flight  
28 is obtained by examining t-The change instability of the gain ratio can be assessed by looking at  
29 the change between successive calibrations in the same flight. Conservatively choosing the mean  
30 difference plus two standard deviations (calculated for all flights with at least two calibrations  
31 per flight in the most recent field campaign) as a realistic limit on the probable upper bound on  
32 the polarization gain ratio systematic error yields 4.7% uncertainty for the 355 nm channel, 5.0%  
33 for the 532 nm channel, and 2.6% for the 1064 nm channel. The fractional relative systematic  
34 uncertainty error from the polarization gain ratio propagates directly to the volume  
35 depolarization ratio, since the volume depolarization ratio is linearly related to the polarization  
36 gain ratio.

37 Residual cross-talk is known to occur in polarization lidars, and must be carefully characterized  
38 and eliminated as much as possible. A well-known potential source of cross talk occurs in the  
39 reflected channel from a polarization beam splitter. Therefore~~However~~, this system has been  
40 designed with extra polarization beam splitters to eliminate that potential concern, as described  
41 in Section 2.a and illustrated in Figure 2. Clear-air studies have found a small residual cross-talk,  
42 which appears as a value of the “clear air” volume depolarization ratio that exceeds the

1 theoretical (molecular only) value. As described in Section 2.a., the narrow bandwidths in the  
 2 system completely eliminate the rotational Raman scattering sidebands, and so the molecular  
 3 depolarization ratio value is temperature independent and is calculated to be known accurately  
 4 to be 0.0036 using N<sub>2</sub> and O<sub>2</sub> molecules (ignoring a negligible wavelength dependence due to  
 5 non-linear molecules like CO<sub>2</sub>) (She, 2001; Behrendt and Nakamura, 2002). Since 2006, we have  
 6 historically measured minimum depolarization ratio values in clear air that exceed the  
 7 theoretical value, namely values of approximately 0.006 in the 355 nm channel, of approximately  
 8 0.008 in the 1064 nm channel, and 0.0085-0.0135 in the 532 nm channel, which we ~~can~~ attribute  
 9 to a small remaining ellipticity in the optics or stress birefringence in the aircraft window. ~~The~~  
 10 ~~cross talk due to ellipticity in the transmission system can be modeled, as follows, as an~~  
 11 ~~ellipticity in the polarization (or, alternately, as an error in the polarization angle, leading to the~~  
 12 ~~same result).~~

13 We start with the polarization Stokes vector (Born and Wolf, 1999)

$$\vec{S} = \begin{pmatrix} 1 \\ \cos(2\theta)\cos(2\psi) \\ \cos(2\theta)\sin(2\psi) \\ \sin(2\theta) \end{pmatrix} \quad (4)$$

14 where the angles  $\theta$  and  $\psi$  represent the ellipticity angle and polarization offset angle, plus the  
 15 Mueller matrix for a partially depolarizing backward scattering process (Mishchenko and  
 16 Hovenier, 1995; Gimmetstad, 2008),

$$\hat{M} = \begin{pmatrix} 1 & 0 & 0 & 0 \\ 0 & 1 - \frac{2\delta_{tot}}{\delta_{tot} + 1} & 0 & 0 \\ 0 & 0 & \frac{2\delta_{tot}}{\delta_{tot} + 1} - 1 & 0 \\ 0 & 0 & 0 & \frac{4\delta_{tot}}{\delta_{tot} + 1} - 1 \end{pmatrix} \quad (5)$$

17 Assuming there is a ~~rotation~~ polarization offset angle (rotation) or ellipticity in the transmission,  
 18 we derive the correction to the measured depolarization ratio to be

$$\delta_{corr} = \frac{\delta_{meas} + \chi + \chi\delta_{meas} - 1}{\chi - \delta_{meas} + \chi\delta_{meas} + 1} \quad (6)$$

19 where

$$\chi = \cos(2\theta)\cos(2\psi) \quad (7)$$

20 ~~The ellipticity and polarization offset angles  $\theta$  and  $\psi$  are treated identically in Eqs (5) and (6), and~~  
 21 ~~are generically considered 'cross talk'.~~ The subscript 'meas' indicates the measured  
 22 depolarization ratio and 'corr' represents the corrected depolarization ratio, assuming the  
 23 measurement to be affected by cross-talk, caused by ellipticity or an angle offset, or both. Eqs (6)  
 24 and (7) make no distinction between the ellipticity and polarization offset angles  $\theta$  and  $\psi$ .  
 25 Therefore, we can model cross talk due to either source using the same correction, although  
 26 noting that an offset angle would additionally affect the polarization gain ratio, treated

1 ~~separately~~. Equation (6) represents a fairly constant shift in the ~~total volume~~ depolarization ratio  
2 approximately equal to the offset between the measured clear air value and the molecular-only  
3 depolarization ~~ratio value~~. An ellipticity angle of  $5.8^\circ$  ( $\chi=0.980$ ) would explain the error in the  
4 depolarization ratio ~~at 532 nm where the error is largest~~. A partial correction for the cross-talk  
5 was implemented in the archived HSRL-2 data (A full correction as in Eq (6) will be included in  
6 the next version of processed HSRL-2 data). Taking the ~~partial correction~~ into account, we  
7 include a ~~component factor~~ of 0.007 (absolute) due to cross-talk in the estimated volume  
8 depolarization ~~ratio error for the 532 nm and 1064 nm channels and 0.001 (absolute) for the 355~~  
9 ~~nm channel~~.

10 ~~We believe that the polarization angle error is much smaller than the inferred angle of  $5.8^\circ$ . An~~  
11 ~~error in the wave plate angle (offset angle calibration) would also affect the volume~~  
12 ~~depolarization ratio according to Eqs (5) and (6), but this effect is much smaller.~~ The ~~angle~~  
13 calibration procedure has been carefully designed and used successfully on both the HSRL-1 and  
14 HSRL-2 systems since 2006, and the ~~accuracy stability~~ of the ~~polarization offset~~ angle is high. ~~The~~  
15 ~~polarization angle calibration indicates the zero-point of the wave-plate angle where the~~  
16 ~~polarization of the detector is properly aligned compared to the transmitted beams; if the wave-~~  
17 ~~plate was not already set at this zero-point it is rotated to that point for subsequent science~~  
18 ~~measurements. Adjustments Changes indicated during polarization angle calibrations are at most~~  
19  $0.4^\circ$  of polarization ( $0.2^\circ$  rotation of the half-wave plate) for all channels (assessed, as before, using  
20 the mean plus two standard deviations for all flights having multiple ~~polarization angle~~  
21 calibrations during the latest field mission), ~~which is a good indicator of the systematic~~  
22 ~~uncertainty in the polarization angle for measurements between calibrations~~. Since the  
23 ~~polarization offset~~ angle calibration error is much smaller than the inferred ellipticity ( $0.4^\circ$   
24 compared to  $6^\circ$ ), we do not include ~~polarization angle~~ calibration directly in the systematic  
25 ~~uncertainty error~~ budget.

26 Note that not only the volume depolarization ~~ratio~~ measurement itself but also the ~~de~~depolarization  
27 gain ratio calibration depend on the correct alignment of the calibration waveplates in Figure 1.  
28 The ~~de~~depolarization gain ratio assessment depends on a polarization alignment of  $45^\circ$  during  
29 calibration. This effect on the measured gain will be reflected in the ~~stability error~~ of the gain  
30 ratio, and so is already included in the ~~polarization gain ratio systematic uncertainty error~~  
31 ~~assessment~~ discussed above.

32 The calculated ~~aerosol depolarization particle depolarization~~ ratio,  $\delta_i$ , is additionally affected by  
33 any errors in the total ~~aerosol~~ scattering ratio,  $R$ , in Eq (2). For 532 nm, the only significant  
34 potential systematic error in  $R$  is an error in the ~~calibration~~ gain ratio between the aerosol and  
35 molecular channels. The ~~uncertainty stability~~ of the ~~is aerosol-to-molecular~~ gain ratio was  
36 assessed in a similar manner to the offset angle and polarization gain ratios given above, ~~by~~  
37 ~~examining the change in the gain ratio on flights where multiple aerosol-to-molecular gain~~  
38 ~~calibrations occurred during a flight~~. The ~~uncertainty upper bound~~ in the 532 nm ~~backscatter~~  
39 ~~aerosol-to-molecular~~ gain ratio is estimated to be 4.1% ~~from the mean difference plus two~~  
40 ~~standard deviations for all flights with multiple calibrations in the latest field mission~~. A  
41 systematic ~~uncertainty error~~ of 4.1% in the ~~aerosol-to-molecular~~ gain ratio propagates directly to

1 a 4.1% ~~uncertainty error~~ in  $R$  for the 532 nm channel, since the aerosol-to-molecular gain ratio and  
2 the total aerosol scattering ratio are linearly related.

3 The 355 nm and 1064 nm channels are somewhat more complicated, because it is not possible to  
4 calibrate them directly in the same way as 532 nm. The iodine filter for the 532 nm HSRL channel  
5 allows for essentially complete separation of the aerosol signal from the total (aerosol plus  
6 molecular) signal, but this is not the case for the interferometer used at 355 nm, and the 1064 nm  
7 channel has only one total channel with no separation. So for these channels, the calibration is  
8 transferred from 532 nm in a cloud-free region in the free troposphere, as described by Hair et al.  
9 (2008). In the calibration transfer region, we do not assume that there is no aerosol, but do look  
10 for regions where the aerosol backscatter ratio is small and can be inferred from the value at 532  
11 nm assuming a constant backscatter Ångström exponent. By using a range of reasonable  
12 backscatter Ångström exponents, we conservatively estimate an ~~uncertainty error~~ of 3% in total  
13 aerosol scattering ratio for the 355 nm channel. The 1064 nm aerosol backscatter ratio is also  
14 affected by the assumption of the lidar ratio to use for separating the aerosol and molecular part;  
15 this sensitivity is relatively small for backscatter at 1064 nm, compared to shorter wavelengths or  
16 compared to the sensitivity of extinction. Taking these sources into account, we conservatively  
17 use 20% as the ~~uncertainty in upper bound on error on~~ total aerosol scattering ratio,  $R$ , at 1064 nm.

18 For the 355 nm channel, the system implements an interferometer to spectrally separate the  
19 aerosol and molecular scattering components. The ratio of the aerosol signal in the aerosol-  
20 dominated channel to the aerosol signal in the molecular-dominated channel is referred to as the  
21 contrast ratio, which needs to be determined to accurately derive the total aerosol scattering ratio.  
22 For the HSRL-2 system, fairly high contrast ratios of 15-20 are routinely achieved. Our estimate  
23 of the error in the contrast ratio definition is usually a few percent but can be up to 20%. A 20%  
24 error in the contrast ratio for the smoke case presented here would produce an error in the total  
25 aerosol scattering ratio of less than 4%. Adding the contrast ratio ~~uncertainty error~~, 4%, and the  
26 calibration transfer ~~uncertainty error~~, 3%, in quadrature yields an uncertainty of 5% for  
27 conservative estimate of the 355 nm total aerosol scattering ratio ~~error of 5%~~.

28 The ~~uncertainties estimates~~ given above are intended to be an ~~conservative~~ upper bound on the  
29 probable systematic errors. The systematic errors on the three quantities,  $\delta_{mol}$ ,  $\delta_{tot}$ , and  $R$ , are  
30 independent and, since their actual values within these ~~uncertainty estimates upper bounds~~ are  
31 unknown, they should be treated statistically. We therefore combine the three sources of  
32 systematic ~~uncertainty error~~ in quadrature to assess the ~~potential~~ systematic ~~uncertainty error~~ in  
33 the ~~aerosol depolarization particle depolarization~~ ratio,  $\delta_a$ . The propagation is described by the  
34 following equation:

$$\left(\frac{\Delta\delta_a}{\delta_a}\right)^2 = F_R \left(\frac{\Delta R}{R}\right)^2 + F_{\delta_{tot}} \left(\frac{\Delta\delta_{tot}}{\delta_{tot}}\right)^2 + F_{\delta_m} \left(\frac{\Delta\delta_m}{\delta_m}\right)^2 \quad (8)$$

35 Here, the  $\Delta$  symbol indicates the systematic ~~uncertainty error~~ associated with the various  
36 quantities and the propagation factors  $F_x$  are defined like this:

$$F_x = \left( \frac{x}{\delta_a} \frac{\partial \delta_a}{\partial x} \right)^2 \quad (9)$$

1 The partial derivatives are calculated easily from Eq. (2) which relates the particle depolarization  
 2 ratio to the factors  $R_s$ ,  $\delta_{tot}$ , and  $\delta_m$ . From Eq. (8), the propagation factors,  $F_x$ , are therefore the  
 3 factors by which the relative uncertainty in the aerosol depolarization particle depolarization  
 4 ratio is magnified with respect to the relative uncertainty in the component variables.

5 These factors vary with total aerosol scattering ratio and ~~volume total~~ depolarization ratio but do  
 6 not depend on the systematic ~~uncertainty errors~~. To illustrate the behavior of the aerosol  
 7 ~~depolarization particle depolarization~~ ratio systematic ~~uncertainty error~~, Table 2 gives the value  
 8 of ~~aerosol depolarization particle depolarization ratio~~ and its propagated systematic  
 9 ~~uncertainty error~~ (as a percent error) for benchmark values of the total aerosol scattering ratio and  
 10 the ~~volume total~~ and molecular depolarization ratios, plus their estimated systematic  
 11 ~~uncertainty errors~~. It also gives the propagation factors,  $F_x$ . From Table 2, it is clear that the  
 12 propagation factor for the ~~uncertainty error~~ in the molecular depolarization ratio is always small,  
 13 the propagation factor for the ~~total volume~~ depolarization ratio ~~uncertainty error~~ is typically 1-2,  
 14 and the propagation factor for uncertainty in the total aerosol scattering ratio,  $F_R$ , varies  
 15 significantly with the total aerosol scattering ratio.  $F_R$  is comparable to  $F_{\delta_{tot}}$  except when the total  
 16 aerosol scattering ratio is fairly small; in the case of small scattering, it is significantly larger.

#### 17 **Acknowledgements**

18 Funding for this research came from the NASA HQ Science Mission Directorate Radiation  
 19 Sciences Program and the DISCOVER-AQ project. M. Kahnert acknowledges funding by the  
 20 Swedish Research Council (*Vetenskapsrådet*) under project 621-2011-3346. The authors also  
 21 acknowledge the NOAA Air Resources Laboratory (ARL) for the provision of the HYSPLIT  
 22 transport and dispersion model and READY website (<http://www.arl.noaa.gov/ready.php>) used  
 23 for some of the analysis described in this work. The MODIS images used in Figure 7 were  
 24 obtained from the MODIS Adaptive Processing System (MODAPS) archive. Thank you to Rich  
 25 Hare and Terry Mack of the NASA Langley Engineering Directorate for their exceptional work  
 26 on the HSRL-2 instrument. The authors are also very grateful to the NASA Langley B200 King  
 27 Air crew from the California and Colorado deployments: Mike Basnett, Dale Bowser, Les Kagey,  
 28 Howie Lewis, Scott Sims, Mike Wusk, and Rick Yasky from LaRC and also Kurt Blankenship and  
 29 Munro Dearing for their dedication in support of HSRL measurements.

1 **Tables**

2 **Table 1.** Measured properties for specific dust and smoke samples. To obtain these values, samples were taken at  
 3 specific times and altitudes comprising 400-4500 distinct measurement points. For the dust cases, values were  
 4 chosen near the peak value of the 532 nm particle depolarization ratio, where it can be inferred that the aerosol is  
 5 nearly pure dust. The values are reported as mean±standard deviation for the sample. Systematic uncertainties  
 6 error bounds for aerosol depolarization particle depolarization ratio from HSRL-2 are indicated in parentheses.

		Layer AOD (532 nm)	<u>Linear p</u> particle depolarization ratio (1064 nm)	<u>Linear p</u> Particle depolarization ratio (532 nm)	<u>Linear p</u> Particle depolarization ratio (355 nm) (HSRL-2 only)	Aerosol Backscatter Ångström exponent (532/1064)
Midwest U.S. 13 July 2014	transported Saharan dust	0.10	0.270±0.005(0.009)	0.304±0.005(0.022)	0.246±0.018(0.055)	0.46±0.03
Caribbean 18 August 2010	transported Saharan dust	0.25	0.278±0.012	0.327±0.018	--	0.68±0.13
Chihuahuan desert 8 February 2013	local North American dust	0.02	0.383±0.006(0.011)	0.373±0.014(0.023)	0.243±0.046(0.045)	-0.09±0.04
Pico de Orizaba 12 March 2006	local North American dust	0.31	0.400±0.009	0.334±0.018	--	-0.9±0.4
Denver 17 July 2014	smoke	0.05	0.018±0.002(0.008)	0.093±0.015(0.012)	0.240±0.010(0.021)	1.1±0.1
East Coast US 2 August 2007	smoke	0.06	0.019±0.005	0.068±0.010	--	0.62±0.25

7

8

1 Table 2. Illustrates the systematic ~~uncertaintyerror~~ in ~~linear aerosol depolarizationparticle depolarization~~ ratio  
2 propagated from the systematic ~~uncertaintieserrors~~ in total aerosol scattering ratio, linear volume depolarization  
3 ratio, and linear molecular depolarization ratio. Benchmark values of R (total aerosol scattering ratio),  $\delta_{tot}$  (the  
4 volume depolarization ratio) and  $\delta_{mol}$  (the molecular depolarization ratio) and typical systematic ~~uncertaintieserrors~~  
5 are given in the first three columns. Columns 4-6 give the propagation factors, as described in the text. Column 7  
6 gives the resulting ~~aerosol depolarizationparticle depolarization~~ ratio and systematic ~~uncertaintyerror~~ for each  
7 benchmark set. Note: percentages given in this table are ~~fractionalrelative uncertaintieserrors~~ (not depolarization  
8 ratio units).

R	$\delta_{tot}$	$\delta_m$	$F_R$	$F_{\delta_{tot}}$	$F_{\delta_m}$	$\delta_a$
3.0±5%	0.15±5%	0.0036±1%	0.37	1.2	1e-4	0.24±6%
3.0±5%	0.05±5%	0.0036±1%	0.26	1.1	8e-4	0.07±6%
2.0±5%	0.2±5%	0.0036±1%	2.2	1.6	3e-4	0.49±10%
2.0±5%	0.1±5%	0.0036±1%	1.4	1.3	6e-4	0.22±8%
2.0±5%	0.05±5%	0.0036±1%	1.1	1.2	0.002	0.10±8%
1.2±5%	0.05±5%	0.0036±1%	45	1.9	0.008	0.37±34%

9

10

1 **Figure Captions**

2 Figure 1. A simplified block diagram of the transmitter optics relevant for [linear](#) depolarization  
3 measurements by HSRL-2. The two Glan Laser Polarizers are the primary components  
4 ensuring the transmitted laser light is polarized. The motorized Calibration Waveplates are  
5 used to align the output polarization to the receiver polarization analyzers. The 532 nm and  
6 1064 nm laser beams are maintained as a single beam. Since they do not exit the laser at the  
7 same polarization, a Co-alignment waveplate is used to align the polarization from the two  
8 wavelengths so that the Glan Laser Polarizer does not significantly reduce the amount of light  
9 transmitted at one of the wavelengths. The attenuator waveplate is used to attenuate the 532  
10 nm beam for eye safety considerations when flying at low altitudes, and for maximizing the  
11 power output otherwise.

12 Figure 2. A simplified block diagram of the receiver optics relevant for [linear](#) depolarization  
13 measurements by HSRL-2. Abbreviations: PMT=Photomultiplier Tube; APD = Silicon  
14 Avalanche Photo Detector; DS = Dichroic Beam Splitter; PBS = Polarizing Beam Splitter; Co-pol  
15 = Co-polarized channel (with respect to the transmitted light); X-pol = Cross-polarized channel.  
16 The collimated light arrives from the telescope and is split into the three wavelengths using  
17 Dichroic Beam Splitters. The first optical component filters solar background using either an  
18 interference filter (indicated "Filter") or an interference filter and etalon in combination  
19 (indicated "Filter\*"). The 1064 nm channel also includes an additional half-wave plate which  
20 can be used to correct any small polarization misalignment in the receiver system since the 532  
21 nm and 1064 nm beams are transmitted together. This half-wave plate is set during installation  
22 and is not rotated during normal operations. The light then passes through Polarization Beam  
23 Splitters to be separated into components co-polarized and cross-polarized with respect to the  
24 transmitted beam. Since the [transmittance](#) ratio of the light exiting a PBS is greater in the  
25 transmitted direction than in the reflected direction, a second "clean-up" PBS is included for  
26 each detector wavelength to further improve the [transmittance](#) ratio for the co-polarized light.  
27 (An extra clean up PBS is also included for the cross-polarized light in the 532 nm channel.) The  
28 co-polarized signal and cross-polarized signal are used to determine [volume](#) depolarization  
29 [ratio](#) at each wavelength. The 355 nm and 532 nm co-polarized channels are split again and  
30 passed through additional optics to separate the aerosol and molecular signals (see text).

31 Figure 3. [Curtains of aerosol](#) backscatter and extinction [coefficients](#) from HSRL-2 for  
32 observations on 13 July 2014 for a flight segment in Missouri and Kansas in the Midwestern  
33 United States.

34 Figure 4. [Linear](#) particle depolarization ratio at three wavelengths measured by the HSRL-2 for  
35 the same flight segment shown in Figure 3.

1 Figure 5. Line plots illustrating the volume and aerosol [linear](#) depolarization ratio profile for the  
2 HSRL-2 measurements at 17.2 UT (17:12 UT) on 13 July 2014. The volume depolarization [ratio](#)  
3 is shown as a thin black line. The error bars on the volume depolarization [ratio](#) represent  
4 random error (most are small and mostly obscured except 1064 nm). The [particle](#)  
5 depolarization [ratio](#) is shown as a thick colored line. Colored error bars indicate random error  
6 (most are small enough to be obscured by the line) while gray error bars indicate systematic  
7 [uncertainty](#), estimated as described in the text. Systematic [uncertainty](#) is not shown for the  
8 volume depolarization [ratio](#) but see text for estimate. The vertical resolution of these  
9 measurements is 30 m and the horizontal resolution is 10 s for all wavelengths.

10 Figure 6. Measurement curtain of aerosol backscatter [coefficient](#) at 532 nm from the HSRL-2  
11 instrument for a 280 km flight segment over the Southwestern U.S. on 8 February 2013, showing  
12 locally generated dust in approximately the first kilometer above the surface, as well as very  
13 tenuous smoke plumes at higher altitude. This flight segment was part of a transit flight from a  
14 field mission in California back to the B200 home base in Virginia. The selected flight segment is  
15 approximately 280 km and begins (at the left margin) on the slopes of the Dos Cabezas  
16 Mountains of Arizona and ends (at the right margin) at the Franklin Mountains in New Mexico.  
17 The ground surface is marked with a white line.

18 Figure 7. [Linear](#) particle depolarization ratio at three wavelengths observed by HSRL-2 on 8  
19 February 2013 in the Southwestern U.S. for the flight segment shown in Figure 6.

20 Figure 8. Line plots illustrating the volume and aerosol [linear](#) depolarization ratio profile for the  
21 HSRL-2 measurements at 17.14 UT (17:08 UT) on 8 Feb 2013. Error bars and resolutions as  
22 described for [Figure 5](#).

23 Figure 9. [Linear](#) particle depolarization ratio measured by HSRL-2 and HSRL-1 for the four dust  
24 cases discussed in the text. Note the spectral dependence (and in particular the 1064 nm  
25 channel) is different for the two local dust-[dominated aerosol](#) cases compared to the transported  
26 Saharan dust-[dominated aerosol](#) cases.

27 Figure 10. MODIS Aqua true color images of much of North America on 17 July 2014,  
28 composited from four granules at 19:45, 19:50, 21:25, and 21:30 UT. [The approximate location of](#)  
29 [the HSRL-2 observations discussed in the text \(Denver, Colorado\) is marked with a yellow dot.](#)  
30 [The bright white is clouds and snow cover and the gray is smoke. Several distinct smoke](#)  
31 [plumes indicate sources in the U.S. Pacific Northwest and in Western Canada within the cloud-](#)  
32 [free area on the western part of the continent. Significant smoke layers from these fires blanket](#)  
33 [the mid-continent cloud-free areas in the northern portion of the image. The HSRL-2](#)  
34 [measurements are close to the southern edge of the extensive smoke field. The approximate](#)

1 ~~location of the HSRL-2 observations discussed in the text (Denver, Colorado) is marked with a~~  
2 ~~yellow dot.~~

3 Figure 11. View of the smoke plume aloft on 17 July 2013 taken from the B200. Photo credit: Tim  
4 Berkoff.

5 Figure 12. 532 nm aerosol backscatter coefficient measurement curtain from HSRL-2 for a  
6 portion of a flight on 17 July 2014 in and around Denver, Colorado. Approximately the first  
7 third of the pictured curtain is a southbound track between the Boulder Atmospheric  
8 Observatory Tall Tower and Chatfield Park, CO. The remainder of the flight is a northbound leg  
9 between Chatfield Park and Fort Collins. The blank region indicates a tight turn at Chatfield  
10 Park where the lasers were shuttered. Scattered clouds are visible at the top of the boundary  
11 layer. Some of these have off-scale backscatter values (tan color) and some are thick enough to  
12 cause significant attenuation of the beam; beneath these, data are blanked out due to low signal.  
13 The white line indicates underlying terrain. The smoke layer at approximately 8 km is discussed  
14 in the text.

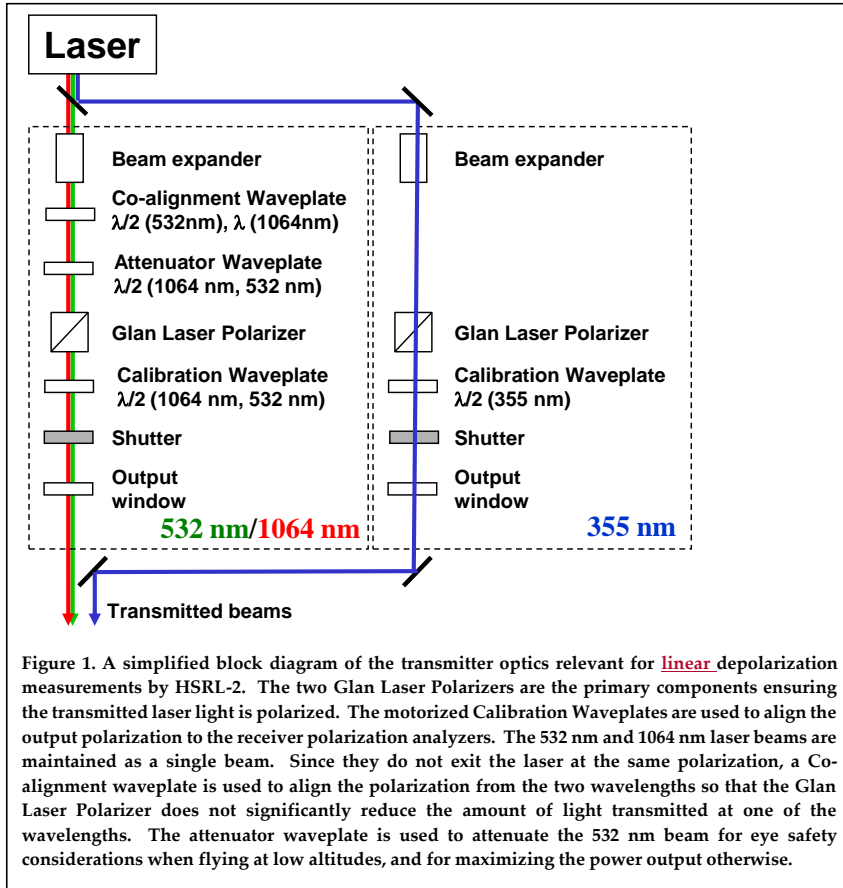
15 Figure 13. Linear particle depolarization ratio measurement curtains for the flight segment  
16 shown in Figure 12.

17 Figure 14. Line plots illustrating the volume and aerosol linear depolarization ratio profile for  
18 the HSRL-2 measurements at 19.3 UT (19:18 UT) on 17 July 2014. Error bars and resolutions as  
19 described for Figure 5.

20 Figure 15. Linear particle depolarization ratio at three wavelengths for soot aggregates  
21 embedded in a sulfate shell reproduced from Kahnert et al. (2012), for 20% LAC volume  
22 fraction. Dots indicate five realizations with randomly generated geometries, per aggregate  
23 volume-equivalent particle radius, and the colored lines connect the averages of the five for  
24 each wavelength. The legend shows the aggregate volume-equivalent particle radii at which the  
25 calculation was performed. The thick black line indicates the particle depolarization ratios  
26 measured by airborne HSRL-2 within a smoke plume observed on 17 July 2014 at 355, 532, and  
27 1064 nm.

1 Figures

2



3

Figure 1. A simplified block diagram of the transmitter optics relevant for linear depolarization measurements by HSRL-2. The two Glan Laser Polarizers are the primary components ensuring the transmitted laser light is polarized. The motorized Calibration Waveplates are used to align the output polarization to the receiver polarization analyzers. The 532 nm and 1064 nm laser beams are maintained as a single beam. Since they do not exit the laser at the same polarization, a Co-alignment waveplate is used to align the polarization from the two wavelengths so that the Glan Laser Polarizer does not significantly reduce the amount of light transmitted at one of the wavelengths. The attenuator waveplate is used to attenuate the 532 nm beam for eye safety considerations when flying at low altitudes, and for maximizing the power output otherwise.

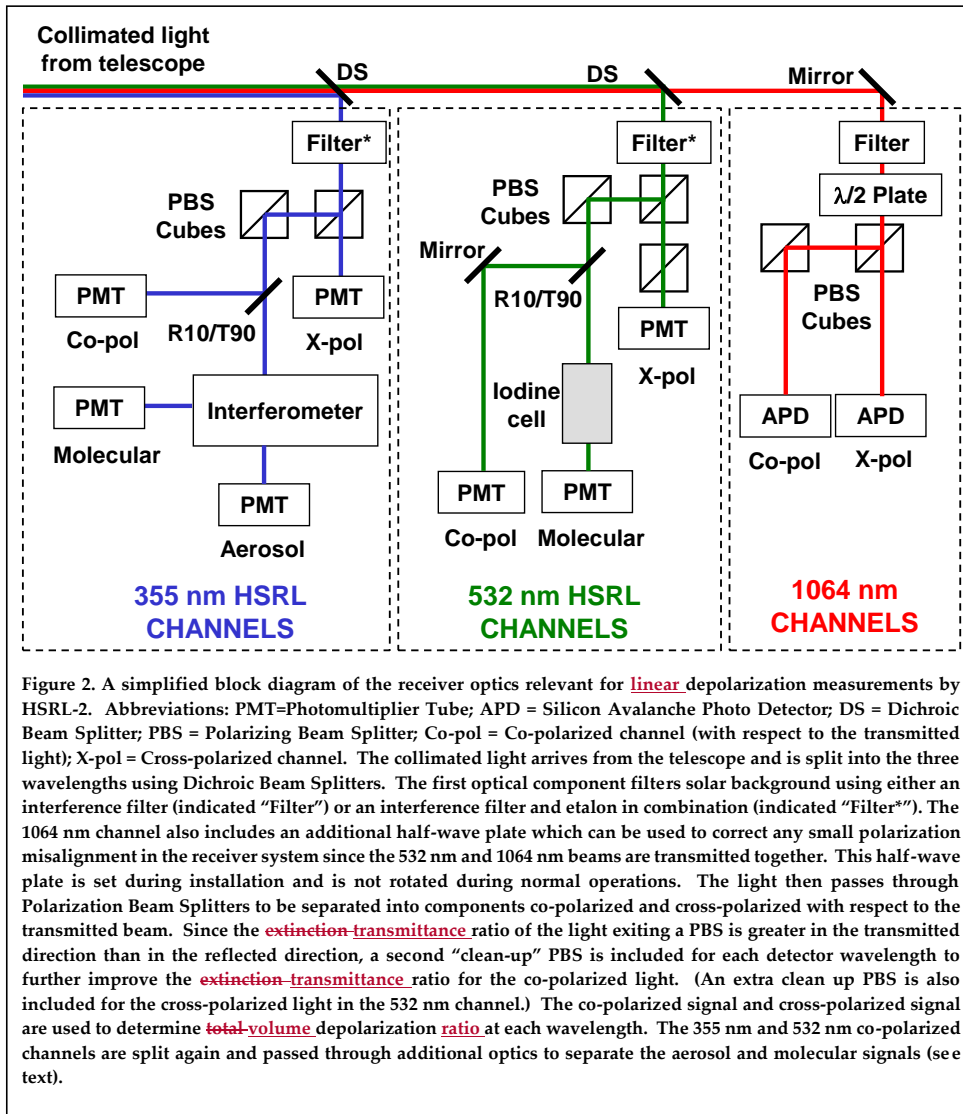


Figure 2. A simplified block diagram of the receiver optics relevant for linear depolarization measurements by HSRL-2. Abbreviations: PMT=Photomultiplier Tube; APD = Silicon Avalanche Photo Detector; DS = Dichroic Beam Splitter; PBS = Polarizing Beam Splitter; Co-pol = Co-polarized channel (with respect to the transmitted light); X-pol = Cross-polarized channel. The collimated light arrives from the telescope and is split into the three wavelengths using Dichroic Beam Splitters. The first optical component filters solar background using either an interference filter (indicated "Filter") or an interference filter and etalon in combination (indicated "Filter\*"). The 1064 nm channel also includes an additional half-wave plate which can be used to correct any small polarization misalignment in the receiver system since the 532 nm and 1064 nm beams are transmitted together. This half-wave plate is set during installation and is not rotated during normal operations. The light then passes through Polarization Beam Splitters to be separated into components co-polarized and cross-polarized with respect to the transmitted beam. Since the extinction-transmittance ratio of the light exiting a PBS is greater in the transmitted direction than in the reflected direction, a second "clean-up" PBS is included for each detector wavelength to further improve the extinction-transmittance ratio for the co-polarized light. (An extra clean up PBS is also included for the cross-polarized light in the 532 nm channel.) The co-polarized signal and cross-polarized signal are used to determine total-volume depolarization ratio at each wavelength. The 355 nm and 532 nm co-polarized channels are split again and passed through additional optics to separate the aerosol and molecular signals (see text).

1  
2

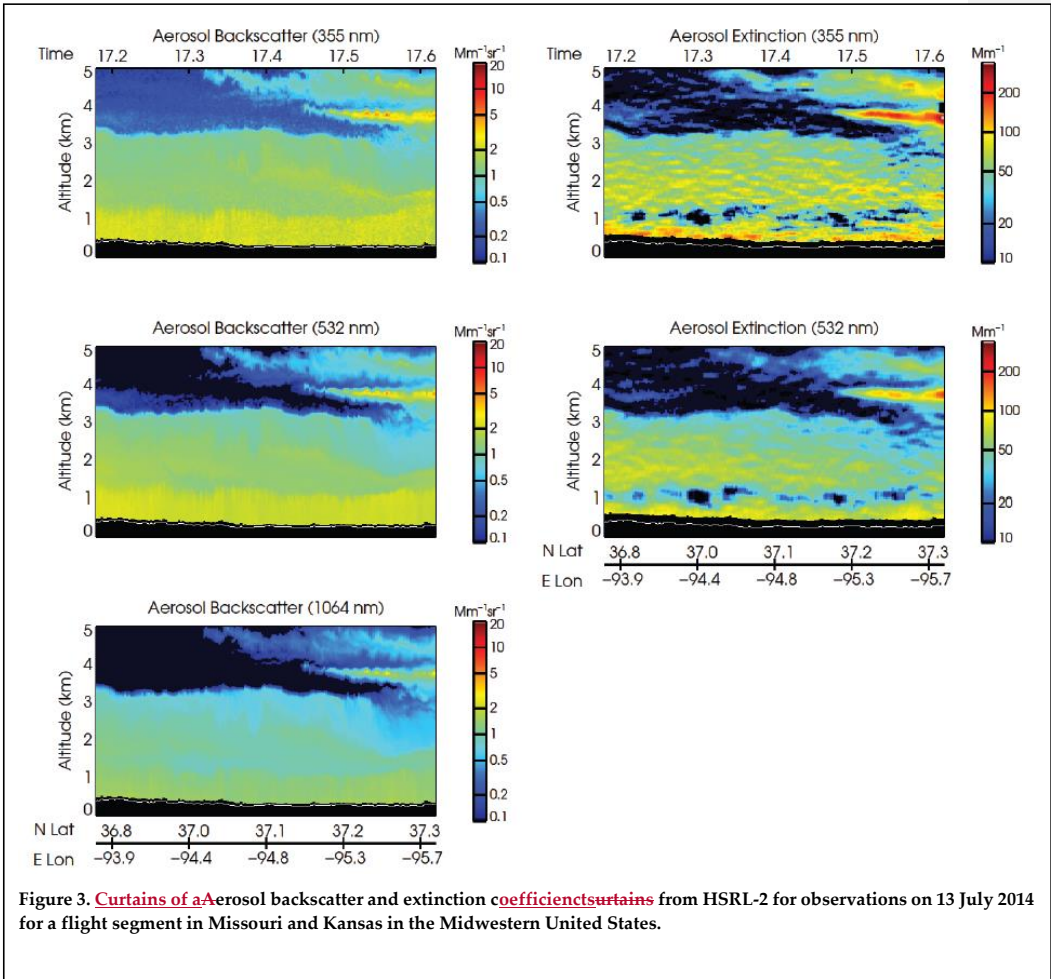
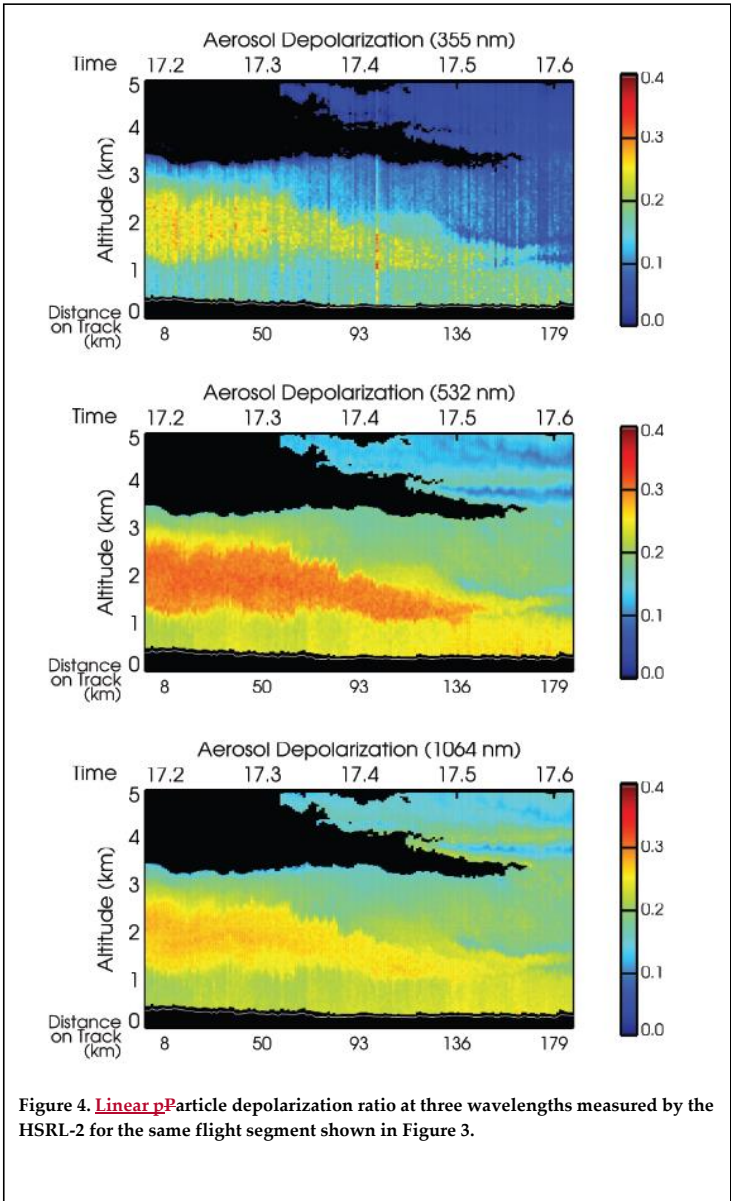


Figure 3. Curtains of aerosol backscatter and extinction coefficients from HSRL-2 for observations on 13 July 2014 for a flight segment in Missouri and Kansas in the Midwestern United States.

1



1

1

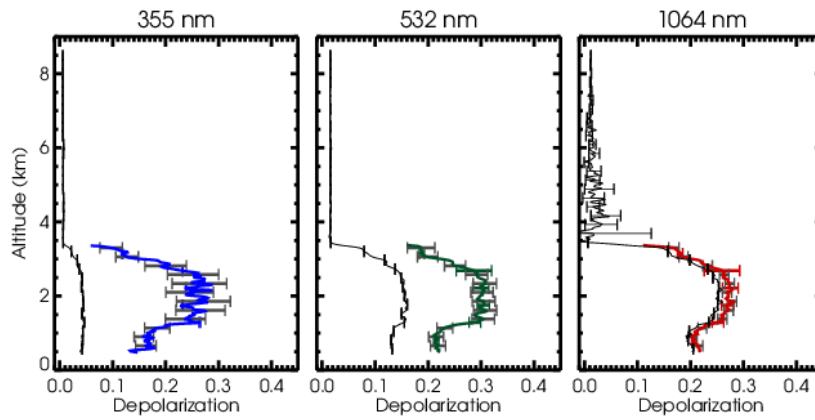
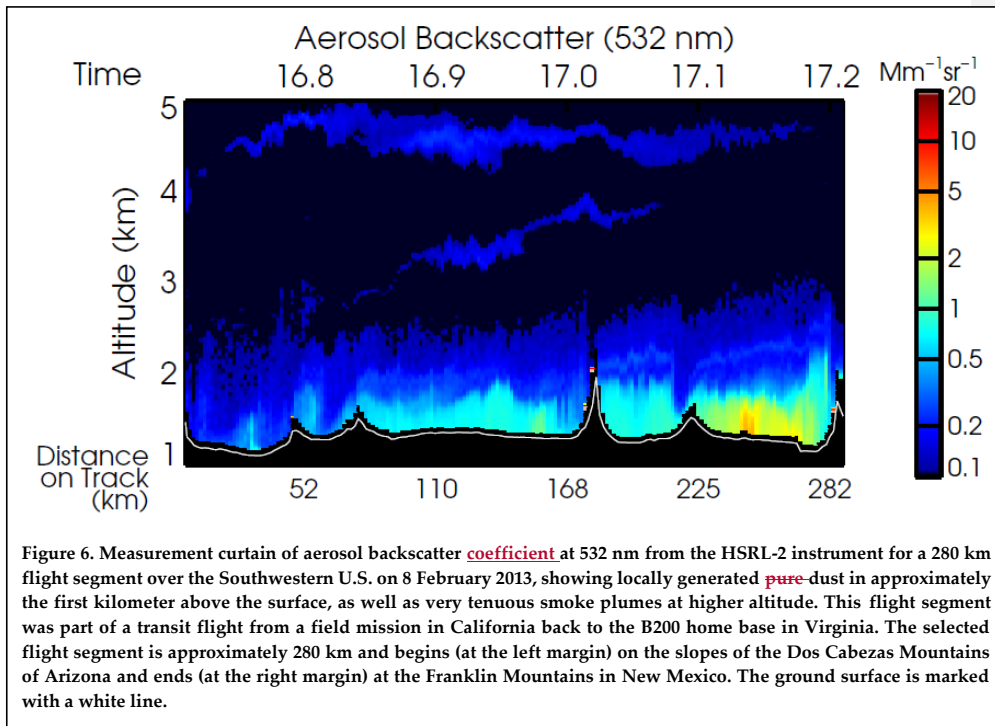


Figure 5. Line plots illustrating the volume and aerosol linear depolarization ratio profile for the HSRL-2 measurements at 17.2 UT (17:12 UT) on 13 July 2014. The volume depolarization ratio is shown as a thin black line. The error bars on the volume depolarization ratio represent random error (most are small and mostly obscured except 1064 nm). The aerosol particle depolarization ratio is shown as a thick colored line. Colored error bars indicate random error (most are small enough to be obscured by the line) while gray error bars indicate systematic uncertainty error bounds, estimated as described in the text. Systematic uncertainty error bars are not shown for the volume depolarization ratio but see text for estimate. The vertical resolution of these measurements is 30 m and the horizontal resolution is 10 s for all wavelengths.

2

1  
2



3

Figure 6. Measurement curtain of aerosol backscatter coefficient at 532 nm from the HSRL-2 instrument for a 280 km flight segment over the Southwestern U.S. on 8 February 2013, showing locally generated pure-dust in approximately the first kilometer above the surface, as well as very tenuous smoke plumes at higher altitude. This flight segment was part of a transit flight from a field mission in California back to the B200 home base in Virginia. The selected flight segment is approximately 280 km and begins (at the left margin) on the slopes of the Dos Cabezas Mountains of Arizona and ends (at the right margin) at the Franklin Mountains in New Mexico. The ground surface is marked with a white line.

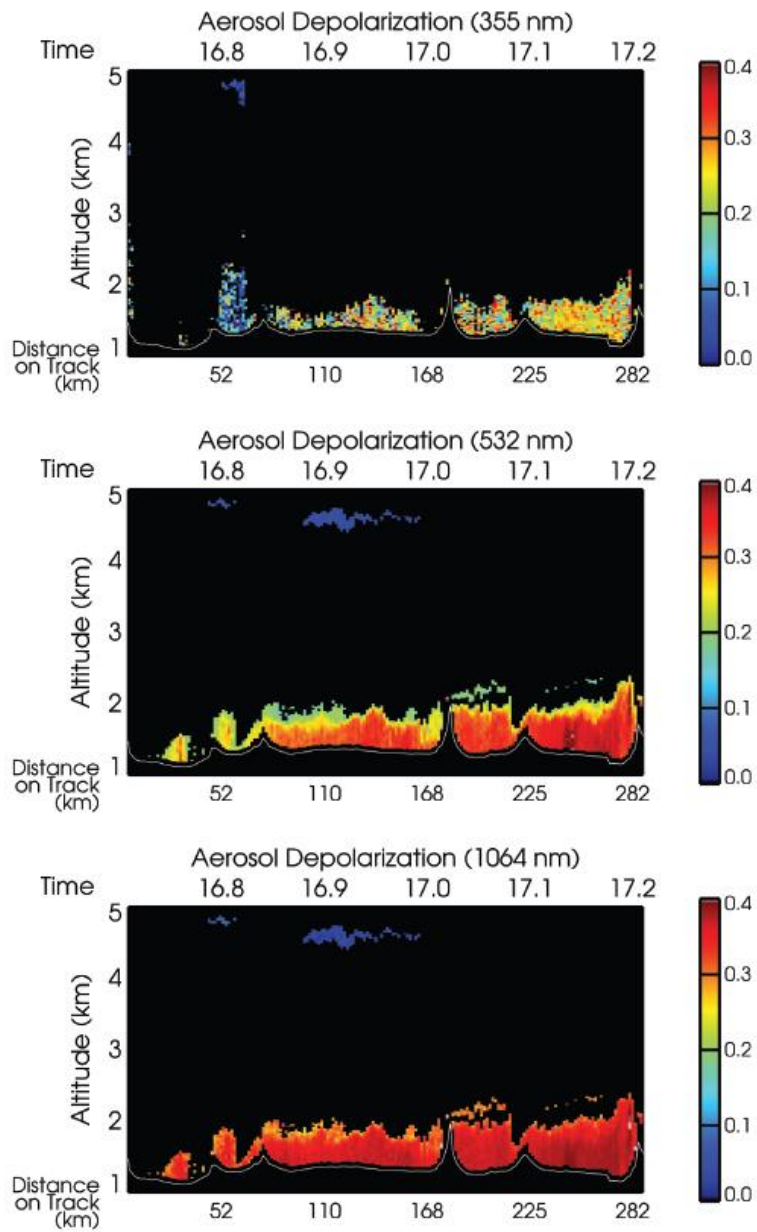


Figure 7. Linear particle depolarization ratio at three wavelengths observed by HSRL-2 on 8 February 2013 in the Southwestern U.S. for the flight segment shown in Figure 6.

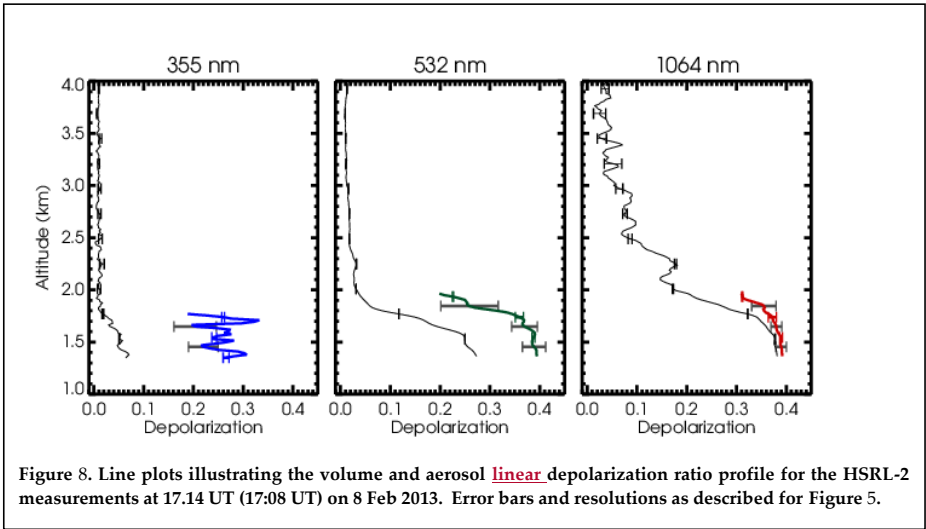


Figure 8. Line plots illustrating the volume and aerosol linear depolarization ratio profile for the HSRL-2 measurements at 17.14 UT (17:08 UT) on 8 Feb 2013. Error bars and resolutions as described for Figure 5.

1  
2

1

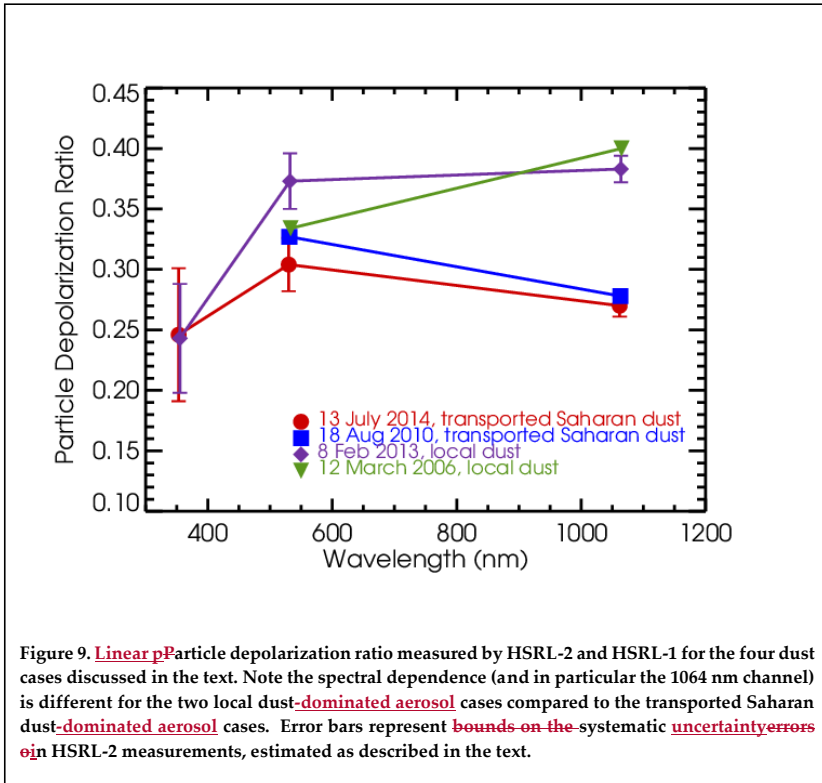


Figure 9. **Linear p**Particle depolarization ratio measured by HSRL-2 and HSRL-1 for the four dust cases discussed in the text. Note the spectral dependence (and in particular the 1064 nm channel) is different for the two local dust-dominated aerosol cases compared to the transported Saharan dust-dominated aerosol cases. Error bars represent bounds on the systematic uncertainty errors in HSRL-2 measurements, estimated as described in the text.

2

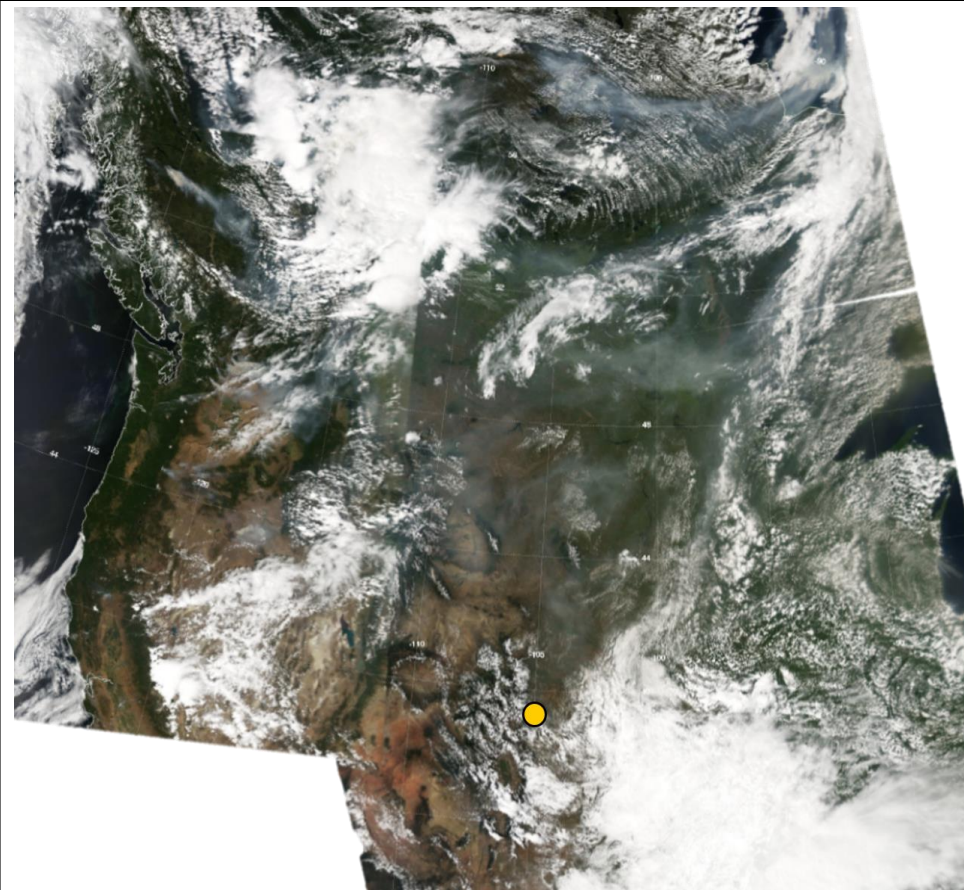


Figure 10. MODIS Aqua true color images of much of North America on 17 July 2014, composited from four granules at 19:45, 19:50, 21:25, and 21:30 UT. The approximate location of the HSRL-2 observations discussed in the text (Denver, Colorado) is marked with a yellow dot. The bright white is clouds and snow cover and the gray is smoke. Several distinct smoke plumes indicate sources in the U.S. Pacific Northwest and in Western Canada within the cloud-free area on the western part of the continent. Significant smoke layers from these fires blanket the mid-continent cloud-free areas in the northern portion of the image. The HSRL-2 measurements are close to the southern edge of the extensive smoke field. Smoke is visible through much of the region. Sources are visible in several places in the U.S. Pacific Northwest and in Western Canada. The approximate location of the HSRL-2 observations discussed in the text (Denver, Colorado) is marked with a yellow dot.

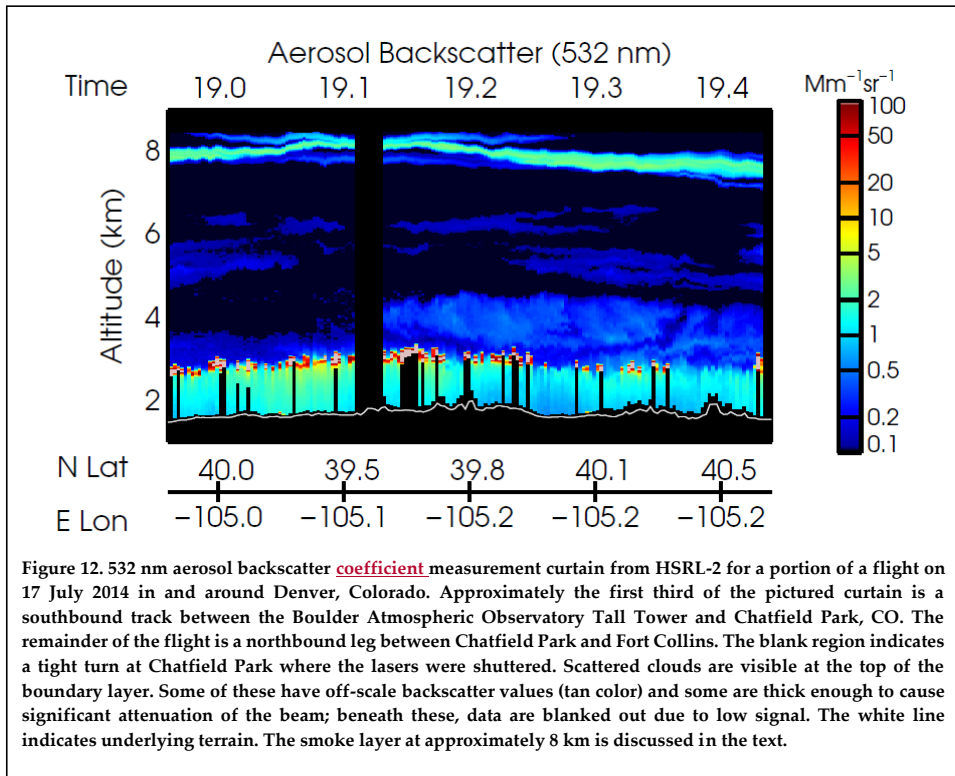
1

2



Figure 11. View of the smoke plume aloft on 17 July 2013 taken from the B200. Photo credit: Tim Berkoff.

1



1

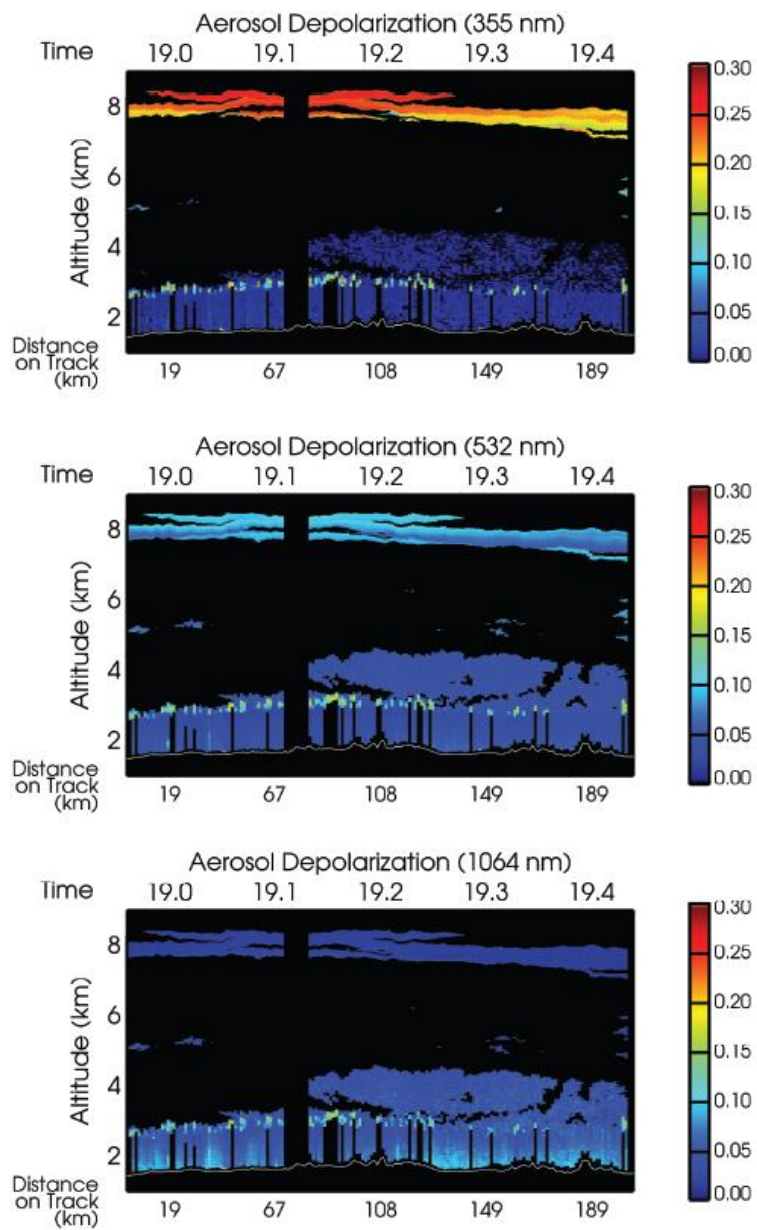


Figure 13. Linear pP Particle depolarization ratio measurement curtains for the flight segment shown in Figure 12.

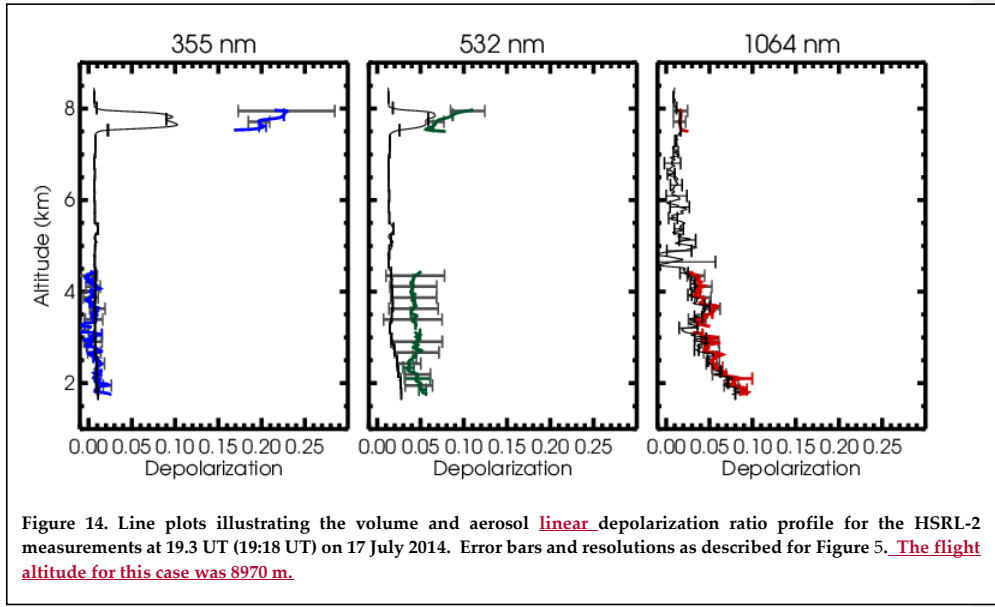


Figure 14. Line plots illustrating the volume and aerosol linear depolarization ratio profile for the HSRL-2 measurements at 19.3 UT (19:18 UT) on 17 July 2014. Error bars and resolutions as described for Figure 5. The flight altitude for this case was 8970 m.

1

2

**Commented [SPB1]:** Note, this figure is revised. Error bars larger than previously on the layer below 4.5 km.

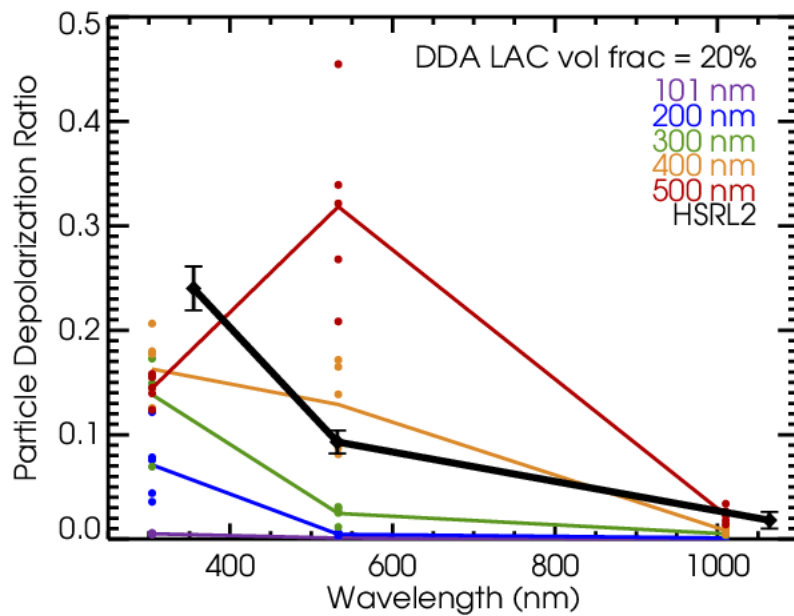


Figure 15. Particle depolarization ratio at three wavelengths for soot aggregates embedded in a sulfate shell reproduced from Kahnert et al. (2012), for 20% LAC volume fraction. Dots indicate five realizations with randomly generated geometries, per aggregate volume-equivalent particle radius, and the colored lines connect the averages of the five for each wavelength. The legend shows the aggregate volume-equivalent particle radii at which the calculation was performed. The thick black line indicates the particle depolarization ratios measured by airborne HSRL-2 within a smoke plume observed on 17 July 2014 at 355, 532, and 1064 nm. Error bars represent systematic uncertainty in bounds on the systematic error of HSRL-2 particle aerosol depolarization ratio, estimated as described in the text.

1

1 **References**

- 2 Adachi, K., and Buseck, P. R.: Internally mixed soot, sulfates, and organic matter in aerosol  
3 particles from Mexico City, *Atmos. Chem. Phys.*, 8, 6469-6481, 10.5194/acp-8-6469-2008,  
4 2008.
- 5 Alvarez, J. M., Vaughan, M. A., Hostetler, C. A., Hunt, W. H., and Winker, D. M.: Calibration  
6 Technique for Polarization-Sensitive Lidars, *J Atmos Ocean Tech*, 23, 683-699,  
7 10.1175/jtech1872.1, 2006.
- 8 Ansmann, A., Tesche, M., Knippertz, P., Bierwirth, E., Althausen, D., Muller, D., and Schulz, O.:  
9 Vertical profiling of convective dust plumes in southern Morocco during SAMUM, *Tellus*  
10 *Ser. B-Chem. Phys. Meteorol.*, 61, 340-353, DOI 10.1111/j.1600-0889.2008.00384.x, 2009.
- 11 [Ansmann, A., Tesche, M., Seifert, P., Groß, S., Freudenthaler, V., Apituley, A., Wilson, K. M.,  
12 Serikov, I., Linné, H., Heinold, B., Hiebsch, A., Schnell, F., Schmidt, J., Mattis, I.,  
13 Wandinger, U., and Wiegner, M.: Ash and fine-mode particle mass profiles from  
14 EARLINET-AERONET observations over central Europe after the eruptions of the  
15 Eyjafjallajökull volcano in 2010. \*Journal of Geophysical Research: Atmospheres\*, 116, n/a/  
16 n/a, 10.1029/2010JD015567, 2011.](#)
- 17 [Ansmann, A., Seifert, P., Tesche, M., and Wandinger, U.: Profiling of fine and coarse particle mass:  
18 case studies of Saharan dust and Eyjafjallajökull/Grimsvötn volcanic plumes. \*Atmos.\*  
19 \*Chem. Phys.\*, 12, 9399-9415, 10.5194/acp-12-9399-2012, 2012.](#)
- 20 Behrendt, A., and Nakamura, T.: Calculation of the calibration constant of polarization lidar and  
21 its dependency on atmospheric temperature, *Optics Express*, 10, 805-817,  
22 10.1364/OE.10.000805, 2002.
- 23 Bescond, A., Yon, J., Girasole, T., Jouen, C., Rozé, C., and Coppalle, A.: Numerical investigation  
24 of the possibility to determine the primary particle size of fractal aggregates by measuring  
25 light depolarization, *Journal of Quantitative Spectroscopy and Radiative Transfer*, 126,  
26 130-139, 2013.
- 27 Born, M., and Wolf, E.: Principles of optics: electromagnetic theory of propagation, interference  
28 and diffraction of light, Cambridge university press, 1999.
- 29 Burton, S. P., Ferrare, R. A., Hostetler, C. A., Hair, J. W., Rogers, R. R., Obland, M. D., Butler, C.  
30 F., Cook, A. L., Harper, D. B., and Froyd, K. D.: Aerosol Classification of Airborne High  
31 Spectral Resolution Lidar Measurements - Methodology and Examples, *Atmospheric*  
32 *Measurement Techniques*, 5, 73-98, 10.5194/amt-5-73-2012, 2012.
- 33 Burton, S. P., Ferrare, R. A., Vaughan, M. A., Omar, A. H., Rogers, R. R., Hostetler, C. A., and  
34 Hair, J. W.: Aerosol classification from airborne HSRL and comparisons with the  
35 CALIPSO vertical feature mask, *Atmos. Meas. Tech.*, 6, 1397-1412, 10.5194/amt-6-1397-  
36 2013, 2013.
- 37 Burton, S. P., Vaughan, M. A., Ferrare, R. A., and Hostetler, C. A.: Separating mixtures of aerosol  
38 types in airborne High Spectral Resolution Lidar data, *Atmos. Meas. Tech.*, 7, 419-436,  
39 10.5194/amt-7-419-2014, 2014.

- 1 [Cairo, F., Di Donfrancesco, G., Adriani, A., Pulvirenti, L., and Fierli, F.: Comparison of Various](#)  
2 [Linear Depolarization Parameters Measured by Lidar, Appl. Opt., 38, 4425-4432, 1999.](#)
- 3 [Dahlkötter, F., Gysel, M., Sauer, D., Minikin, A., Baumann, R., Seifert, P., Ansmann, A., Fromm,](#)  
4 [M., Voigt, C., and Weinzierl, B.: The Pagami Creek smoke plume after long-range](#)  
5 [transport to the upper troposphere over Europe -- aerosol properties and black carbon](#)  
6 [mixing state, Atmos. Chem. Phys., 14, 6111-6137, 10.5194/acp-14-6111-2014, 2014.](#)
- 7 [David, G., Thomas, B., Nousiainen, T., Miffre, A. and Rairoux, P.: Retrieving simulated volcanic,](#)  
8 [desert dust and sea-salt particle properties from two/three-component particle mixtures](#)  
9 [using UV-VIS polarization lidar and T matrix, Atmos. Chem. Phys., 13, 6757-6776,](#)  
10 [10.5194/acp-13-6757-2013, 2013.](#)
- 11 de Foy, B., Burton, S. P., Ferrare, R. A., Hostetler, C. A., Hair, J. W., Wiedinmyer, C., and Molina,  
12 L. T.: Aerosol plume transport and transformation in high spectral resolution lidar  
13 measurements and WRF-Flexpart simulations during the MILAGRO Field Campaign,  
14 Atmos Chem Phys, 11, 3543-3563, 10.5194/acp-11-3543-2011, 2011.
- 15 Fernald, F. G.: Analysis of Atmospheric Lidar Observations - Some Comments, Appl Optics, 23,  
16 652-653, 1984.
- 17 Fiebig, M., Petzold, A., Wandinger, U., Wendisch, M., Kiemle, C., Stifter, A., Ebert, M., Rother, T.,  
18 and Leiterer, U.: Optical closure for an aerosol column: Method, accuracy, and inferable  
19 properties applied to a biomass-burning aerosol and its radiative forcing, J. Geophys. Res.,  
20 107, 8130, 10.1029/2000jd000192, 2002.
- 21 Freudenthaler, V., Esselborn, M., Wiegner, M., Heese, B., Tesche, M., Ansmann, A., Müller, D.,  
22 Althausen, D., Wirth, M., Fix, A., Ehret, G., Knippertz, P., Toledano, C., Gasteiger, J.,  
23 Garhammer, M., and Seefeldner, M.: Depolarization ratio profiling at several wavelengths  
24 in pure Saharan dust during SAMUM 2006, Tellus B, 61, 165-179, 10.1111/j.1600-  
25 0889.2008.00396.x, 2009.
- 26 Gasteiger, J., Wiegner, M., Groß, S., Freudenthaler, V., Toledano, C., Tesche, M., and Kandler, K.:  
27 Modelling lidar-relevant optical properties of complex mineral dust aerosols, Tellus B, 63,  
28 725-741, 10.1111/j.1600-0889.2011.00559.x, 2011.
- 29 Gasteiger, J., and Freudenthaler, V.: Benefit of depolarization ratio at  $\lambda = 1064$  nm for the retrieval  
30 of the aerosol microphysics from lidar measurements, Atmos. Meas. Tech., 7, 3773-3781,  
31 10.5194/amt-7-3773-2014, 2014.
- 32 Gimmetstad, G. G.: Reexamination of depolarization in lidar measurements, Appl. Opt., 47, 3795-  
33 3802, 2008.
- 34 Groß, S., Esselborn, M., Weinzierl, B., Wirth, M., Fix, A., and Petzold, A.: Aerosol classification by  
35 airborne high spectral resolution lidar observations, Atmos. Chem. Phys., 13, 2487-2505,  
36 10.5194/acp-13-2487-2013, 2013.
- 37 Groß, S., Freudenthaler, V., Wirth, M., and Weinzierl, B.: Towards an aerosol classification scheme  
38 for future EarthCARE lidar observations and implications for research needs,  
39 Atmospheric Science Letters, n/a-n/a, 10.1002/asl2.524, 2014.

- 1 [Groß, S., Freudenthaler, V., Schepanski, K., Toledano, C., Schäfler, A., Ansmann, A., and](#)  
2 [Weinzierl, B.: Optical properties of long-range transported Saharan dust over Barbados as](#)  
3 [measured by dual-wavelength depolarization Raman lidar measurements, Atmos. Chem.](#)  
4 [Phys., 15, 11067-11080, 10.5194/acp-15-11067-2015, 2015.](#)
- 5 [Haarig, M., Althausen, D., Ansmann, A., Klepel, A., Baars, H., Engelmann, R., and Groß, S.:](#)  
6 [Measurement of the linear depolarization ratio of aged dust at three wavelengths \(355,](#)  
7 [532 and 1064 nm\) simultaneously over Barbados, International Laser Radar Conference,](#)  
8 [New York, NY, 2015.](#)
- 9 Hair, J. W., Hostetler, C. A., Cook, A. L., Harper, D. B., Ferrare, R. A., Mack, T. L., Welch, W.,  
10 Izquierdo, L. R., and Hovis, F. E.: Airborne High Spectral Resolution Lidar for profiling  
11 aerosol optical properties, *Appl Optics*, 47, 6734-6752, 10.1364/AO.47.006734, 2008.
- 12 Illingworth, A. J., Barker, H. W., Beljaars, A., Ceccaldi, M., Chepfer, H., Cole, J., Delanoë, J.,  
13 Domenech, C., Donovan, D. P., Fukuda, S., Hiraakata, M., Hogan, R. J., Huenerbein, A.,  
14 Kollias, P., Kubota, T., Nakajima, T., Nakajima, T. Y., Nishizawa, T., Ohno, Y., Okamoto,  
15 H., Oki, R., Sato, K., Satoh, M., Shephard, M., Wandinger, U., Wehr, T., and van Zadelhoff,  
16 G. J.: THE EARTHCARE SATELLITE: The next step forward in global measurements of  
17 clouds, aerosols, precipitation and radiation, *B Am Meteorol Soc*, 10.1175/BAMS-D-12-  
18 00227.1, 2015.
- 19 Johnson, M. S., Meskhidze, N., and Praju Kiliyanpilakkil, V.: A global comparison of GEOS-  
20 Chem-predicted and remotely-sensed mineral dust aerosol optical depth and extinction  
21 profiles, *Journal of Advances in Modeling Earth Systems*, 4, M07001,  
22 10.1029/2011MS000109, 2012.
- 23 Kahnert, M., Nousiainen, T., Lindqvist, H., and Ebert, M.: Optical properties of light absorbing  
24 carbon aggregates mixed with sulfate: assessment of different model geometries for  
25 climate forcing calculations, *Optics express*, 20, 10042-10058, 10.1364/OE.20.010042, 2012.
- 26 Liu, Z., Fairlie, T. D., Uno, I., Huang, J., Wu, D., Omar, A., Kar, J., Vaughan, M., Rogers, R., Winker,  
27 D., Trepte, C., Hu, Y., Sun, W., Lin, B., and Cheng, A.: Transpacific transport and evolution  
28 of the optical properties of Asian dust, *Journal of Quantitative Spectroscopy and Radiative*  
29 *Transfer*, 116, 24-33, 10.1016/j.jqsrt.2012.11.011, 2013.
- 30 [Mamouri, R. E., and Ansmann, A.: Fine and coarse dust separation with polarization lidar,](#)  
31 [Atmos. Meas. Tech., 7, 3717-3735, 10.5194/amt-7-3717-2014, 2014.](#)
- 32 Maring, H., Savoie, D. L., Izaguirre, M. A., Custals, L., and Reid, J. S.: Mineral dust aerosol size  
33 distribution change during atmospheric transport, *Journal of Geophysical Research:*  
34 *Atmospheres*, 108, 8592, 10.1029/2002jd002536, 2003.
- 35 Martins, J. V., Hobbs, P. V., Weiss, R. E., and Artaxo, P.: Sphericity and morphology of smoke  
36 particles from biomass burning in Brazil, *Journal of Geophysical Research: Atmospheres*,  
37 103, 32051-32057, 10.1029/98JD01153, 1998.
- 38 Mattis, I., Ansmann, A., Wandinger, U., and Müller, D.: Unexpectedly high aerosol load in the  
39 free troposphere over central Europe in spring/summer 2003, *Geophys Res Lett*, 30,  
40 D2178, 10.1029/2003gl018442, 2003.

- 1 McGill, M. J., Welton, E. J., Yorks, J. E., and Scott, V. S.: CATS: A New Earth Science Capability,  
2 in *The Earth Observer*, edited, pp. 4-8, NASA Earth Observing System Project Science  
3 Office 2012.
- 4 Mishchenko, M. I., and Hovenier, J. W.: Depolarization of light backscattered by randomly  
5 oriented nonspherical particles, *Opt. Lett.*, 20, 1356-1358, 1995.
- 6 Mishchenko, M. I., and Sassen, K.: Depolarization of lidar returns by small ice crystals: An  
7 application to contrails, *Geophys Res Lett*, 25, 309-312, 1998.
- 8 Müller, D., Mattis, I., Wandinger, U., Ansmann, A., Althausen, D., and Stohl, A.: Raman lidar  
9 observations of aged Siberian and Canadian forest fire smoke in the free troposphere over  
10 Germany in 2003: Microphysical particle characterization, *J Geophys Res-Atmos*, 110,  
11 D17201, 10.1029/2004jd005756, 2005.
- 12 Müller, D., Hostetler, C. A., Ferrare, R. A., Burton, S. P., Chemyakin, E., Kolgotin, A., Hair, J. W.,  
13 Cook, A. L., Harper, D. B., Rogers, R. R., Hare, R. W., Cleckner, C. S., Obland, M. D.,  
14 Tomlinson, J., Berg, L. K., and Schmid, B.: Airborne Multiwavelength High Spectral  
15 Resolution Lidar (HSRL-2) observations during TCAP 2012: vertical profiles of optical and  
16 microphysical properties of a smoke/urban haze plume over the northeastern coast of the  
17 US, *Atmos. Meas. Tech.*, 7, 3487-3496, 10.5194/amt-7-3487-2014, 2014.
- 18 Murayama, T., Müller, D., Wada, K., Shimizu, A., Sekiguchi, M., and Tsukamoto, T.:  
19 Characterization of Asian dust and Siberian smoke with multiwavelength Raman lidar  
20 over Tokyo, Japan in spring 2003, *Geophys Res Lett*, 31, 10.1029/2004gl021105, 2004.
- 21 [Nisantzi, A., Mamouri, R. E., Ansmann, A., and Hadjimitsis, D.: Injection of mineral dust into the](#)  
22 [free troposphere during fire events observed with polarization lidar at Limassol, Cyprus,](#)  
23 [Atmos. Chem. Phys., 14, 12155-12165, 10.5194/acp-14-12155-2014, 2014.](#)
- 24 Nishizawa, T., Sugimoto, N., Matsui, I., Shimizu, A., and Okamoto, H.: Algorithms to retrieve  
25 optical properties of three component aerosols from two-wavelength backscatter and one-  
26 wavelength polarization lidar measurements considering nonsphericity of dust, *Journal*  
27 *of Quantitative Spectroscopy and Radiative Transfer*, 112, 254-267, DOI:  
28 10.1016/j.jqsrt.2010.06.002, 2011.
- 29 Omar, A. H., Winker, D. M., Kittaka, C., Vaughan, M. A., Liu, Z. Y., Hu, Y. X., Trepte, C. R.,  
30 Rogers, R. R., Ferrare, R. A., Lee, K. P., Kuehn, R. E., and Hostetler, C. A.: The CALIPSO  
31 Automated Aerosol Classification and Lidar Ratio Selection Algorithm, *J Atmos Ocean*  
32 *Tech*, 26, 1994-2014, 10.1175/2009jtecha1231.1, 2009.
- 33 Pappalardo, G., Amodeo, A., Apituley, A., Comeron, A., Freudenthaler, V., Linné, H., Ansmann,  
34 A., Bösenberg, J., D'Amico, G., Mattis, I., Mona, L., Wandinger, U., Amiridis, V., Alados-  
35 Arboledas, L., Nicolae, D., and Wiegner, M.: EARLINET: towards an advanced  
36 sustainable European aerosol lidar network, *Atmos. Meas. Tech.*, 7, 2389-2409,  
37 10.5194/amt-7-2389-2014, 2014.
- 38 Rogers, R. R., Hair, J. W., Hostetler, C. A., Ferrare, R. A., Obland, M. D., Cook, A. L., Harper, D.  
39 B., Burton, S. P., Shinozuka, Y., McNaughton, C. S., Clarke, A. D., Redemann, J., Russell,  
40 P. B., Livingston, J. M., and Kleinman, L. I.: NASA LaRC airborne high spectral resolution

- 1 lidar aerosol measurements during MILAGRO: observations and validation, *Atmos*  
2 *Chem Phys*, 9, 4811-4826, 10.5194/acp-9-4811-2009, 2009.
- 3 Rogers, R. R., Hostetler, C. A., Hair, J. W., Ferrare, R. A., Liu, Z., Obland, M. D., Harper, D. B.,  
4 Cook, A. L., Powell, K. A., Vaughan, M. A., and Winker, D. M.: Assessment of the  
5 CALIPSO Lidar 532 nm attenuated backscatter calibration using the NASA LaRC airborne  
6 High Spectral Resolution Lidar, *Atmos. Chem. Phys.*, 11, 1295-1311, 10.5194/acp-11-1295-  
7 2011, 2011.
- 8 Rogers, R. R., Vaughan, M. A., Hostetler, C. A., Burton, S. P., Ferrare, R. A., Young, S. A., Hair, J.  
9 W., Obland, M. D., Harper, D. B., Cook, A. L., and Winker, D. M.: Looking Through the  
10 Haze: Evaluating the CALIPSO Level 2 Aerosol Layer Optical Depth using Airborne High  
11 Spectral Resolution Lidar Data, *Atmos. Meas. Tech.*, 7, 4317-4340, 10.5194/amt-7-4317-  
12 2014, 2014.
- 13 [Sakai, T., Nagai, T., Zaizen, Y., and Mano, Y.: Backscattering linear depolarization ratio](#)  
14 [measurements of mineral, sea-salt, and ammonium sulfate particles simulated in a](#)  
15 [laboratory chamber, \*Appl. Opt.\*, 49, 4441-4449, 2010.](#)
- 16 Sasano, Y., and Browell, E. V.: Light-Scattering Characteristics of Various Aerosol Types Derived  
17 from Multiple Wavelength Lidar Observations, *Appl Optics*, 28, 1670-1679, 1989.
- 18 Sassen, K., and Khvorostyanov, V. I.: Cloud effects from boreal forest fire smoke: Evidence for ice  
19 nucleation from polarization lidar data and cloud model simulations, *Environ Res Lett*, 3,  
20 025006, [10.1088/1748-9326/3/2/025006](#), 2008.
- 21 Scarino, A. J., Obland, M. D., Fast, J. D., Burton, S. P., Ferrare, R. A., Hostetler, C. A., Berg, L. K.,  
22 Lefer, B., Haman, C., Hair, J. W., Rogers, R. R., Butler, C., Cook, A. L., and Harper, D. B.:  
23 Comparison of mixed layer heights from airborne high spectral resolution lidar, ground-  
24 based measurements, and the WRF-Chem model during CalNex and CARES, *Atmos.*  
25 *Chem. Phys.*, 14, 5547-5560, 10.5194/acp-14-5547-2014, 2014.
- 26 She, C.-Y.: Spectral Structure of Laser Light Scattering Revisited: Bandwidths of Nonresonant  
27 Scattering Lidars, *Appl. Opt.*, 40, 4875-4884, 2001.
- 28 Shipley, S. T., Tracy, D. H., Eloranta, E. W., Trauger, J. T., Sroga, J. T., Roesler, F. L., and Weinman,  
29 J. A.: High Spectral Resolution Lidar to Measure Optical-Scattering Properties of  
30 Atmospheric Aerosols .1. Theory and Instrumentation, *Appl Optics*, 22, 3716-3724, 1983.
- 31 Sorensen, C.: Light scattering by fractal aggregates: a review, *Aerosol Science & Technology*, 35,  
32 648-687, 2001.
- 33 Su, W. Y., Schuster, G. L., Loeb, N. G., Rogers, R. R., Ferrare, R. A., Hostetler, C. A., Hair, J. W.,  
34 and Obland, M. D.: Aerosol and cloud interaction observed from high spectral resolution  
35 lidar data, *J Geophys Res-Atmos*, 113, D24202, 10.1029/2008jd010588, 2008.
- 36 Sugimoto, N., Uno, I., Nishikawa, M., Shimizu, A., Matsui, I., Dong, X., Chen, Y., and Quan, H.:  
37 Record heavy Asian dust in Beijing in 2002: Observations and model analysis of recent  
38 events, *Geophys Res Lett*, 30, 1640, 10.1029/2002gl016349, 2003.

- 1 Sugimoto, N., and Lee, C. H.: Characteristics of dust aerosols inferred from lidar depolarization  
2 measurements at two wavelengths, *Appl Optics*, 45, 7468-7474, 2006.
- 3 Sugimoto, N., Tatarov, B., Shimizu, A., Matsui, I., and Nishizawa, T.: Optical Characteristics of  
4 Forest-Fire Smoke Observed with Two-Wavelength Mie-Scattering Lidars and a High-  
5 Spectral-Resolution Lidar over Japan, *SOLA*, 6, 93-96, 10.2151/sola.2010-024, 2010.
- 6 Tesche, M., Ansmann, A., Müller, D., Althausen, D., Engelmann, R., Freudenthaler, V., and Groß,  
7 S.: Vertically resolved separation of dust and smoke over Cape Verde using  
8 multiwavelength Raman and polarization lidars during Saharan Mineral Dust  
9 Experiment 2008, *J. Geophys. Res.*, 114, D13202, 10.1029/2009jd011862, 2009a.
- 10 Tesche, M., Ansmann, A., Müller, D., Althausen, D., Mattis, I., Heese, B., Freudenthaler, V.,  
11 Wiegner, M., Esselborn, M., Pisani, G., and Knippertz, P.: Vertical profiling of Saharan  
12 dust with Raman lidars and airborne HSRL in southern Morocco during SAMUM, *Tellus*  
13 *Ser. B-Chem. Phys. Meteorol.*, 61, 144-164, 10.1111/j.1600-0889.2008.00390.x, 2009b.
- 14 Tesche, M., Müller, D., Gross, S., Ansmann, A., Althausen, D., Freudenthaler, V., Weinzierl, B.,  
15 Veira, A., and Petzold, A.: Optical and microphysical properties of smoke over Cape  
16 Verde inferred from multiwavelength lidar measurements, *Tellus B*, 63, 677-694,  
17 10.1111/j.1600-0889.2011.00549.x, 2011.
- 18 Wiegner, M., Gasteiger, J., Kandler, K., Weinzierl, B., Rasp, K., Esselborn, M., Freudenthaler, V.,  
19 Heese, B., Toledano, C., Tesche, M., and Althausen, D.: Numerical simulations of optical  
20 properties of Saharan dust aerosols with emphasis on lidar applications, *Tellus Ser. B-*  
21 *Chem. Phys. Meteorol.*, 61, 180-194, DOI 10.1111/j.1600-0889.2008.00381.x, 2009.
- 22 Winker, D. M., Hunt, W. H., and McGill, M. J.: Initial performance assessment of CALIOP,  
23 *Geophys. Res. Lett.*, 34, L19803, 10.1029/2007gl030135, 2007.
- 24 Yang, W., Marshak, A., Kostinski, A. B., and Várnai, T.: Shape-induced gravitational sorting of  
25 Saharan dust during transatlantic voyage: Evidence from CALIOP lidar depolarization  
26 measurements, *Geophys Res Lett*, 40, 3281-3286, 10.1002/grl.50603, 2013.

27  
28  
29  
30  
31